Sede Amministrativa: Università degli Studi di Padova

Dipartimento di Medicina Molecolare

CORSO DI DOTTORATO DI RICERCA IN: Biomedicina

CURRICOLO: Medicina Rigenerativa

CICLO: XXIX

A NOVEL ROLE FOR HEPARANASE IN THE ONSET OF LIVER FIBROSIS ESTABLISHMENT

Coordinatore: Ch.mo Prof. Stefano Piccolo

Supervisore: Ch.ma Prof.ssa Annarosa Floreani

Co-Supervisore: Ch.mo Prof. Maurizio Onisto

Dottorando: Maria Francesca Secchi

Index

List of abbreviations

α-SMA	alpha smooth muscle actin
AIH	Autoimmune hepatitis
BCA	Bicinchoninic acid
BSA	Bovine serum albumin
CCl_4	Carbon tetrachloride
DAMPs	Damage associated pattern molecules
DTT	Dithiothreitol
ECL	Enhanced chemiluminescence
ECM	Extracellular matrix
ELISA	Enzyme-linked immunosorbent assay
EMT	Epithelial-mesenchymal transition
FBS	Fetal bovine serum
FFPE	Formalin-fixed paraffin-embedded
FGF-2	Fibroblast growth factor-2
FGFR1	Fibroblast growth factor receptor-1
FN	Fibronectin
GAG	Glycosaminoglycan
GalNAc	N-acetylgalactosamine
GBSS	Gey's balanced salt solution
GlcA	Glucuronic acid
GlcNAc	N-acetylglucosamine
GlcNS	N-sulfoglucosamine
GPI	Glycosil-phophatydil-inositol
HCC	Hepatocellular carcinoma
H-E	Hematoxylin-eosin
HPSE	Heparanase
HRP	Horseradish peroxidase
HS	Heparan sulfate
HSC	Hepatic stellate cell
HSPG	Heparan sulfate proteoglycan

IdoA	Iduronic acid
IF	Immunofluorescence
IFN-γ	Interferon gamma
IL	Interleukin
IHC	Immunohistochemistry
KO	Knock out
LMWH	Low molecular weight heparin
LPS	Lipopolysaccharide
MMP	Matrix metalloprotease
P/S	Penicillin/streptomycin
PBC	Primary biliary cholangitis
PBS	Phosphate buffered saline
PSC	Primary sclerosing cholangitis
PDGF	Platelet derived growth factor
PFA	Paraformaldehyde
PKA	Protein kinase A
PI3K	Phosphatidylinositol 3-kinase
PMA	Phorbol myristate acetate
ROS	Reactive oxygen species
RT	Room temperature
RT-PCR	Reverse transcriptase-polymerase chain reaction
SDC	Syndecan
STZ	Streptozotocin
TBS	Tris buffered saline
TBST	Tris buffered saline Tween-20
TGF-β	Transforming growth factor beta
TLR	Toll-like receptor
TNF-α	Tumor necrosis factor alpha
VEGF	Vascular endothelial growth factor

Sommario

I proteoglicani dell'eparan solfato sono importanti componenti strutturali e funzionali delle membrane basali costituiti da un asse proteico (solubile o transmembrana) legato covalentemente a catene altamente solfatate di glicosaminoglicani chiamate eparan solfato. L'eparanasi è l'unico enzima in grado di tagliare le catene di eparan solfato a livello di specifici siti intracatena, generando frammenti di circa 5-7kDa. Essa si definisce endo-β-D-glucuronidasi, in quanto capace di tagliare i legami glicosidici tra i monomeri di acido glucuronico a glucosamina che costituiscono l'eparan solfato. A livello intracellulare (endosomale e lisosomale), l'eparanasi partecipa al turnover dei proteoglicani dell'eparan solfato associati alla membrana cellulare mentre, quando secreta, è coinvolta nella degradazione e nel rimodellamento della matrice extracellulare. Data l'interazione elettrostatica dell'eparan solfato con fattori di crescita, citochine ed enzimi, il suo taglio da parte dell'eparanasi facilita indirettamente anche il rilascio e la diffusione di queste molecole. L'eparanasi svolge poi funzioni non enzimatiche in quanto è in grado di regolare l'espressione genica attraverso l'attivazione di vie di segnalazione intracellulari. Nello svolgere queste funzioni, l'eparanasi è coinvolta sia in processi fisiologici che patologici. In particolare l'eparanasi ha un ruolo significativo nella progressione tumorale e nelle malattie glomerulari renali. Inoltre, è stato recentemente dimostrato il suo coinvolgimento anche nell'infiammazione cronica a livello intestinale e renale così come nella fibrosi tubulo-interstiziale. In generale, la fibrosi è un processo sregolato di riparazione tissutale che insorge in seguito ad un danno persistente e ad infiammazione cronica. Nel fegato, il progressivo accumulo di matrice extracellulare può portare a cirrosi e insufficienza epatica. In questo processo, l'attivazione delle cellule di Kupffer e delle cellule stellate (HSC) svolge un ruolo fondamentale, le prime nella risposta infiammatoria, le seconde nella fibrogenesi.

Finora, nessuno studio ha dimostrato un coinvolgimento dell'eparanasi nello sviluppo della malattia cronica epatica. Considerata la riproducibilità dei meccanismi che concorrono allo sviluppo delle malattie croniche, questo studio ha lo scopo di: i) verificare se l'eparanasi sia up-regolata nel corso della malattia

cronica di fegato, ii) studiare l'eventuale regolazione della sua espressione e iii) studiare i possibili effetti sullo sviluppo della malattia.

Il quadro di espressione temporo-spaziale dell'eparanasi è stato studiato in topi con danno cronico epatico indotto da somministrazioni di tetracloruro di carbonio (CCl_4) per 1, 2, 8 e 12 settimane. La progressione del danno cronico e della fibrosi è stata valutata tramite le colorazioni istologiche di Azan-Mallory ed Ematossilina-Eosina. Estese aree centrolobulari ad elevata attività necro-infiammatoria e fibrosi si sono osservate dopo 1 e 2 settimane di trattamento che hanno progressivamente generato fasci fibrotici e cirrosi micronodulare osservati dopo 8 e 12 settimane di trattamento. Analisi di espressione genica (tramite real time RT-PCR) e proteica (tramite Western blot e immunofluorescenza), hanno dimostrato un significativo aumento di espressione dell'eparanasi dopo 1 e 2 settimane di trattamento ma non dopo 8 e 12 settimane suggerendo un possibile ruolo dell'enzima nelle fasi iniziali del danno cronico. Analisi di immunoistochimica hanno poi evidenziato una localizzazione dell'eparanasi nelle aree centrolobulari con danno necro-infiammatorio e fibrosi. Per identificare la sorgente cellulare di eparanasi responsabile del suo aumento tissutale, sono state condotte analisi *in vitro* su colture cellulari ed analisi di co-immuofluorescenza su sezioni di fegato trattato con CCl_4 per 1 e 2 settimane. Data la localizzazione dell'eparanasi nelle aree fibrotiche e il ruolo fondamentale delle HSC nella malattia cronica di fegato, ci siamo chiesti se l'espressione di eparanasi aumenti nelle HSC durante la loro attivazione. A tal scopo, cellule primarie sono state isolate da fegato di ratto e indotte ad attivarsi tramite coltura su plastica. Dopo 15 giorni dall'isolamento, i livelli di espressione dell'eparanasi e di marcatori del transdifferenziamento (α-SMA, fibronectina, TGF-β e collagene I) sono significativamente aumentati rispetto a cellule coltivate per 7 giorni. Tuttavia, nonostante analisi di immunofluorescenza abbiano evidenziato l'espressione di eparanasi da parte di HSC attivate *in vivo* a 1 e 2 settimane di trattamento con CCl_4, un più significativo grado di co-localizzazione è stato osservato con i macrofagi marcati con F4/80 e CD68.

Dato il principale coinvolgimento dei macrofagi nell'aumento di eparanasi epatica in sede di infiammazione, è stata quindi condotta un'analisi sui possibili meccanismi di up-regolazione dell'eparanasi da parte dei macrofagi infiammatori. A tal scopo, cellule primarie di Kupffer sono state isolate da fegato di ratto e

trattate con LPS e TNF-α, due importanti stimoli pro-infiammatori. Al contrario dell'LPS che non ha alterato l'espressione dell'eparanasi, il TNF-α ne ha indotto un significativo aumento. Anche macrofagi umani U937, trattati con concentrazioni crescenti di TNF-α, hanno aumentato l'espressione genica e proteica dell'eparanasi, con un meccanismo dose-dipendente. Tramite Western blot sui mezzi condizionati di U937 trattate o meno con TNF-α, abbiamo inoltre dimostrato un incremento di enzima extracellulare in presenza di TNF-α, suggerendo come questo fattore stimoli anche la secrezione di eparanasi. Due osservazioni hanno poi fornito ulteriori evidenze sul possibile ruolo del TNF-α come regolatore dell'espressione dell'eparanasi nella malattia cronica epatica: in primo luogo il significativo aumento di espressione del TNF-α nel tessuto epatico solo a 1 e 2 settimane di intossicazione da CCl_4 e, in secondo luogo, la sua co-localizzazione con l'eparanasi alle stesse settimane di trattamento. Tra le altre molecole pro-infiammatorie testate, mentre IFN-γ ha stimolato la trascrizione genica dell'eparanasi, IL-4 ne ha ridotto l'espressione suggerendo una diversa regolazione dell'eparanasi da parte dei macrofagi a seconda del loro stato di polarizzazione M1 e M2.

L'elevata espressione dell'eparanasi negli stadi iniziali della malattia cronica di fegato ha portato a chiederci quale potesse essere il suo ruolo nel processo di fibrogenesi. Dato il coinvolgimento delle cellule di Kupffer nell'attivazione delle HSC tramite il rilascio di stimoli pro-fibrotici, abbiamo verificato se fosse possibile un meccanismo di regolazione anche attraverso il rilascio di eparanasi. A tale scopo, cellule stellate LX-2 sono state trattate con i mezzi condizionati delle U937 precedentemente indotte a produrre eparanasi tramite stimolazione con TNF-α. Il coinvolgimento dell'eparanasi nell'attivazione delle LX-2 è stato verificato utilizzando un inibitore dell'eparanasi durante il trattamento. I risultati hanno dimostrato come l'eparanasi sia in grado di regolare l'espressione di α-SMA e di fibronectina da parte delle LX-2.

Oltre alla degradazione della matrice extracellulare, anche la capacità di promuovere l'attivazione dei macrofagi è un'attività dell'eparanasi già nota. In questo studio, tramite un saggio di migrazione *in vitro*, è stato dimostrato come la forma latente dell'eparanasi sia in grado di stimolare anche la migrazione dei macrofagi.

Infine, per verificare il coinvolgimento dell'eparanasi nella fibrosi epatica umana, i livelli di attività dell'eparanasi sono stati misurati nel plasma di soggetti sani e pazienti affetti da malattia cronica di fegato, ad eziologia virale o autoimmune e a diversi stadi di fibrosi. A conferma di quanto riscontrato nel modello animale, abbiamo osservato come, indipendentemente dall'eziologia della malattia epatica, l'attività plasmatica dell'eparanasi aumenti nei pazienti con fibrosi lieve e moderata rispetto ai soggetti sani, ma ritorni basale nei pazienti cirrotici. Inoltre, nei pazienti, l'attività plasmatica dell'eparanasi correlava negativamente con il grado di stiffness epatica.

Complessivamente, i nostri risultati indicano un coinvolgimento dell'eparanasi nella malattia cronica di fegato ma solo nelle sue fasi iniziali. Macrofagi infiammatori e, in misura minore, HSC attivate costituiscono un'importante fonte di eparanasi. In questo contesto, l'eparanasi secreta nell'ambiente extracellulare può avere un ruolo nell'attivazione delle HSC mediata dai macrofagi e nella migrazione dei macrofagi stessi.

Summary

Heparan sulfate proteoglycans are important structural and functional components of basal membranes composed of a core protein (soluble or transmembrane) covalently linked to highly sulfated chains of glycosaminoglycans called heparan sulfate. Heparanase is the only endoglucuronidase capable of cleaving heparan sulfate chains of heparan sulfate proteoglycans. It exerts its enzymatic activity by catalyzing the cleavage of the β(1,4)-glycoside bond between glucuronic acid and glucosamine residues, generating fragments of about 5–7kDa. At intracellular level (endosomal and lysosomal), heparanase participates in the turnover of membrane-associated heparan sulfate proteoglycans, while secreted enzyme is involved in the remodeling and degradation of extracellular matrix. Given the electrostatic interaction of heparan sulfate with growth factors, cytokines and enzymes, heparanase cleavage indirectly facilitates the release and diffusion of these molecules. Heparanase exerts also non-enzymatic functions since it regulates gene expression by the activation of specific signaling pathways. Through degradation of heparan sulfate chains and heparan sulfate-independent functions, HPSE regulates several physiological and pathological processes. In particular, heparanase has a significant role in tumor progression and in renal glomerular diseases. In addition, it was recently shown its involvement also in bowel and kidney chronic inflammation as well as in tubulo-interstitial fibrosis. In general, fibrosis is an unregulated process of tissue repair that occurs in response to persistent damage and chronic inflammation. In the liver, the progressive accumulation of extracellular matrix can lead to cirrhosis and organ failure. In this process, activated Kupffer cells and hepatic stellate cells (HSCs) play a fundamental role, the first in the inflammatory response, the latter in fibrogenesis.

The involvement of heparanase in the development of chronic liver disease has not been demonstrated so far. Given the reproducibility of the mechanisms that contribute to the development of chronic diseases, this study was aimed to: i) investigate whether heparanase is up-regulated during chronic liver disease, ii) study the possible regulation of its expression and iii) study the possible effects on the development of the disease.

The tempo-spatial expression of heparanase was studied in mice with chronic hepatic damage induced by carbon tetrachloride (CCl_4) administration for 1, 2, 8 and 12 weeks. The progression of chronic injury and fibrosis was assessed by Azan-Mallory and Hematoxylin-Eosin histological stainings. Extensive centrilobular areas with necro-inflammatory activity and fibrosis were observed after 1 and 2 weeks of treatment that progressively developed fibrotic septa and micronodular cirrhosis observed after 8 and 12 weeks of treatment. Analyses of gene expression (by real time RT-PCR) and protein expression (by western blot and immunofluorescence), showed a significant increase of heparanase expression after 1 and 2 weeks of treatment but not after 8 and 12 weeks suggesting a possible role in the early stages of chronic damage. Immunohistochemical analyses revealed the localization of heparanase in the centrilobular areas with necro-inflammatory damage and fibrosis. To identify the cellular source responsible for heparanase increase in tissue, *in vitro* analyses on cell cultures and co-immunofluorescence analyses on sections from 1 and 2 week-treated livers were performed. Given heparanase localization in fibrotic areas and the fundamental role of the HSCs in chronic liver disease, we wondered if the expression of heparanase increases in HSC during their activation. For this purpose, primary HSCs were isolated from rat livers and induced to activate through culture on plastic dishes. After 15 days of isolation, the levels of heparanase and transdifferentiation markers (α-SMA, fibronectin, TGF-β and collagen I) expression increased significantly compared to cells cultured for 7 days. However, despite immunofluorescence analyses on liver sections revealed the expression of heparanase by *in vivo* activated HSCs at 1 and 2 weeks of treatment with CCl_4, a more significant degree of co-localization was observed with macrophages labeled with F4/80 and CD68.

Given the main involvement of macrophages in increasing hepatic heparanase in the sites of inflammation, an analysis of the possible mechanisms of heparanase up-regulation by inflammatory macrophages was then conducted. To this purpose, primary Kupffer cells were isolated from rat livers and treated with LPS and TNF-α, two important pro-inflammatory stimuli. In contrast to LPS, that did not alter the expression of heparanase, TNF-α induced a significant increase of heparanase expression. Also human U937 macrophages, treated with increasing concentrations of TNF-α, increased the heparanase gene and protein levels, in a

dose-dependent mechanism. By Western blot on the conditioned media from cells treated or not with TNF-α, we also showed an increase of extracellular enzyme in the presence of TNF-α, indicating that this factor stimulates also heparanase secretion. In addition, two observations provided further evidence on the possible role of TNF-α as a regulator of heparanase expression in chronic liver disease: first, the significant increase in TNF-α expression in the liver tissue only at 1 and 2 weeks of intoxication by CCl4 and, secondly, its co-localization with heparanase at the same weeks of treatment. Among the other pro-inflammatory molecules tested, while IFN-γ stimulated heparanase gene transcription, IL-4 reduced its expression thus suggesting a different regulation of heparanase by macrophages depending on their state of M1 or M2 polarization.

The observation of enhanced heparanase expression in the early stages of chronic liver disease led to wonder what it could be its role in the process of fibrogenesis. Given the involvement of Kupffer cells in the activation of HSC through the release of pro-fibrotic stimuli, we examined whether a mechanism of regulation through the release of heparanase was also possible. For this purpose, LX-2 stellate cells were treated with the conditioned media of U937 cells that were previously induced to produce heparanase by stimulation with TNF-α. The involvement of heparanase in the activation of LX-2 has been verified using an heparanase inhibitor during treatment. The results showed that heparanase is able to regulate the expression of α-SMA and fibronectin by LX-2 cells.

Besides extracellular matrix degradation, the promotion of macrophage activation by heparanase is already known. In this study, using an *in vitro* migration assay, we demonstrated that heparanase is also able to stimulate the migration of macrophages.

Finally, to verify the involvement of heparanase also in human liver fibrosis, the levels of heparanase activity were measured in the plasma of healthy subjects and patients with chronic liver disease, of viral or autoimmune etiology and at different stages of fibrosis. Accordingly to the animal model, we showed that, regardless of the etiology of hepatic disease, heparanase plasma activity increased in patients with mild and moderate fibrosis compared to healthy subjects, but returned to baseline in patients with cirrhosis. In addition, in patients, plasma heparanase activity negatively correlated with the degree of liver stiffness.

Overall, our results indicate the involvement of heparanase in chronic liver disease but only in its early stages. Inflammatory macrophages and, to a lesser extent, activated HSCs are an important source of heparanase. In this context, secreted heparanase in the extracellular environment may play a role in the macrophage-mediated activation of HSCs and in the migration of macrophages themselves.

1. Introduction

1.1 General overview of proteoglycans

Proteoglycans are high molecular mass molecules formed by a core protein and one or more polysaccharide chains covalently bound to the core protein. The polysaccharide chains, named glycosaminoglycans (GAGs), are constituted by a disaccharide unit of an uronic acid (either D-glucuronic, GlcA or L-iduronic, IdoA) and a hexosamine (either N-acetylglucosamine, GlcNAc or N-acetylgalactosamine, GalNAc) which is repeated linearly. The glycosidic linkage (α or β) connects hexosamine and uronic acid at position (1→3) or (1→4). Inter-disaccharide linkages are always (1→4). Upon macromolecular assembly in Golgi apparatus, the disaccharide unit undergoes sulfation reactions in different positions conferring to GAGs an elevated negative charge. The high structural heterogeneity of proteoglycans is mainly given by: 1) the huge number of core protein identified, 2) the number of GAGs chains attached to the core protein and 3) the type of GAG which, according to its component sugars and pattern of modifications, is categorized in chondroitin sulfate, dermatan sulfate, keratan sulfate and heparan sulfate/heparin. In addition, proteoglycans may contain different types of GAGs along the core protein (hybrid proteoglycans) [1].

Proteoglycans are also heterogeneously localized. Condroitin and dermatan sulfate proteoglycans are main structural components of extracellular matrix (ECM). The major biological function of ECM proteoglycans is given by their highly anionic GAGs which provide tissue hydration and viscosity and favour nutrient, metabolites and hormones diffusion. Pericellular proteoglycans (mostly heparan sulfate proteoglycans) are structural constituents of basement membranes and modulators of signaling pathways and morphogen gradients through the interaction with regulatory and signaling factors. Cell surface proteoglycans are closely associated with cell membrane through a membrane-spanning core protein or a glycosil-phophatydil-inositol (GPI) anchor and may function as adhesion molecules, endocytic receptors and as co-receptors thus controlling cell signaling, adhesion and motility. Serglycin is the only intracellular proteoglycan, localized primarily, but not exclusively, in the secretory granules of mast cells in which has a role in proteases packaging [2].

1.2 Heparan sulfate proteoglycans

1.2.1 Structure

Heparan sulfate proteoglycans (HSPGs) contain heparan sulfate (HS) chains. The disaccharide unit of HS consists of a negatively charged GlcA or its epimer IdoA and a GlcNAc or GlcNS (N-sulfoglucosamine). The intra-disaccharide glycosidic linkage is α (1→4) or β (1→4). Inter-disaccharide linkages are always α (1→4). HSPGs are assembled in the endoplasmic reticulum and Golgi apparatus compartments. HS chains are polymerized starting from a tetrasaccharide linkage region (xylose, galactose, galactose, glucuronic acid) which is synthesized on different serine residues in the core protein (Fig.1a). Throughout elongation, HS is modified by sequential reactions of specific enzymes: N-deacetylation/N-sulfation of GlcNAc, C5-epimerization of GlcA to IdoA, 2-O-sulfation of IdoA and 6-O-sulfation of GlcNAc. Depending on sulfation pattern, HS contains low sulfated domains and highly sulfated domains. A heavily sulfated variant of HS is called heparin [3]. The structure of HS and heparin unit is shown in Figure 1b.

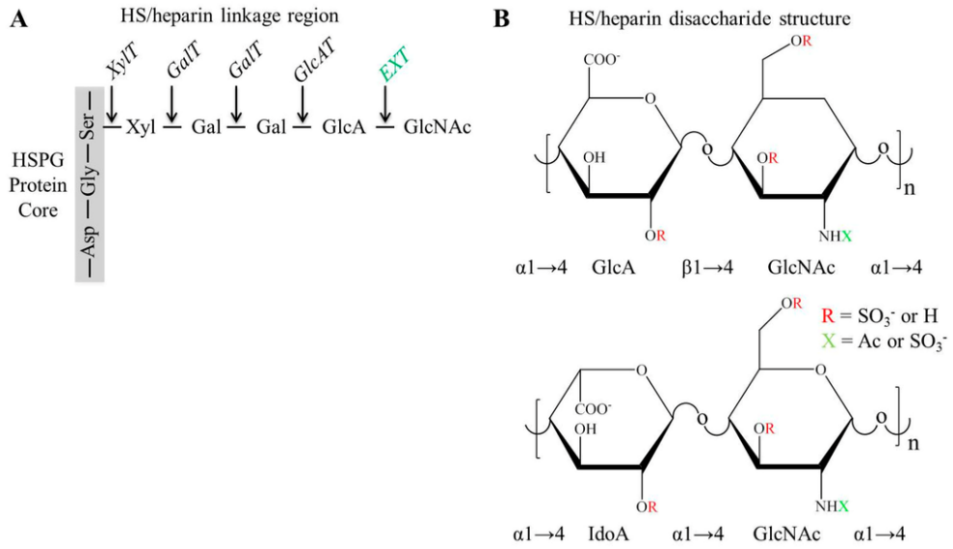

Figure 1. HSPGs structure. (a) A chain of four monosaccharides (tetrasaccharide linker) connects HS to the protein core. This linkage region is assembled by the sequential action of specific enzymes: xylosyltransferase (XylT), galactosyltransferase (GalT) and glucuronic acid transferase (GlcAT). Acceptor serines residues are flanked by a glycine/aspartic acid sequence. **(b)** Structure of HS/heparin disaccharide unit. The glycosidic linkages and structure modifications are shown. Heparin is structurally related to HS but with an higher sulfate content. From [3].

1.2.2 HSPGs localization and functions

Mammalian HSPGs are prevalently cell surface and pericellular proteoglycans. With the exception of two chondroitin sulfate proteoglycans (NG2 and phosphacan), all cell surface proteoglycans are HSPGs. This class includes transmembrane betaglycan, four transmembrane syndecans and six GPI-anchored glypicans. In transmembrane HSPGs, HS chains are attached to the ectodomain, distal to the plasma membrane on betaglycan and syndecans while proximal on glypicans. Syndecan-1 and -3 also contain proximal chondroitin sulfate chains (Fig.2a). Cell surface HSPGs bind several ligands through electrostatic interaction with anionic HS chains, acting as a reservoir for growth factors, chemokines, cytokines and morphogens and as regulators of cell signaling and morphogenesis [4]. Membrane HSPGs can activate receptors on the same cells *(in cis)* or on adjacent cells *(in trans)* promoting cell-cell cross talk [5]. A well known example is represented by syndecan-1 which promotes basic fibroblast growth factor (FGF-2) binding and activation of FGF-2 receptor-1 (FGFR1) [6]. More specifically, released HS fragments bound to FGF-2 are potent activators of FGFR1. Betaglycan, also known as transforming growth factor (TGF-β) type III receptor, is a TGF-β co-receptor which promotes TGF-β binding to type II receptor. However, the presentation of TGF-β to the receptor does not involve HS chains. The biological activity of membrane proteoglycans is post-translational modulated by the enzymatic release of HSPGs ectodomain in the pericellular space (ectodomain shedding). HSPGs shedding generates diffusing soluble HSPGs which re-localize HS-bound ligands and act as autocrine or paracrine effectors. Syndecans are shed by metalloproteases (MMPs) while glypicans can be cleaved by a protease or a lipase, releasing the ectodomain in the first case and the entire molecule in the second case. Shedding is known to contribute to the progression of several tumors by the generation of soluble bioactive syndecan-1 which, once released in the microenvironment, promotes angiogenesis and invasiveness [7]. Besides their function as co-receptors, transmembrane HSPGs act also as endocytic and adhesion receptors with the collaboration of cytoscheletal proteins, fibronectin and integrins. [5].

Pericellular HSPGs are important extracellular scaffold of basement membrane barriers and include perlecan, agrin and collagen XVIII. Perlecan contains a multi-

domain protein core and three HSPGs chains at its N-terminus (Fig.2a). Besides its structural role, perlecan is known to regulate several biological processes by its interaction with ECM, growth factors and membrane proteins (integrins and tyrosine kinase receptors). In particular, perlecan HS chains are a reservoir for vascular endothelial growth factor (VEGF), platelet-derived growth factor (PDGF), TGF-β and FGF family members. By the release of these factors, perlecan is a potent regulator of vascularization and tumor angiogenesis [8]. As perlecan, agrin is a multimodular HSPGs containing three HS chains. Agrin, abundant in synaptic region, is an important example of *in trans* cellular crosstalk mediated by HSPGs. Indeed, motor neuron-derived agrin is a crucial organizer of the neuromuscular junction at post-synaptic membrane by the high affinity of its N- and C-terminal domain for laminin in basal membrane and low-density lipoprotein-like receptor 4 (LRP4) in skeletal muscle respectively [9]. Agrin is also a major component of the glomerular basement membrane (GBM) in the kidney. Collagen XVIII, which contains a collagenous domain and three HS chains, is a GBM component as well [10]. Figure 2b summarized the above-mentioned biological activities of HSPGs.

As introduced in paragraph 1.1, serglycin is an intracellular HSPG localized in secretory vesicles of hematopoietic and endothelial cells. Serglycin is an hybrid proteoglycan, containing both heparin and chondroitin sulfate chains. In secretory granules, the highly anionic heparin mediate electrostatic interaction with proteases and inflammatory mediators, favouring their packaging [11]. Upon activation, degranulated mast cells release heparin which acts as an anticoagulant factor. The anticoagulant effect of heparin is due to its ability to interact with and activate antithrombin which, in turn, inhibits the coagulant factor thrombin. The interaction is mediated by a specific pentasaccharide sequence with an high affinity for antithrombin [12]. Several commercially produced low molecular weight heparins (LMWHs) are used as anticoagulant in clinic. Serglycin has long been regarded as the unique intracellular HSPGs. To date, there are several report about HS and HSPGs in cell nucleus where they affect gene transcription by the inhibition of histone acetyltransferase (HAT) [13].

Together with shedding, the remove of specific sulfate groups by endosulfatases and the cleavage of HS chains are other post-biosynthetic modifications of

HSPGs. The enzyme able to cut HS polysaccharide and to release diffusible HS fragments is called heparanase (Fig.2).

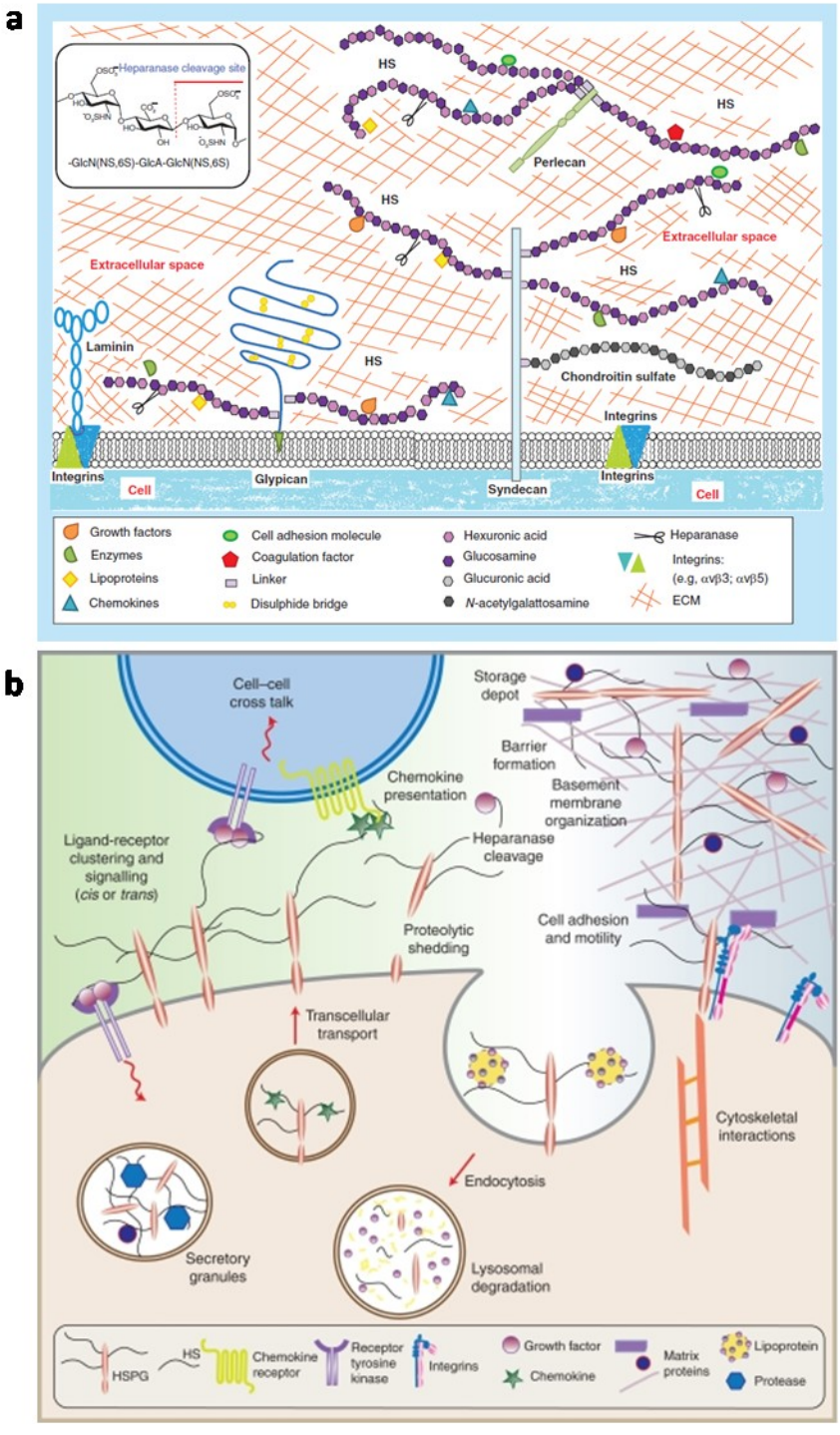

Figure 2. HSPGs localization and biological roles. (a) Principal cell surface (syndecan and glypican) and pericellular (perlecan) HSPGs. Because of their negative charge, HS binds to several proteins including growth factors, chemokines, enzymes, lipoproteins and plasma proteins. HS chains are cleaved by heparanase enzyme. From [14]. **(b)** HSPGs are multitasking molecules functioning as scaffold proteins, co-receptors, endocytic and adhesion receptors. From [5].

1.3 Heparanase

Heparanase (HPSE) is the only endo-β-D-glucuronidase with an HS cleavage activity that has been discovered so far in mammals. Human HPSE gene (*HPSE-1*) is located on chromosome 4q21.3 and it is expressed by alternative splicing as two mRNA, both containing the same open reading frame [15]. *HPSE-1* was first cloned in 1999 by four distinct groups [16-19] followed by the cloning in mouse [20], chicken [21], rat [18], *Spalax* [22] and bovine [23]. In 2000, *HPSE-2* gene was cloned [24]. Interestingly, HPSE-2 protein, which shares ~40% similarity with HPSE, does not have glycosidase activity but seems to inhibit HPSE by interacting with HS [25].

HPSE cleavage site is the β (1,4) glycosidic linkage between GlcA and GlcNS in HS chains. Only a limited number of sites are cleaved by HPSE leading to the formation of 5-10kDa HS fragments (10-20 sugar units). The specificity is due to the recognition of a trisaccharide substrate (GlcNS/GlcNAc-GlcA-GlcNS) with a defined HS sulfation pattern (Fig.3) [26]. HPSE exerts its activity also on heparin, generating 5-20kDa fragments [27].

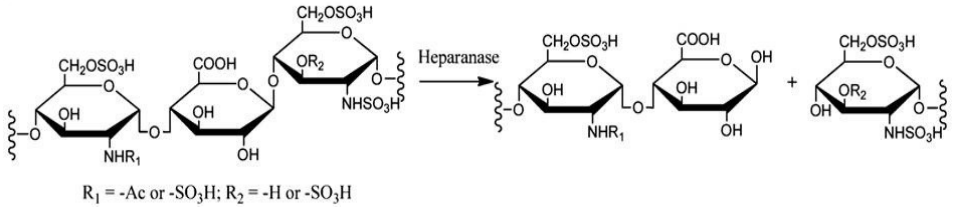

Figure 3. Sequence recognized and cleaved by HPSE in HS. The minimum substrate is a trisaccharide with a specific sulfation pattern. For the trisaccharide substrate recognition, the N-sulfated group on the reducing side and the 6-O-sulfated group on the non-reducing side are essential. Modified from [26].

1.3.1 Heparanase biogenesis and structure

HPSE is a 58kDa dimer of a 50kDa and 8kDa subunits non-covalently linked. HPSE dimer is the result of an intracellular and an extracellular processing which starts in the endoplasmic reticulum where pre-proHPSE is synthesized. This precursor of 543 residues and 68kDa is then processed in proHPSE (65kDa) by the removal of the N-terminal signal peptide (Fig.4a). From the Golgi apparatus,

pro-HPSE is secreted extracellularly. HPSE glycosylation at six predicted sites has been proved to be important for the transport across the endoplasmic reticulum and Golgi apparatus and its final secretion [28]. The conversion of the inactive proHPSE into the active dimeric enzyme requires its re-uptake via endocytosis pathway and its conveyance to lysosomes. In lysosome, cathepsin L protease catalyzes the excision of a 6kDa linker region giving rise to the two subunits that form the mature enzyme (Fig.4a). Several membrane molecules has been demonstrated to mediate the binding and internalization of proHPSE, alone or in cooperation between them. Low-density lipoprotein receptor-related protein and mannose 6-phosphate receptor have been described as high affinity, low abundant HPSE receptors while membrane HSPGs (in particular syndecans) as low affinity, high abundant [29]. However, the molecular mechanism underlying HPSE uptake is unknown yet. A recent study has proposed that syndecan-mediated HPSE endocytosis occurs via clathtrin-coated pits [30]. Moreover, syndecan-1 mediates HPSE internalization through the conserved domain 2 and the variable region of cytoplasmic tail and its interaction with intracellular protein syntenin and α actinin [31]. In Figure 5 the cellular processing and trafficking of HPSE is represented.

HPSE is a member of the glycoside hydrolases 79 (GH79) family and of the larger glycoside hydrolases clan A (GH-A). As the other family members, HPSE requires a proton donor and a nucleophile residues for catalytic mechanism. Glu^{225} and Glu^{343}, both localized in the major subunit, have been identified as the two critical catalytic residues in HPSE. Human HPSE crystal structure has been solved both in apo and in ligand-bound forms [32] (Fig.4b). HPSE is characterized by a $(\beta/\alpha)_8$ domain (a TIM-barrel fold of eight alternating β-strands and α-helices) and a β-sandwich domain of which the 8kDa subunit provides one β sheet of β-sandwich and the first β-α-β motif of $(\beta/\alpha)_8$ domain. $(\beta/\alpha)_8$ domain contains two heparin/HS binding domains (HBDs): HBD1 comprises Lys^{158}-Asp^{162} at the N-terminus of the major subunit while HBD2 (Gln^{270}-Lys^{280}) the fifth α-helix of TIM barrel [33]. The C-terminal domain of the 50kDa subunit (413-Ile^{543} aminoacids) contributes to the remaining β-sandwich and is critical for protein secretion, enzymatic and non-enzymatic activity of HPSE [34].

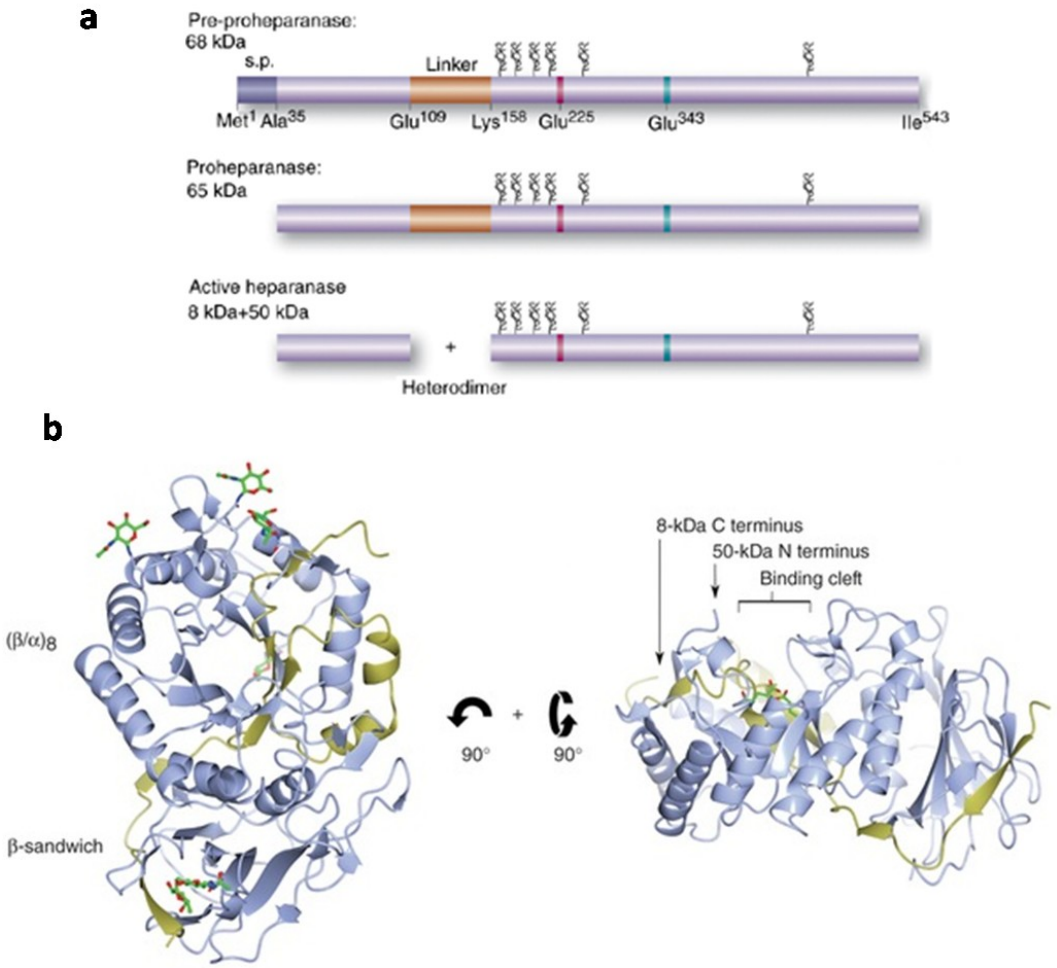

Figure 4. HPSE processing and molecular structure. (a) Schematic representation of pre-proHPSE, proHPSE and active HPSE. HPSE is translated as pre-proHPSE. A signal peptidase generates proHPSE by the excision of the signal peptide (s.p.) spanning Met^{1}-Ala^{35}. In lysosomes, cathepsin L generates active HPSE by the excision of the linker region spanning Glu^{109}-Lys^{158}. Glu^{225}, Glu^{343} and the 6 putative N-glycosylation sites are shown on the major subunit. From [35]. **(b)** Front (left) and side (right) views of HPSE structure. The 8kDa (in yellow) and 50kDa (in blue) subunits are organized to form a (β/α)8 domain and a β-sandwich domain. In the (β/α)8 domain, a cleft contains the HS-binding site. Modified from [32].

1.3.2 Heparanase enzymatic and non-enzymatic activities

Consistent with its primary localization in late endosomes and perinuclear lysosomes, the physiological cellular role of active HPSE is to take part to the degradation and turnover of cell surface HSPGs. However, HPSE localization is not restricted to intracellular vesicles. In response to proper stimuli, mature HPSE

can be secreted. Protein kinase A (PKA) and protein kinase C (PKC) pathways are involved in the excretion process [36]. Extracellular active HPSE contributes to the HSPGs degradation by the cleavage of HS. HPSE-mediated breakdown of HS affects not only the structure of basal membranes and ECM but also the pool of HS-bound ligands which are released in the surrounding environment. In turn, the remodeling of ECM network and the diffusion of cytokines and growth factors facilitate cell motility and promote cell proliferation, angiogenesis and inflammation [14] (Fig.5).

Beside its well-known enzymatic role, it is increasingly emerging that HPSE is a multitasking protein. HPSE functions are not limited to HS cleavage but include also activities which are independent of HS and enzymatic reaction. By the interaction with not-yet identified cell membrane receptor(s), both proHPSE and mature HPSE activate signaling pathways and regulate gene expression associated to several cellular processes (Fig.5). Cell adhesion, migration and angiogenesis are stimulated by HPSE-induced pathways that mainly involve PI3K/Akt, Src and p38 MAPK. HPSE-mediated Akt activation requires RICTOR-mTOR and is promoted by integrins [37]. Efforts are now focused in the identification of the receptor(s) that mediates HPSE non-enzymatic functions. Consistently, it has been recently shown that the receptor that binds HPSE inducing Akt phosphorylation is localized in lipid rafts [30]. Moreover, HPSE signaling is mediated by the C-domain [34].

Given nuclear localization of HSPGs, it is not surprising that also HPSE has been discovered in cell nucleus. Upon lysosome permeabilization and via interaction with the chaperon heat shock protein 90, active HPSE can translocate in the nucleus where it degrades nuclear HS and regulates gene expression [38, 39] (Fig.5). Two different modes of gene expression regulation by HPSE have been described so far: the promotion of HAT activity by the cleavage of nuclear HS [38] and through direct interaction with DNA [40]. HPSE regulates the expression of genes associated to glucose metabolism and inflammation in endothelial cells [38], to differentiation in pro-myeloblast and tumorigenesis in melanoma cell lines [39, 40]. In addition to mature HPSE, also latent proHPSE has been detected in cell nucleus. Moreover, the observation that exogenously added proHPSE can

be translocated in nucleus and converted in the mature enzyme has led to the hypothesis that HPSE processing may occur also in this compartment [41].

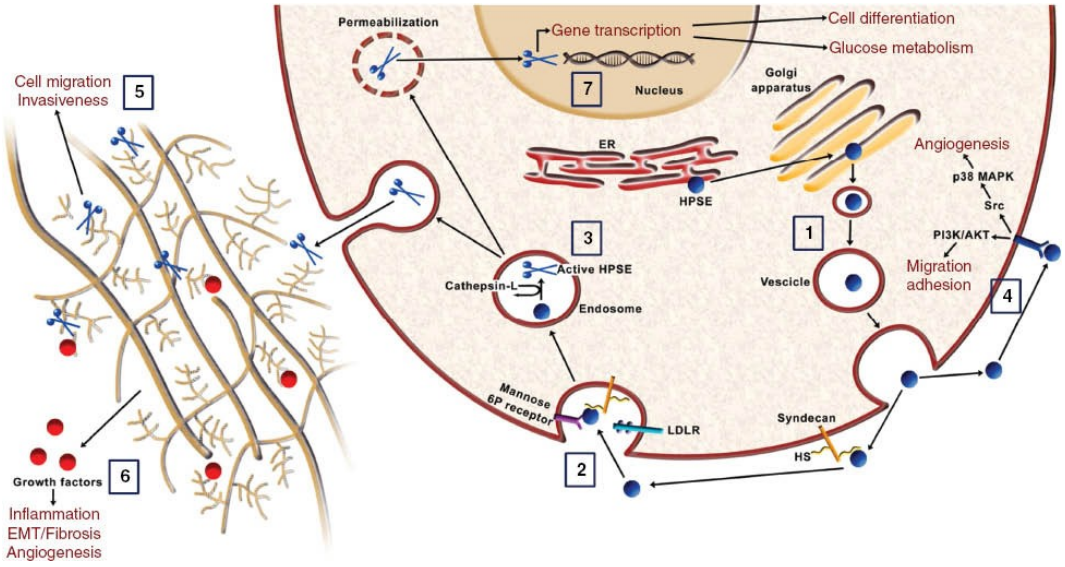

Figure 5. HPSE biosynthesis, trafficking and functions. HPSE is synthesized in the endoplasmic reticulum and secreted from the Golgi apparatus as proHPSE (1). This precursor interacts with different membrane proteins leading to its uptake (2) and converging to endosomes and lysosomes where it is activated by cathepsin L (3). Secreted proHPSE may activate intracellular signaling pathways by the interaction with unidentified receptor/s (4). Secretion of active HPSE occurs in specific conditions. Extracellular active HPSE affects several cellular processes by basement membranes disassembly (5) and HS-bound bioactive molecules release (6). From endosomal permeabilization, HPSE is shuttled in cell nucleus where it affects gene transcription (7). From [42].

1.3.3 Heparanase in physiology

Cellular HPSE expression is tightly regulated to prevent uncontrolled HS cleavage and adverse biological processes. The epigenetic regulation of HPSE gene promoter by methylation [43] and the activity of the wild-type transcription factor p53 [44] inhibit constitutively its expression in most tissues. Thus, HPSE expression is restricted only to keratinocytes, placental trophoblasts, platelets and activated blood-born cells (mast cells and leukocytes) [16, 45].

Enzymatic remodeling of HS is essential in physiological processes that require cell movement and growth factors bioavailability such as embryo development,

hair growth, wound healing and angiogenesis. Consequently, HPSE is involved in all these events [46].

In murine early pregnancy, HPSE increases in uterus and contributes to the tissue remodeling and growth factors release that are necessary for blastocyst implantation and embryo development [47]. In human fetus, HPSE is expressed by liver, skeletal muscle and colon [48]. Interestingly, the expression of HPSE homologous in chick embryo is restricted to the developing nervous and vascular systems [21].

Hair follicle growth is regulated by HPSE both in mouse and human despite its source seems to be different in the two species. In the mouse follicle, HPSE localizes in bulge-derived keratinocytes and helps their migration through the outer root sheath [49]. On the contrary, in human follicle, HPSE localizes in the inner root sheath and controls its differentiation [50]. In a model of skin wound healing, HPSE is required for tissue reorganization by stimulating angiogenesis and keratinocytes migration [51]. HPSE derived from degranulated platelets and immune cells facilitates the interaction of inflammatory cells with the subendothelial membranes and their extravasation as well as blood coagulation [45, 52]. The more recent discovered hemostatic non-enzymatic activity of HPSE is exerted in three main ways: 1) HPSE induces the expression of coagulation tissue factor (TF) in endothelial cells [53]; 2) HPSE induces tissue factor pathway inhibitor (TFPI) expression and release in endothelial cells [54]; 3) HPSE enhances TF activity and increases factor Xa levels [55].

1.3.4 Heparanase in disease

Through HS degradation and non-catalytic mechanisms, HPSE is strongly implicated in several pathological conditions. Up-regulation of HPSE has been demonstrated in tumors, inflammatory and degenerative diseases [42]. In non-physiological conditions, several factors induce HPSE up-regulation: mutated variants of p53, estrogen, reactive oxygen species (ROS), hypoxia, inflammatory cytokines, iperglycemia and albuminuria.

1.3.4.1 Heparanase in cancer

In addition to physiological conditions, it is well-accepted that HPSE sustains angiogenesis and cell migration also in cancer progression, as cancer cells may up-regulate HPSE, thus promoting tumor growth and metastasis. Both HPSE enzymatic and non-enzymatic activities are crucial for cancer progression [56]. The cleavage of HS chains contributes to the disruption of matrix integrity and promotes tumor cell invasion and migration. By its enzymatic activity, HPSE also induces tumor neo-vascularization: on one hand, the disassembly of the subendothelial capillary basal membrane contributes to a favourable environment for endothelial cell sprouting toward the growing tumor; on the other, HSPGs cleavage leads to the release and diffusion of the HS-bound pro-angiogenic factors VEGF-A and FGF-2 [57]. The mechanisms by which HPSE sustains tumor metastasis and angiogenesis are also enzymatic-independent. HPSE directly induces endothelial cell migration via PI3K/Akt pathway [58] and VEGF expression through p38 MAPK phosphorylation and Src activation [59]. p38 signaling pathway has been reported to mediate HPSE induction of TF in tumor cells as well. In this way, HPSE has also a pro-coagulant activity in cancer, which contributes to the pro-thrombotic state of cancer patients [60]. By the cooperation of HS dependent and independent functions, HPSE is an important modulator of syndecan-1 expression, clustering and shedding (heparanase-syndecan-1 axis), which are known to enhance angiogenesis and metastasis, in particular in multiple myeloma. In myeloma cells, HPSE/syndecan interaction results in syndecans clustering and Rac1 activation prior to endocytosis, thus improving cell adhesion and spreading [61]. Secondly, HPSE enhances syndecan-1 shedding through the release of sequestered growth factors which, in turn, induce the expression of the sheddase MMP-9 via ERK signaling pathway [62, 63].

All together, HPSE activities result in extravasation of cancer cells and increased risk of metastasis. In line with this, HPSE expression is elevated in most malignant tumor-derived cell types and primary human tumor biopsies. These includes solid tumors (carcinoma of the colon, thyroid, liver, pancreas, bladder, cervix, breast, prostate, gastric, head and neck) and hematological tumors (multiple myeloma, leukemia and lymphoma). HPSE correlates to tumor size,

microvessel density, metastatic potential and poor prognosis. High HPSE levels are also associated with reduced post-operative survival [64].

Although mutated p53 and hypomethylation contribute for increased HPSE expression in tumors, several transcription factors have been shown to positively regulate HPSE expression in cancer cells. Sp1 and GA-binding protein (GABP) transcription factors control HPSE expression in thyroid tumor cells [65], NF-kB in lung alveolar and gastric cancer cells [66, 67], early growth responce-1 (EGR1) in prostate and bladder cancer cells [68, 69] and Ets1, Ets2 in breast tumor cells [70]. In estrogen receptor-positive breast cancer cells, estrogen is a potent stimulator of HPSE expression, although the transcription factor involved is ignored yet [71].

1.3.4.2 Heparanase in inflammatory diseases

Considering the important roles of HS and heparin in several aspects of inflammation [72], increasing attention has been focused on the modulation of inflammatory reactions by HPSE. Up-regulation of HPSE has been observed in mouse models of delayed-type hypersensitivity [73], chronic colitis [74] and lung injury [75] and in human inflammatory bowel diseases [74, 76] inflammatory lung disease [75], rheumatoid arthritis [77] and atherosclerosis [78]. Inflammation is a defence response to a tissue damage which implies the recruitment of circulating immune cells to the site of injury. Secreted HPSE by neutrophils, activated T-lymphocytes and platelets favours extravasation of immune cells by the remodeling and the increased permeability of subendothelial basement membrane. In addition, HPSE activity affects immunocytes recruitment, the release of cytokines and chemokines and the activation of immune cells [79].

Recent findings on inflammatory diseases of the intestinal tract have pointed HPSE as an important link between inflammation and cancer [80]. Investigating colon tissues from patients with inflammatory bowel diseases (Crohn's disease and ulcerative colitis), it is emerged that HPSE is preferentially expressed by injured colonic epithelial cells. This observation was also confirmed in a mouse model of acute and chronic colitis [74]. In the setting of colitis it seems that epithelial-derived HPSE modulates and sustains chronic activation of inflammatory macrophages by luminal flora. In turn, activated macrophages

further induce epithelial colon cells to express and release HPSE (via TNF-α) and promote its activation by secretion of cathepsin L. This chronic inflammatory circuit creates a tumor-promoting microenvironment which may sustain early steps of colitis-associated carcinogenesis [74]. An inflammatory role of HPSE in diabetic nephropathy has been recently described and resembles that in inflammatory bowel diseases. Overloaded HPSE in the interstitium sustains persistent macrophages activation by diabetic milieu components and a chronic inflammatory microenvironment [81]. The way through which HPSE induces macrophage activation and cytokine release is still under investigation but it seems to be mediated by Toll-like receptors (TLR-2 and TLR-4) [78, 82].
TNF-α-mediated induction of HPSE occurs also in pulmonary endothelial cells in the mouse model of sepsis-associated inflammatory lung disease. Luminal HPSE degrades endothelial glycocalyx and promotes leucocytes recruitment by the uncovering of endothelial adhesion molecules [75].

1.3.4.3 Heparanase in glomerular diseases

HSPGs are important components of barrier basal membranes such as the GBM in the kidney. In glomerulus, this specialized membrane lies between podocytes and endothelial cells. Podocytes, GBM and endothelium form the glomerular filtration barrier that permits the flow of plasma and small solutes and retains high molecular weight proteins. Anionic HSPGs (predominantly agrin and collagen XVIII) contribute to the selectivity of the glomerular filter in a charge-dependent way, creating an electrostatic barrier to anionic plasma proteins such as albumin. Several experimental and human glomerulopathies (diabetic nephropathy, passive Heymann nephritis, puromycin-induced nephrosis, adryamycin-induced nephrosis) are characterized by a decreased content in glomerular HSPGs and a concomitant increase in HPSE expression [35]. Several factors induce HPSE expression in glomerular disease. Aldosterone, angiotensin II and ROS, which mediate progressive renal damage, increase HPSE expression in cultured podocytes [83]. Hyperglycemia contributes to increased HPSE levels in diabetic nephropathy and a glucose-response element has been identified in HPSE gene promoter [84]. As in some cancer cells, glucose-induced EGR1 transcription factor is responsible for HPSE up-regulation in kidney diseases [85]. In

glomerulopathies, HPSE-mediated degradation of HSPGs destabilizes the charge-selective barrier and promotes proteinuria. This is supported by the fact that inhibition of HPSE reduced proteinuria [86, 87] and, on the contrary, HPSE-overexpressing transgenic mice increase proteinuria and do not express HS in the glomerulus [88]. Nevertheless, in the last years different studies have questioning the role of HSPGs in the glomerular charge selectivity and other mechanisms have been postulated for HPSE-induced proteinuria: degradation of HS by HPSE may weaken glomerular cell-GBM interaction and favour lost of podocytes; the release of growth factors and bioactive HS fragments may activate cellular processes that mediate proteinuria; HPSE itself may activate signaling pathways on podocytes and endothelial cells [35].

The involvement of HPSE in diabetic nephropathy pathogenesis is the most documented. Diabetic nephropathy is a major cause of end-stage renal disease. It affects type 1 and type 2 diabetic patients and it is characterized by persistent albuminuria, decreased glomerular filtration rate and hypertension. Both in human biopsies and in the animal model of streptozotocin (STZ)-induced diabetes, HPSE is up-regulated by podocytes and endothelial cells in the glomerulus and by epithelial cells in the proximal tubule and its expression is negatively correlated with that of HS [88]. Increased HPSE levels are also detected in urine of patients with diabetic nephropathy [89] and type 2 diabetes [90]. Consistently with these findings, the treatment with sulodexide (a mixture of 80% LMWH and 20% dermatan sulfate), reduces albuminuria and loss of HS in experimental adryamicin-induced diabetic nephropathy [91] most likely by sulodexide inhibition of HPSE [92]. Moreover, injection with another heparin-derived HPSE inhibitor (roneparstat or SST0001) results in amelioration of albuminuria and serum creatinine level in mice with diabetes [85]. The strongest evidence for the essential role of HPSE in the development of diabetic nephropathy has been provided by inducing diabetes in HPSE-null mice (HPSE-KO). Compared to wild-type mice, HPSE-KO mice fail to develop glomerular damage, albuminuria and mesangial matrix expansion upon STZ administrations [85]. Together with glomerular alterations, another feature of diabetic nephropathy is tubulo-interstitial injury, characterized by peritubular inflammation and fibrosis. Along with glomerular damage amelioration, HPSE-KO mice have also reduced TGF-β

levels, less macrophage infiltration and less tubulo-interstitial fibrosis compared to wild-type mice [85]. In agreement, our recent studies have highlighted the involvement of HPSE in the regulation of TGF-β expression and in the establishment of tubulo-interstitial fibrosis, a process that, beyond diabetic nephropathy, characterized all chronic kidney diseases (discussed in paragraph 1.4.2).

1.4 Fibrosis and heparanase

1.4.1 Overview of parenchymal organ fibrosis

Tissue fibrosis (scarring) is defined as un unregulated wound-healing response characterized by progressive accumulation of ECM and its concomitant decreased remodeling. Common pathways and players characterize fibrosis of different parenchymal organs (e.g. lung, liver, kidney): 1) chronic injuries directed to parenchymal cells are main triggers of fibrosis and cause apoptotic/necrotic cell death; 2) a chronic inflammatory response is activated by injured cells and it is sustained by recruited inflammatory cells (e.g., leukocytes, macrophages and T-cells) and secreted cytokines (interleukins and TNF-α); 3) fibrogenic cells are activated by inflammatory cells and drive the scarring process by the secretion of abundant ECM proteins (predominantly collagens type I and III, fibronectin and laminin); 4) pro-fibrotic factors (TGF-β and FGF-2), produced by inflammatory and fibrogenic cells, are implicated in fibrosis through ECM induction and ECM degradation inhibition; 5) the persistence of chronic injury together with the fact that the synthesis of matrix is not counterbalanced by its resorption, progressively lead to organ architecture destruction and functional impairment [93].

Myofibroblasts are the main fibrogenic cells and source of ECM in fibrosis. Myofibroblasts are highly proliferative cells with contractile feature due to the expression of alpha isoform of smooth muscle actin (α-SMA). The initial consideration that myofibroblasts derive from the activation and proliferation of resident fibroblast has been substituted by the observation that myofibroblast source is variable. Indeed, bone marrow-derived fibrocytes, epithelial cells undergoing epithelial to mesenchymal transition (EMT) and endothelial cells

undergoing endothelial to mesenchymal transition (EndMT) also contribute to the myofibroblast pool [94].

1.4.2 Heparanase in tubulo-interstitial fibrosis

Fibrosis of the renal tubulo-interstitium is the pathological process of ECM accumulation that characterizes chronic kidney disease. The tubulo-interstitium comprises the tubular epithelium, the vasculature and the interstitium which, in turn, includes fibroblasts and immune cells. Activated interstitial fibroblasts, are the main players of the fibrogenic response by the synthesis of abundant ECM proteins [95].

The fact that HPSE expression increases in the tubulo as well as in the glomerulus in diabetic nephropathy [88] and the less extensive tubulo-interstitial fibrosis in diabetic HPSE KO mice [85], have put the attention of our research to the possible role of HPSE also in tubular injury. In chronic kidney diseases, tubular cells are subjected to different influences from the glomerular effluent and the interstitium. High glucose levels, albuminuria and advance glycosylation end products (AGEs) are responsible of tubular injury in diabetes and all these factors stimulate HPSE expression in renal tubular cells *in vitro* [84, 96]. Moreover, a thorough study of the pathway involved has led to the identification of PI3K/Akt as the signaling cascade activated by albuminuria and AGEs [96]. Increased HPSE activity at tubular level has been demonstrated to regulate EMT of proximal tubule cells, an important source of myofibroblasts in tubulo-interstitial fibrosis [97]. In the process of transdifferentiation into myofibroblast-like cells, tubular cells undergo four key events: 1) loss of epithelial marker (E-cadherin) and cell polarity; 2) expression of mesenchymal markers (i.e. α-SMA, vimentin, fibronectin); 3) degradation of tubular basement membrane by MMPs; 4) migration into the interstitium [98]. In the onset of fibrogenesis, tubular injury attracts immune cells that, once activated, release FGF-2 and TGF-β which are the main pro-fibrotic triggers of tubular EMT [99, 100]. By regulating the availability and activity of these growth factors, HPSE promotes tubular EMT. *In vitro* demonstration of the inhibition or delay of tubular EMT following HPSE gene silencing, provides evidence for the role of HPSE in this process [101, 102]. In addition, FGF-2 and TGF-β induce HPSE expression in tubular cells, thus

creating an autocrine loop that sustains EMT. In response to FGF-2, HPSE-silenced cells do not up-regulate mesenchymal markers (α-SMA, vimentin, fibronectin), do not increase the expression and activity of MMPs and do not migrate [101]. Regarding TGF-β, all these events are delayed in the absence of HPSE. HPSE also regulates the induction of TGF-β expression by pro-fibrotic stimuli [102]. The precise mode of action of HPSE in regulating EMT has not been fully characterized. However, it is reasonable to think that it involves the HS turnover and the expression of cell surface HSPGs. In fact, HPSE silenced tubular cells up-regulate syndecan-1 that sequesters FGF-2 from receptor binding. Moreover, HPSE cooperates with MMP-9 to the shedding of syndecan-1 and the release of HS-FGF-2 fragments which are potent activators of FGFR1 [101]. As already mentioned in paragraph 1.3.4.2, a chronic inflammatory condition is fostered by HPSE in diabetic nephropathy. Latent HPSE secreted by injured glomerular and tubular cells in the interstitium may be also activated by up-regulated tubular cathepsin L and modulate the activation of inflammatory macrophages. Activated macrophages produce pro-fibrotic growth factors which, in turn, stimulate HPSE expression (Fig.6).

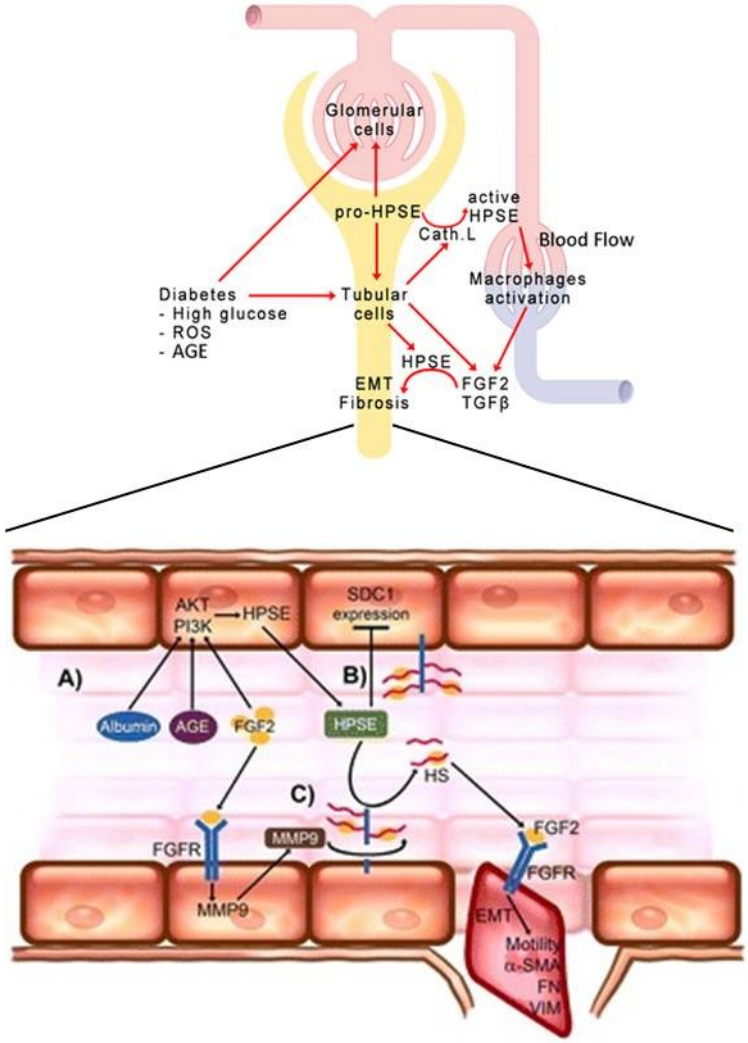

Figure 6. HPSE regulation and activity in kidney inflammation and fibrosis. In the interstitial milieu of diabetic nephropathy, overloaded HPSE produced by glomerular and tubular cells helps the activation of macrophages and triggers tubular EMT. In the tubule, different pro-fibrotic factors acting on epithelial cells, up-regulate HPSE (A), which, once secreted, regulates the bioavailability and activity of HS/FGF-2 and the expression of syndecan-1 (SDC-1) (B). FGF-2 induces an autocrine loop through the induction of HPSE and MMP-9 which cooperate to the shedding of syndecan-1 (C). Modified from [97].

1.4.3 Heparanase in chronic liver disease

1.4.3.1 Chronic liver disease

Chronic liver injury of any etiology is characterized by progressive fibrosis which culminates in cirrhosis and organ failure. Cirrhosis is the leading cause of hepatocellular carcinoma (HCC). Viral hepatitis B or C, alcohol abuse, non-

alcoholic steatohepatitis (NASH), autoimmune hepatitis, cholestatic disorders and metabolic dysfunction are the prevalent causes of liver fibrosis/cirrhosis. Common risk factors are genetic polymorphisms, obesity and age. Regardless the etiology, a protracted injury directed to hepatocytes and/or cholangiocytes causes the activation of an inflammatory and pro-fibrogenic response which drives hepatic fibrosis. Progression to cirrhosis is accompanied by architectural and vascular distortion and aberrant hepatocytes proliferation with the formation of regenerative nodules surrounded by fibrotic septa. Cirrhosis leads to reduced liver function and increased risk of hepatocellular carcinoma (HCC). While early fibrosis can resolve following damage resolution, cirrhosis can only incompletely regress and liver transplant is the only treatment for end-stage liver disease [103] (Fig.7).

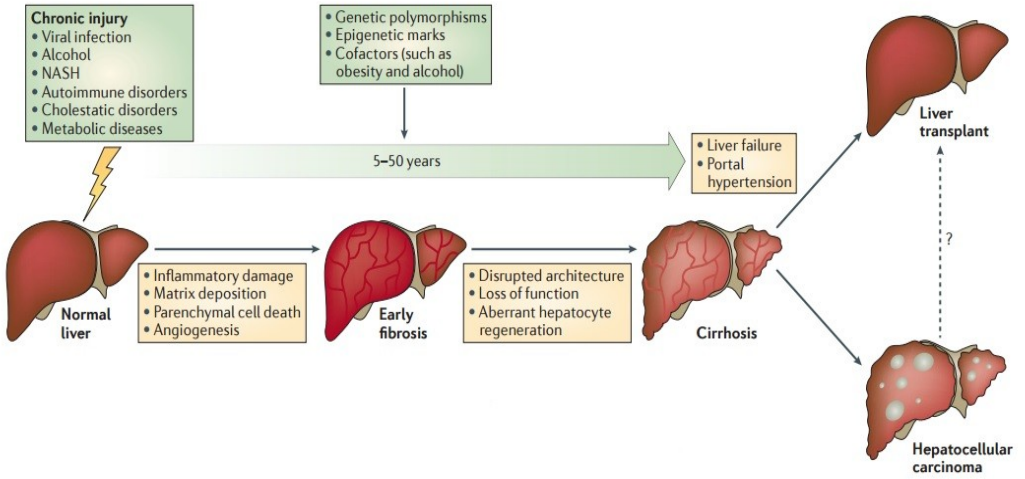

Figure 7. Chronic liver disease progression from early fibrosis to cirrhosis and HCC. Multiple etiologies and risk factors lead to liver fibrosis and sustained fibrogenesis leads to cirrhosis. The excessive ECM deposition disrupts hepatic architecture and vasculature and results in hepatic insufficiency and portal hypertension. Modified from [103].

Liver injury causes parenchymal cell death. Apoptotic bodies, damage-associated molecular patterns (DAMPs), ROS and inflammatory mediators, which are released upon cell apoptosis/necrosis, mediate leucocytes and monocytes recruitment and resident liver macrophages (Kupffer cells) and fibrocytes (hepatic stellate cells) activation [104]. Activated Kupffer cells and hepatic stellate cells (HSCs) are the main cell types involved in the pathogenesis of liver fibrosis.

Kupffer cells promote inflammatory and fibrogenic responses by the release of cytokines, chemokines and growth factors that exacerbate the inflammation and participate to the activation of HSCs, a central event during liver fibrosis. HSCs (also known as Ito cells) are the pericytes of the liver, which resident in the perisinusoidal space between endothelial cells and hepatocytes (space of Disse). They contain vitamin-A lipid droplets and express desmin and the neural marker glial fibrillary acidic protein (GFAP). In normal liver, HSCs functions range from retinoid storage and lipid metabolism to drug detoxification and immunotolerance [105]. In injured liver, quiescent HSCs undergo transdifferentiation into fibrogenic myofibroblasts-like cells and maintain their activated status in response to paracrine and autocrine stimulations. This process implies the loss of lipid droplets and GFAP, *de novo* α-SMA expression, enhanced contractility, proliferation, fibrogenesis and migration. The fibrogenic role of activated HSCs resides in their acquired ability to synthesize and secrete large amount of ECM proteins (mainly collagens and fibronectin) which progressively accumulate in the tissue. [106] (Fig.8). Early changes in gene expression and phenotype occur in the initiation phase of activation, from paracrine stimulation by neighbouring cells (pro-fibrotic factors derived from sinusoidal endothelium and Kupffer cells and lipid peroxides from hepatocytes). Changes in cell behaviour occur in the perpetuation phase of activation, from both paracrine and autocrine stimulations. HSCs self-sustain activation by the secretion of pro-inflammatory and pro-fibrogenic molecules. TGF-β is the most potent stimulus for the synthesis of collagen type I and ECM proteins while cellular proliferation is mainly driven by PDGF, FGF-2, EGF and VEGF mitogens. The development of fibrosis derives not only from matrix synthesis but also from unbalanced matrix degradation. TGF-β-activated HSCs express tissue inhibitors of MMPs (mainly TIMP-1 and TIMP-2) which promote scar accumulation by inhibiting the matrix degradation activity of MMPs. However, the expression of degradative MMPs upon HSCs activation is also modulated and it is dictated by the necessity to remodel surrounded tissue prior to migration and ECM deposition [107]. Several MMPs are expressed by early activated cells (i.e. MMP-13 and MMP-3) [108]

Activated HSCs are the major but not unique producers of fibrotic ECM in injured liver. Myofibroblasts derive also from portal fibroblasts and fibrocytes while the contribution of EMT in hepatic fibrogenesis is still debated [109].

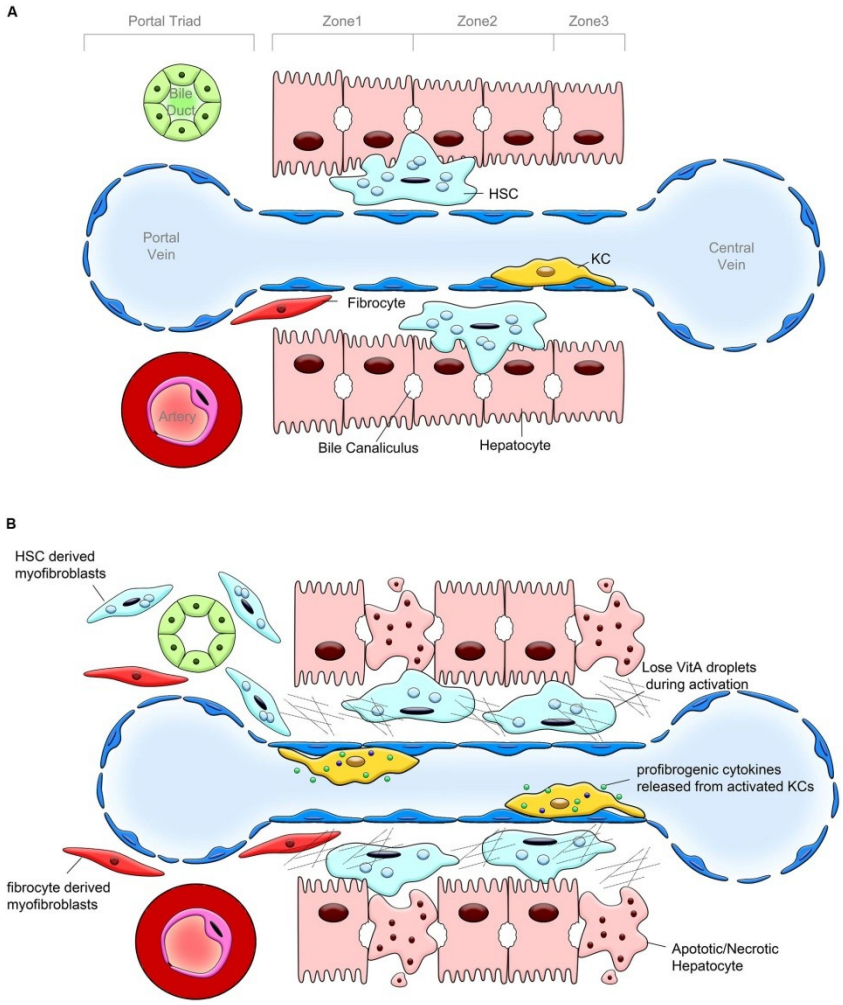

Figure 8. Liver alterations after injury. (a) Healthy liver. The hepatic lobule comprises a central vein surrounded by portal trials each composed of a bile duct, a portal vein and an arteriole. Blood flows from the portal vein into the central vein through hepatic fenestrated sinusoids. Hepatocytes are functionally divided in three zones according to the distance from the arteriole. HSCs reside in the space of Disse, between hepatocytes and sinusoids. Kupffer cells (KC) are found within the lumen of sinusoids. **(b)** Injured liver. Following liver injury, hepatocytes undergo apoptosis/necrosis and activate Kupffer cells which release inflammatory and fibrogenic mediators. HSCs undergo activation enhancing contractility, proliferation and secreting large amount of ECM proteins. To a lesser extent, fibrogenic myofibroblasts derive also by portal fibroblast and bone marrow-derived fibrocytes. Another consequence of injury is the defenestration of sinusoids. From [110].

1.4.3.2 Heparanase in HCC and fibrosis

Although HPSE is widely expressed during human embryonic liver development, it is weakly expressed in mature healthy liver [48] and it has been found to be up-regulated during liver regeneration and in HCC. Regarding liver regeneration, increased HPSE expression has been observed in a rat model of partial hepatectomy. Interestingly, HPSE does not increase linearly during liver regeneration but it reaches a peak of expression after 12 hours and after 7 days post-surgery. HPSE cellular localization changes as well, from a diffuse hepatocyte cytoplasm pattern at early phase of regeneration to a peripheral distribution at later time [48]. A stimulatory effect on hepatocytes and endothelial cells proliferation has been demonstrated by exogenously injected HPSE following partial hepatectomy [111].

The role of HPSE as a pro-metastatic and generically pro-cancerous agent has been widely characterized in liver cancer. Several studies have reported the up-regulation of HPSE by cancer cells in liver tissues from patients with HCC. Moreover, HPSE positively correlates with tumor stage, tumor size, portal vein invasion, tumor invasiveness and microvessel density [112, 113]. Although conflicting data about HPSE gene expression in HCC are actually emerging [114], significant clinical benefits have been demonstrated for the heparanase inhibitor PI-88 (phosphomannopentaose sulfate) in different phase II trials for HCC recurrence after surgical resection [115, 116] and thus PI-88 is actually under phase III trial. Regarding non-cancerous chronic liver disease, HPSE involvement is poorly understood thus far and controversial results have been obtained both from human tissues and from animal models of liver fibrosis [42]. The comparison performed by Xiao et al. on HPSE expression in normal, cirrhotic and cancer livers has revealed a non significant different in mRNA and protein levels between normal and cirrhotic tissues as opposed to the increased levels in HCC tissue. From these observations, they conclude that HPSE participates in the late steps of carcinogenesis but not in pre-cancerous fibrosis/cirrhosis [112]. Surprisingly, the Japanese research group of Ikeguchi has found a decrease amount of HPSE mRNA in HCC tumors compared to adjacent non-cancerous tissue. Moreover, HPSE expression in non-cancerous tissue negatively correlates with fibrosis stage [114]. Increased HPSE protein levels have been also observed

in the liver of thioacetamide-treated fibrotic rats despite discordant results regarding the fibrogenesis stage of the up-regulation. Goldshmidt *et al*., have induced fibrosis in rats through injection of thioacetamide for 2, 4 and 8 weeks. Hepatic HPSE protein levels increased at early stage of the disease (2 weeks of treatment) but declines in 4 and 8 week fibrotic livers [48]. In their model of thioacetamide-induced fibrosis, Ohayon and colleagues obtained opposite results. Treating rats for 1, 3 and 6 weeks, HPSE decreased at early stage of injury (1 and 3 weeks of treatment) and rised almost 2-fold in 6 week treated rats compared to controls [117]. Notably, the same rat strain and injected thioacetamide concentration have been used in the two studies.

2. Aims

Through degradation of HS chain and HS-independent functions HPSE regulates several physiological and pathological processes. HPSE expression, which is limited in normal tissues, becomes deregulated in major human disease and it is not surprising that several HPSE inhibitors have entered clinical trials. HPSE is primarily involved in cancer metastasis and angiogenesis, diabetic nephropathy, atherosclerosis and inflammatory disorders. Among the last, the role of HPSE in inflammatory bowel diseases and in kidney inflammation and fibrosis have been deeply investigated [74, 81, 97]. From these studies, a pro-inflammatory and a pro-fibrogenic role has emerged for HPSE. Both in kidney and bowel, HPSE sustains inflammation by enhancing macrophage activation. Moreover, in an effort to investigate the contribution of HPSE in kidney tubulo-interstitial fibrosis, our research group has discovered an interesting role for HPSE in regulating the transition of tubular epithelial cells into myofibroblast fibrogenic cells.

Although some works have investigated the expression of HPSE in injured livers [48, 117], these data are limited and discordant and HPSE involvement in chronic liver disease is still unknown. The conservative cascade of events and pathways that are involved in parenchymal organ chronic diseases and the necessity to identify common pharmacological targets, led us to focus on HPSE in liver fibrosis. According to this, the major intent of our investigation was to shed light on the possible involvement of HPSE in chronic liver diseases. In particular, with this work, we aimed at: i) investigating whether increased hepatic HPSE expression occurred during chronic liver disease; ii) studying the mechanism of HPSE up-regulation upon hepatic injury; iii) addressing the effects of HPSE up-regulation on fibrogenesis; iv) investigating HPSE activity in plasma of patients with chronic liver disease.

3. Materials and methods

3.1 Carbon tetrachloride - induced liver fibrosis in mice

The hepatotoxin carbon tetrachloride (CCl_4) was used for the experimental induction of liver fibrosis in mice. Single dose or repeated CCl_4 administration is a widely used toxic-induced model of acute and chronic liver injury respectively. The hepatotoxicity of CCl_4 results from its conversion in free radical products. In hepatocytes, CCl_4 is metabolized by cytochrome P-450 2E1 (CYP2E1) into the highly reactive trichloromethyl radical (CCl_3^-) that triggers lipid peroxidation and alter plasma and mitochondria membranes permeability. Due to the prevalent expression of CYP2E1 by centrilobular zone 3 hepatocytes, CCl_4 leads to massive centrilobular necrosis and inflammation. Chronic CCl_4 administration results in fibrosis and micronodular cirrhosis [118].

3.1.1 Animals

Animal studies followed the guidelines of the National Institutes of Health (CEASA protocol number 108288/2013, approved by the Ethics Committee of the University of Padova, Italy).

Male Balb/cJ mice from breeding colony, 6 weeks old, were maintained in a pathogen-free and temperature-controlled environment at 12h light/dark cycle and were fed with a standard rodent diet (Mucedola s.r.l.) with water a*d libitum*.

3.1.2 Experimental design

A total of 20 mice were randomly divided into CCl_4 -treated (n=12) and control (n=8) groups. Animals were intraperitoneally (i.p.) injected with a mixture of CCl_4 in olive oil, at a dose of 1,2µl/g body weight twice a week and sacrificed after 1, 2, 8 and 12 weeks from the beginning of the treatment. Control mice received no treatment. Animals (2 controls and 3 treated mice at each time point) were sacrificed by cervical dislocation 72 hours after the last injection (washout). After a rapid perfusion with PBS via portal vein to clean from blood, livers were collected and sectioned. The left lobe was immediately fixed in phosphate-buffered 10% formaldehyde for histology and immunostaining. The median lobe was collected in RNase-free tubes and snap-frozen in liquid nitrogen for RNA/protein extraction and molecular biology analyses (Fig.9).

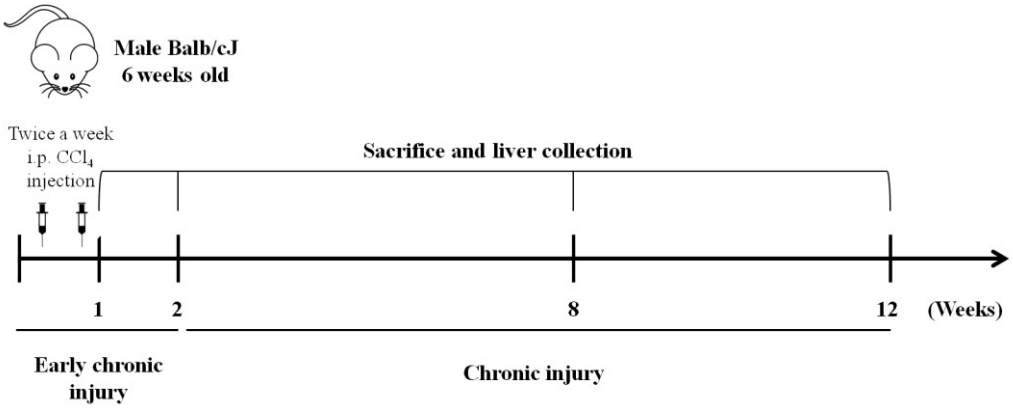

Figure 9. Experimental design of CCl_4-induced chronic liver injury. Male Balb/cJ mice were i.p. injected with CCl_4 twice a week for 1 and 2 weeks to induce early chronic injury and for 8 and 12 weeks to induce advance chronic injury. At each time-point, mice were sacrificed after a washout of 72 hours from the last injection.

3.1.3 Histopathology and immunostaining

Each formaldehyde-fixed sample was embedded in paraffin and cut into 5µm thick sections on a microtome. For paraffin inclusion, tissues were dehydrated through a series of graded ethanol to displace water, cleared in xylene and then embedded in paraffin blocks at 60°C. After deparaffinization and rehydration, Hematoxylin-Eosin and Azan-Mallory stainings were performed on liver sections. Immunohistochemistry and immunofluorescence stainings for proteins of interest were also performed. The entire protocols for paraffin inclusion and deparaffinization are shown in Table 1.

Table 1. Paraffin and deparaffinization protocols used in histopathology and immunostaining.

Paraffin inclusion		**Deparaffinization**	
EtOH 25%	2 x 10 min	Xylene	3 x 10 min
EtOH 50%	2 x 30 min	Xylene/EtOH (1:1)	10 min
EtOH 70%	2 x 60 min	EtOH 100%	2 x 10 min
EtOH 95%	overnight	EtOH 95%	10 min
EtOH 100%	2 x 60 min	EtOH 70%	10 min
Xylene	2 x 60 min	H_2O mQ	10 min
Paraffin	2 x 60 min		

3.1.3.1 Hematoxylin-Eosin staining

Hematoxylin-Eosin (H-E) staining was used for the histopathological examination of mouse livers. Deparaffinized liver sections were treated for 30 seconds with hematoxylin. After recovering the reagent, slices were rinsed with dH_2O to remove the excess of hematoxylin and with tap water to allow stain to develop. Then, slices were incubated with eosin Y solution (0.5% in water, acidified with acetic acid) for 1 minute. After washes with dH_2O and tap water, sections were dehydrated in increasing concentration of ethanol (70% for 5 seconds, 95% for 5 seconds, 100% for 2 minutes) and xylene for 5 minutes. Cover slips were mounted using Pertex®.

3.1.3.2 Azan-Mallory trichrome staining

Azan-Mallory trichrome (modified by Heidenhain) was used to assess the extent of induced fibrosis by the selective staining of collagen fibers. Deparaffinized slices were first incubated in Azocarmine G solution (0,1% azocarmine G, 1% acetic acid in dH_2O) at 50°C for 1 hour. After cooling and washing in dH_2O for 5 minutes, differentiation was performed with 0.1% aniline oil in ethanol 60%. Then slices were washed in 1% glacial acetic acid in ethanol 95% and incubated from 1 to 3 hours in 5% phosphotungstic acid in dH_2O. After wash, slices were incubated from 1 to 3 hours in Mallory solution (0.5% methyl blue, 2% orange G, 2% ossalic acid in dH_2O) diluted 1:3 in dH_2O. Finally, sections were washed in dH_2O and dehydrated in increasing concentration of ethanol (70% for 5 seconds, 95% for 5 seconds, 100% for 2 minutes) and xylene for 5 minutes. Cover slips were mounted using Pertex®.

3.1.3.3 Immunohistochemistry

For immunohistochemistry (IHC) analysis, after deparaffinization, antigen unmasking was carried out by heating slices in sodium citrate buffer (10mM sodium citrate, 0.05% Tween-20, pH 6), in a microwave oven twice for 5 minutes. Slices were left 30 minutes at room temperature (RT) and washed 3 times for 5 minutes in dH_2O. Blocking of endogenous peroxidase was performed by incubation with 0.3% H_2O_2 for 10 minutes. Slices were washed twice with dH_2O and once in Tris-buffered saline with 0.1% Tween-20 (0.1% TBST) 5 minutes

each. Sections were circled with PapPen and saturated with blocking solution (TBST supplemented with 5% goat serum) for 90 minutes at RT. Sections were incubated with primary antibody anti-HPSE (Santa Cruz) diluted 1:300 in antibody buffer (TBST, 2.5% goat serum) overnight at 4°C. Then, slices were rinsed three times with TBST for 5 minutes and incubated with the biotinylated goat anti-rabbit IgG secondary antibody (1:200 in antibody buffer) for 30 minutes at RT. After incubation, slices were washed three times with TBST for 5 minutes and incubated with the Avidin-Biotin Complex (ABC) for 30 minutes following by three washes with TBST for 5 minutes. For signal detection, enzymatic reaction was developed by adding diaminiobenzidine (DAB) substrate for 2 minutes and washing in dH_2O. After hematoxylin counterstaining for 2 minutes and two washing in tap water for 5 minutes, sections were dehydrated in increasing concentration of ethanol (80% for 5 minutes, 95% for 5 minutes, 100% for 5 minutes) and xylene for 15 minutes. Cover slips were mounted using Entellan.

3.1.3.4 Immunofluorescence

For immunofluorescence (IF) analysis, after deparaffinization, antigen unmasking was carried out by heating slices in a microwave oven in sodium citrate buffer (10mM sodium citrate, 0.05% Tween-20, pH 6), twice for 5 minutes. Slices were left 30 minutes at RT and washed three times for 5 minutes in dH_2O. Slices were circled with PapPen and maintained 5 minutes in PBS. Tissues were permeabilized with 0.2% Triton X-100 in PBS for 10 minutes at RT and washed twice for 5 minutes with PBS. Saturation was carried out by incubating in PBS supplemented with 1% BSA and 0.1% Triton X-100 for 1 hour at RT. Slices were incubated overnight at 4°C with the primary antibody in a humid chamber. Antibody were diluted in PBS supplemented with 1% BSA and 0.3% Triton X-100 as reported in Table 2. When a double immunofluorescence staining was performed, slices were incubated with a mix of the two antibodies overnight at 4°C. The following day, slices were washed with PBS three times for 5 minutes and incubated with the secondary antibody for 1 hour at RT at the concentrations listed in Table 2. Following three washes with PBS for 5 minutes, nuclei were counterstained with Hoechst diluted 1:1000 in PBS for 20 minutes at RT. Finally,

sections were washed three times for 5 minutes with PBS and mounted using Fluoromount aqueous mounting medium. Immunofluorescence images were acquired using confocal microscope Leica TCS SP5. Z-stacks imaging was performed using 40x and 63x immersion objectives. Laser excitation line, power intensity and emission range were chosen accordingly to each fluorophore in order to minimize bleed-through.

Table 2. List of primary and secondary antibodies used for immunofluorescence on liver tissues.

	Target	Company	Host species	Dilution
Primary antibody	HPSE	Santa Cruz	rabbit	1:50
	F4/80	Abcam	chicken	1:50
	CD-68	eBioscience	rat	1:50
	TNF-α	Santa Cruz	goat	1:50
	α-SMA	Sigma-Aldrich	mouse	1:100
Secondary antibody	anti-rabbit Alexa 488	Thermo Scientific	goat	1:300
	anti-chicken Alexa 568	Thermo Scientific	goat	1:300
	anti-rat Alexa 568	Abcam	goat	1:300
	anti-goat Alexa 633	Thermo Scientific	donkey	1:300
	anti-mouse Alexa 594	Abcam	goat	1:300

3.1.4 Gene expression analysis

3.1.4.1 RNA isolation

Total RNA from liver tissue was extracted using TRIzol reagent (Sigma-Aldrich), according to the manufacturer's instructions. Briefly, liver lobe was weighed and homogenized in TRIzol (1mL per 50-100mg of tissue sample) with TissueLyserII (Quiagen) homogenizer. After addition of 200µL chloroform per 1mL TRIzol, the tube was centrifuged at 12000 x g for 15 minutes at 4°C and the upper aqueous phase containing RNA removed into a new microtube. For RNA precipitation, 500µL isopropanol per 1mL TRIzol was added. The tube was centrifuged at 12000 x g for 10 minutes at 4°C and the supernatant was discarded. The RNA pellet was washed twice with 1mL ethanol 75% and centrifuged at 7600 x g for 5

minutes at 4°C. After air-drying, the pellet was diluted in RNase-free water and stored at -80°C. The concentration and purity of RNA were determined using a Nanodrop Spectrophotometer (Thermo Scientific). Absorbance ratios at 260/280nm and 260/230nm were used to assess the purity of the samples.

3.1.4.2 First-strand cDNA synthesis

First-strand cDNA was generated using SuperScript II Reverse Transcriptase (Invitrogen) according to the manufacturer's instructions. 500ng of total RNA were mixed with 1µL dNTPs Mix (10mM each), 1µL random examer primers and RNase-free water to a 6µL final volume. To denature RNA and to allow the primers annealing, the mix was incubated at 65°C for 5 minutes and immediately cooled on ice. Then the following components were added: 2µL 5X First-Strand buffer (250mM Tris-HCl pH 8.3, 375mM KCl, 15mM $MgCl_2$), 1µL DTT 0.1M, 0.5µL SuperScript II Reverse Transcriptase and 0.5µl RNase-free water. This 10µL reaction mix was incubated at 25°C for 10 minutes, 42°C for 50 minutes, and 70°C for 15 minutes. cDNA was stored at -20°C until use.

3.1.4.3 Real time RT-PCR

Quantitative real time reverse transcriptase-polymerase chain reaction (real time RT-PCR) was performed on the ABI 7900HT Fast system (Applied Biosystem) using a SYBR-Green Master Mix (BIOLINE). Each reaction mix (10µL total volume) was prepared as reported in Table 3. The following PCR conditions (2-step cycling) were used: polymerase activation at 95°C for 2 minutes followed by 40 cycles of 95°C for 5 seconds (denaturation) and 60-62°C for 30 seconds (combined annealing/extension). To confirm the specificity of the reactions, dissociation curves between 60°C and 95°C were constructed and analyzed for each primer pair. For the determination of the relative concentration, gene expression was normalized to the level of a ubiquitously expressed gene (GAPDH) and quantified by the $\Delta\Delta C_T$ method (ΔC_T target-ΔC_T reference). All reaction were performed in duplicates for each sample. Primers used for real time RT-PCR are listed in Table 4.

Table 3. Real time RT-PCR reaction mix.

Reagent	Volume
2X SensiFAST SYBER Hi-ROX Mix	5µL
forward primer (5µM)	0.4µL
reverse primer (5µM)	0.4µL
cDNA template (4ng/µL)	2µL
H_2O	2.2µL

Table 4. Primers used for real time RT-PCR on total RNA from liver extracts.

Gene	Primer Sequences (5'-3')	Product length (bp)
GAPDH	Forward: GGCAAATTCAACGGCACAGT	84
	Reverse: GTCTCGCTCCTGGAAGATGG	
HPSE	Forward: GTTCCTGTCCATCACCATCGA	72
	Reverse: CTTGGAGAGCCCAGGAAGGT	
TNF-α	Forward: CATCTTCTCAAAATTCGAGTGACAA	175
	Reverse: TGGGAGTAGACAAGGTACAACCC	

3.1.5 Western blot

Snap-frozen liver tissues were homogenized in RIPA buffer (150mM NaCl, 1% Triton X-100, 0.5% Sodium deoxycholate, 0.1% SDS, 50mM Tris-HCl pH 8) supplemented with protease inhibitor cocktail using TissueLyserII (Quiagen) homogenizer. Lysates were maintained at constant agitation for 2 hours at 4°C and centrifuged for 20 minutes at 12000 rpm at 4°C. Supernatants were collected and transferred in new tubes. Protein concentration was determined using the bicinchoninic acid (BCA) assay. Protein aliquots were frozen at -80°C until use. For electrophoresis, equal protein amounts (20µg) were prepared in loading Laemmli buffer and boiled at 100°C for 10 minutes. Proteins were separated by SDS-PAGE on 10% acrylamide gel at 100V in running buffer (25mM Tris, 190mM glycine, 0.1% SDS). An electrophoresis marker was used to monitor the progress of the run and to check sample molecular weight. Proteins were then

electro-transferred to a 0.45µm nitrocellulose membrane at 350mA in transfer buffer (25mM Tris, 190mM glycine, 20% methanol) for 2 hours. Membranes were blocked with 5% non-fat milk in 0.1% TBST and incubated overnight at 4°C with primary antibody in antibody buffer (2.5% non-fat milk in TBST). After three washes of 10 minutes with 0.1% TBST, membranes were incubated with the HRP-conjugated secondary antibody for 90 minutes at RT. Primary and secondary antibodies dilution are reported in Table 5. After three washes of 10 minutes with 0.1% TBST, membranes were incubated with home-made ECL. Signal detection was performed on Uvitec Cambridge. For densitometry analysis ImageJ software was used.

Table 5. Primary and secondary antibodies used for Western Blot on liver tissue lysates.

	Target	Company	Host species	Dilution
Primary antibody	GAPDH	Santa Cruz	rabbit	1:1000
	HPSE	Santa Cruz	rabbit	1:500
Secondary antibody	anti-rabbit IgG HRP	Santa Cruz	goat	1:1000 - 1:2000

3.2 Cell culture

For this work, both primary isolated cell and cell line were used. Cells were grown in a humidified atmosphere, at 37°C and 5% CO_2. For cryopreservation, cell were harvested at 1200 rpm and resuspended in 1mL growth medium supplemented with 50% Fetal Bovine Serum (FBS) and 10% DMSO. Cells were collected in cryovials and stored in liquid nitrogen. For recovering, vials were rapidly thawed at 37°C. Cells were transferred in a tube, diluted in complete medium and centrifuged at 1200 rpm for 5 minutes. Cell pellets were resuspended in complete medium and dispensed.

3.2.1 Primary isolated cells

3.2.1.1 Kupffer cells

Primary Kupffer cells were isolated from adult male Wistar rats according to the method described by Kitani *et al*., [119]. Immediately after sacrifice, rat liver was collected and all the steps of isolation were performed *in vitro*. Extracted livers were washed from blood through PBS perfusion and digested with collagenase at 0.12U/mL in Gey's Balanced Salt Solution (GBSS) for 1 hour at 37°C. After stopping the enzymatic digestion with cold PBS, the cell suspension was filtered using a 50µm cell strainer to remove connective and undigested tissue and centrifuged at 50 x g for 5 minutes (without brake) to pellet parenchymal cells. The supernatant was discarded and the cell pellet was resuspended in DMEM-HG and centrifuged again. This step was repeated twice. The hepatocyte-rich cell pellet was finally resuspended in DMEM-HG supplemented with 10% FBS, 1% penicillin/streptomycin (P/S), 100µM β-mercaptoethanol and 10µg/mL insulin and seeded in three T-75 culture flasks. After 12-15 days of cultures, round macrophages were grown on the parenchymal cell sheet and were gently resuspended by shaking the flask for 30 minutes at 37°C. To remove contaminant cells, medium was transferred to a non-tissue culture Petri dish in which Kupffer cells are selectively able to attach. After 30 minutes, cells were detached from the dish with trypsin and plated in tissue culture multi-well plates. Kupffer cells were cultured in DMEM-HG supplemented with 10% FBS and 1% P/S. The purity of isolated Kupffer cells was determined by immunofluorescence staining of ED1 (CD68). For activation, cells were serum starved overnight in 0.5% FBS and treated with LPS (1µg/mL) and TNF-α (20ng/mL) for 6 hours. After treatment, total RNA was extracted and expression of interested genes was analyzed.

3.2.1.2 Hepatic stellate cells

Primary HSCs were isolated from male Wistar rats combining two well-standardized protocols. After sacrificed, extracted livers were washed from blood with PBS perfusion and digested with collagenase solution (0.12U/mL in GBSS) for 1 hour at 37°C. After stopping the enzymatic digestion with cold PBS, the cell suspension was filtered using a 50µm cell strainer and centrifuge at 50 x g for 5

minutes (without brake) to pellet parenchymal cells. The supernatant (containing HSCs) was aspirated and fractioned on a density gradient of OptiPrep (60% iodixanol) prepared as followed: cell suspension in 17% iodixanol on the bottom of the tube, 11.5% iodixanol in the middle and GBSS on the top. After centrifuging at 1400 x g for 17 minutes (without brake), cells were collected at the interface between GBSS and the 11.5% iodixanol solution. Isolated cells were seeded on uncoated plastic plates to induce spontaneous activation and were maintained in DMEM-HG supplemented with 20% FBS. After 48 hours, medium was replaced with DMEM-HG supplemented with 10% FBS and 1% P/S. The purity of isolation was assessed by desmin immunopositivity. For immunofluorescence analysis, freshly isolated cells were seeded on uncoated coverslips. Morphologic features of isolated HSCs were periodically examined by means of phase-contrast light microscopy. RNA isolation and gene expression analysis through PCR and real time RT-PCR were performed at different days post isolation.

3.2.2 Cell lines

3.2.2.1 U937

U937 is a human monocyte cell line derived from histiocytic lymphoma. U937 suspension monocytes can differentiate in adherent macrophages in the presence of phorbol myristate acetate (PMA). U937 monocytes/macrophages were cultured in RPMI-1640 medium supplemented with 10% FBS, 2mM L-glutamine and 1% P/S in T75 flasks. Cells density was maintained at a maximum of 2 x 10^6 cells/mL. For sub-culturing, cells were harvested by centrifugation at 1200 rpm for 5 minutes. After suspending the pellet with fresh medium, cells were counted using a Bürker chamber and splitted 1:10. Prior to each experiment, U937 monocytes were counted and the necessary number of cells were differentiated in macrophages by treating with 20ng/mL PMA for 48 hours. At the end of PMA stimulation, U937 adherent macrophages were washed twice with PBS without Ca^{2+} and Mg^{2+} and detached from the flask by incubation with trypsin at 37°C. Cells were recovered in a tube and seeded in 6- or 12-well plates at a density of 10^5 cells/cm^2. For treatment, cells were serum starved overnight and stimulated

with TNF-α (1, 10 and 20ng/mL), IFN-γ (20ng/mL), IL-1β (10ng/mL) and IL-4 (20ng/mL) for 24 hours. Genes of interest and protein expression were analyzed by real time RT-PCR and Western blot respectively. Conditioned media from U937 pre-stimulated with or without TNF-α was prepared as followed: 8 x 10^6 adherent U937 macrophages were seeded in a 100mm dish and serum starved for 24 hours. Cells were treated with or without TNF-α (10ng/mL) for 24 hours. After treatment, medium was replaced with fresh medium (without FBS) for another 24 hours. Conditioned media were collected, filtered and stored at -20°C until use.

3.2.2.2 LX-2[1]

The human hepatic stellate cell line LX-2 was cultured in RPMI-1640 medium supplemented with 10% FBS, 2mM L-glutamine and 1% P/S in 100mm dishes. Split was performed 3 times per week by washing cells twice with PBS without Ca^{2+} and Mg^{2+} and incubating them with trypsin at 37°C. After blocking trypsin action with fresh medium, cells were collected in a tube, counted and splitted 1:3. For experiments, cells were seeded in 6-well plates at 2 x 10^5 cells/well and serum starved in RPMI-1640 medium supplemented with 0.5% FBS.

3.2.2.3 RAW 264.7[2]

The murine macrophage cell line RAW 264.7 was cultured in DMEM-HG medium supplemented with 10% FBS, 2mM L-glutamine and 1% P/S. RAW 264.7 are semi-adherent, loosely attached cells which were detached from the surface by scraping. For subculturing, medium was aspirated and cells were washed with PBS. Fresh medium was added and cells were detached from plate with a cell scraper and splitted 1:3.

3.2.3 RNA extraction, RT-PCR and real time RT-PCR

RNA from monolayer cells was extracted with TRizol reagent (Sigma-Aldirch) according to the manufacturer's instructions. After removing medium, cells were

[1] LX-2 cells were a gift from Dr.ssa Elena Tibaldi and Prof.ssa Anna Maria Brunati (University of Padova, Padova)

[2] RAW 264.7 were a gift from Dr.ssa Elisa Duregotti and Prof. Cesare Montecucco (University of Padova, Padova)

washed twice with PBS and lysed with TRizol reagent using a cell scraper. RNA was isolated as described in paragraph 3.1.4.1. 500ng of total RNA was subjected to a reverse transcription reaction using SuperScript II Reverse Transcriptase (Invitrogen) according to the manufacturer's instructions and as described in paragraph 3.1.4.2. RT-PCR and real-time RT-PCR were used for semi-quantitative or quantitative mRNA expression analysis. A total of 12ng cDNA was used as a template for PCR amplification. The PCR reaction mix (15µL total volume) was prepared as reported in Table 6 using MyTaq Polymerase (BIOLINE). Primers used for PCR are listed in Table 7.

Table 6. RT-PCR reaction mix.

Reagent	Volume
5X MyTaq Reaction Buffer	3µL
cDNA template (4ng/µL)	3µL
MyTaq Polymerase	0.15µL
forward primer (10µM)	0.6µL
reverse primer (10µM)	0.6µL
H_2O	7.65µL

Table 7. Primers used for RT-PCR on total RNA cell extracts.

Gene	Primer Sequences (5'-3')	Product length (bp)
GAPDH	Forward: TGAGGACCAGGTTGTCTC Reverse: TCCACCACCCTGTTGCTGTA	147
Col1α1	Forward: GGTGGTTATGACTTCAGCTTCC Reverse: CATGTAGGCTACGCTGTTCTTG	552
FN	Forward: TTACGGTGGCAACTCAAA Reverse: GGTCATGCTGCTTATCCC	419

Amplification was performed using the thermocycler (Applied Biosystem) programmed as followed: an initial denaturation step at 95°C for 1 minutes, 25 cycles of amplification and last extension at 72°C for 7 minutes. For each cycle, denaturation step was performed at 95°C for 15 seconds, annealing at 55°C for GAPDH and fibronectin and 60°C for collagen I and extension at 72°C for 30

seconds. PCR products were mixed with DNA gel loading buffer and run in 2% agarose gels in TAE buffer (40mM Tris, 20mM acetic acid, 1mM EDTA) at 120V. For real time RT-PCR, reaction mix was prepared as shown in Table 3 and performed as described in paragraph 3.1.4.3. Primer sequences are reported in Table 8.

Table 8. Primers used for real time RT-PCR on total RNA cell extracts.

	Gene	Primer Sequences (5'-3')	Product length (bp)
rat	***GAPDH***	Forward: TGAGGACCAGGTTGTCTC	147
		Reverse: TCCACCACCCTGTTGCTGTA	
	HPSE	Forward: AAAGGCCCAGACAGAAGCAA	75
		Reverse: CCTTCCCGATACCTTGGGTG	
	TGF-β	Forward: ATACGCCTGAGTGGCTGTCT	153
		Reverse: TGGGACTGATCCCATTGATT	
	α-SMA	Forward: CCGAGATCTCACCGACTACC	120
		Reverse: TCCAGAGCGACATAGCAGAG	
	IL-1β	Forward: CCTGTCCTGCGTGTTGAAAGA	150
		Reverse: GGGAACTGGGCAGACTCAAA	
human	***GAPDH***	Forward: ACACCCACTCCTCCACCTTT	112
		Reverse: TCCACCACCCTGTTGCTGTA	
	HPSE	Forward: CCCTTGCTATCCGACACCTT	78
		Reverse: CACCACTTCTATTCCCATTCG	
	TNF-α	Forward: AATAGGCTGTTCCCATGTAGC	131
		Reverse: AGAGGCTCAGCAATGAGTGA	
	IL-1β	Forward: CCTGTCCTGCGTGTTGAAAGA	150
		Reverse: GGGAACTGGGCAGACTCAAA	
	α-SMA	Forward: TACTACTGCTGAGCGTGAGA	131
		Reverse: CATCAGGCAACTCGTAACTC	
	VEGF	Forward: AGACGTGTAAATGTTCCTGCAAAA	78
		Reverse: TGCAAGTACGTTCGTTTAACTCAAG	
	FN	Forward: GTGTGTTGGGAATGGTCGTG	113
		Reverse: GACGCTTGTGGAATGTGTCG	

3.2.4 Western blot

For protein sample preparation, cell culture plates were placed on ice and the cells were washed twice with ice-cold PBS. Cells were lysed in ice-cold lysis buffer (50mM Tris, 150mM NaCl, 1% Triton) supplemented with Protease Inhibitor Cocktail. Lysates were collected using a cell scraper and transferred in a tube and maintained for 30 minutes on ice, vortexing every 5 minutes. After being centrifuged at 12000 rpm for 20 minutes, supernatants were collected and transferred in new tubes. Protein concentration was determined using BCA assay according to the manufacturer's instructions. Proteins were aliquoted and frozen at -80°C until use. For conditioned medium preparation, cell supernatants were collected, centrifuged at 1000 x g for 10 minutes to remove detached cells and stored at -20°C until use. For electrophoresis, equal protein aliquots (10µg) and conditioned medium (40µL) were prepared in loading Laemmli buffer and boiled at 100°C for 10 minutes. SDS-PAGE and transfer were performed as described in paragraph 3.1.5. Membranes were blocked with 5% non-fat milk or 3% BSA in 0.1% TBST for 2 hours and incubated overnight with primary antibody. After 3 washes of 10 minutes with 0.1% TBST, membranes were incubated with the HRP-conjugated secondary antibody for 90 minutes at RT. Primary and secondary antibodies were prepared in 2.5% non-fat milk or 1.5% BSA according to the antibody datasheet. Antibodies were diluted as reported in Table 7. After 3 washes of 10 minutes with 0.1% TBST, membranes were incubated with home-made ECL. Signal detection was performed on Uvitec Cambridge. For densitometry analysis ImageJ software was used.

Table 9. Primary and secondary antibodies used for Western Blot on cell lysates.

	Target	Company	Host species	Dilution
Primary antibody	α-SMA	Sigma-Aldrich	mouse	1:1000
	Fibronectin	Santa Cruz	rabbit	1:400
	GAPDH	Santa Cruz	mouse	1:2000
	HPSE	ProSpec	mouse	1:500
	VEGF	Santa Cruz	rabbit	1:400
Secondary antibody	anti-rabbit IgG HRP	Santa Cruz	goat	1:1000
	anti-mouse IgG HRP	Santa Cruz	goat	1:2000 - 1:4000

3.2.5 Immunofluorescence

For immunofluorescence staining, cells were grown on 12mm glass coverslips and fixed with 4% paraformaldehyde (PFA) for 10 minutes at RT. Fixed cells were washed three times with PBS and immediately stained or stored in PBS at 4°C for at least one week. Quenching solution (50mM glycine, 50mM ammonium chloride in PBS) was added for 10 minutes. Cells were washed three times with PBS and permeabilized with 0.2% Triton X-100 in PBS for 10 minutes. After three washing with PBS for 5 minutes, saturation was carried out with 1% BSA in PBS for 1 hour at RT. Cells were then incubated with primary antibody in 1% BSA in a humid chamber overnight at 4°C. For double immunofluorescence staining, cells were incubated with a mix of the two different antibodies. After three washing with PBS, 5 minutes each, cells were incubated with secondary antibody in 1% BSA for 1 hour at RT in the dark. Primary and secondary antibody dilutions are reported in Table 10. After washing, nuclei were counterstained with Hoechst diluted 1:1000 in PBS for 20 minutes at RT. Cells were finally washed with PBS and coverslips were mounted with Fluoromount aqueous mounting medium. Immunofluorescence images were acquired using confocal microscope Leica TCS SP5.

Table 10. Primary and secondary antibodies used for immunofluorescence on cultured cells.

	Target	Company	Host species	Dilution
Primary antibody	HPSE	Santa Cruz	rabbit	1:50
	ED-1	Santa Cruz	mouse	1:50
	IL-β	Santa Cruz	rabbit	1:50
	α-SMA	Sigma-Aldrich	mouse	1:100
Secondary antibody	anti-rabbit Alexa 488	Thermo Scientific	goat	1:300
	anti-mouse Alexa 594	Abcam	goat	1:300

3.2.6 Wound-healing assay

Wound-healing assay or scar assay is an easy method to study cell migration *in vitro*. The protocol is to create a wound in a cell monolayer and observe cells migrating to close the scratch. By capturing images at regular intervals, scratch areas are measured and used to quantify the migration rate of the cells [120]. For our experiment, RAW 264.7 were seeded in 6-well plates and allowed to grow until confluence. The cell monolayers were scraped with the end of a 200µL pipette tip to create the wound and washed twice with PBS to remove detached cells (time 0). Cells were maintained in DMEM-HG without FBS in three experimental conditions: control medium without treatment, treatment with latent HPSE precursor (1µg/mL) and treatment with HPSE latent precursor (1µg/mL) in addition to the HPSE inhibitor SST0001 (200µg/mL). Cell migration into the wounded area was followed through light microscope and images were captured at time 0 and after 6, 24 and 30 hours. Wound areas were measured using the wound healing tool of Image J software.

3.3 Human patients

3.3.1 Study population

A total of 86 subjects were consecutively enrolled in the study, including 14 healthy volunteers (controls) and 35 patients with different chronic liver diseases. Patients had been diagnosed for hepatitis B (HBV, n=8), hepatitis C (HCV, n=27), primary biliary cholangitis (PBC, n=18), primary sclerosing cholangitis (PSC, n=9), autoimmune hepatitis (AIH, n=7), PBC/AIH overlap (n=2), PSC/AIH overlap (n=1). Patients with HCV and HBV were categorized in viral hepatitis subgroup. Patients with PBC, PSC, AIH and overlap syndrome were categorized in autoimmune disease subgroup. The baseline characteristics of the patients are shown in Table 11. Exclusion criteria were as follows: diabetes, ulcerative colitis, Chron's disease, cancer and glomerulopathies.

Table 11. Patient characteristics. Data are mean ± s.d.

	Healthy controls	Viral hepatitis	Autoimmune disease
Population (n.)	14	35	37
Male/Female	7/7	21/14	8/29
Age (years)	40.58 ± 13.15	57.03 ± 16.35	52.57 ± 15.42

3.3.2 Liver Transient Elastography (Fibroscan)

Liver fibrosis was assessed in patients by Fibroscan device. Fibroscan is a method for the determination of hepatic fibrosis by measuring liver stiffness. The exam is non-invasive, rapid and easily performed. Briefly, an ultrasound probe is connected to a vibrator. The probe is placed on the skin at the level of the right lobe of the liver. Transmitted vibrations induce an elastic wave that propagates through the liver. According to the principle that the harder the tissue, the faster the wave propagates, ultrasound is acquired and the velocity of propagation is used to determine liver stiffness, expressed in kPa. The histological stage of fibrosis was graded according to the Metavir score (ranging from F0 to F4) using the liver stiffness cut-off values recommended by Castera and colleagues [121]. As shown in Figure 10, liver stiffness values below 7kPa correspond to absent or

mild fibrosis. Values for liver stiffness of 9.5 and 12.5kPa represent the cut-offs for F3 and F4 stages (severe fibrosis and cirrhosis respectively).

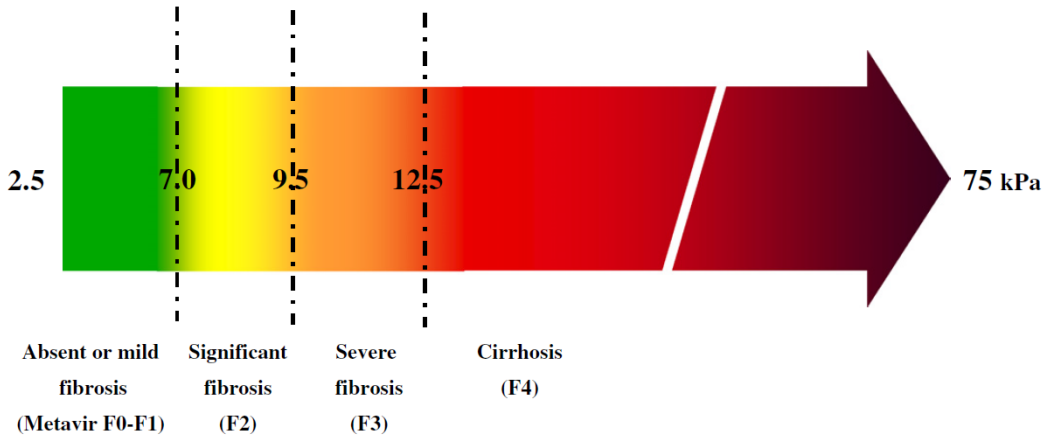

Figure 10. Liver stiffness cut-off values used for fibrosis staging. In the Metavir score, fibrosis is graded from 0 to 4: F0, no fibrosis; F1, portal fibrosis without septa; F2, portal fibrosis with few septa; F3, numerous septa without cirrhosis; F4, cirrhosis. From [121].

3.3.3 Plasma collection

A total of 3mL of peripheral blood was collected from patients and healthy subjects after signing a written informed consent. Blood was collected in EDTA-anticoagulant tubes and processed by centrifugation at 1500 x g for 15 minutes. Plasma was collected, aliquoted and stored at -20°C until use. All samples were thawed once.

3.3.4 Heparanase activity assay

HPSE plasma activity was measured using an ELISA-modified assay based on the ability of HPSE to degrade HS present in Matrigel. Matrigel was let thaw overnight at 4°C, diluted in ice-cold PBS at the concentration of 200µg/mL and used to coat ELISA plates (25µL/well). Matrigel manipulation was performed with ice-cold tips and tubes. Plates were left at RT for 2 hours. Plasma samples were diluted 1:4 in HPSE buffer (0.1M sodium acetate pH 5, 0.1% BSA, 0.01% Triton X-100, Protease Inhibitor Cocktail) in the presence or absence of LMWH (50µg/mL). Plates were washed once with 0.05% PBST (PBS with 0.05% Tween-

20) and 25µL of each sample was loaded in triplicate. Plates were incubated overnight at 37°C. The day after plates were washed with 0.05% PBST and saturated with blocking buffer (1% BSA, 0.1% Triton X-100 in PBS) at RT for 2 hours. After washing, plates were incubated with anti-HS-specific monoclonal antibody (clone HepSS-1) diluted 1:500 in blocking buffer at RT for 1 hour. Plates were washed three times for 5 minutes with 0.05% PBST and incubated with secondary antibody (HRP-conjugated goat anti-mouse IgM) diluted 1:1000 in blocking buffer for 1 hour at RT. Plates were washed three times for 5 minutes with 0.05% PBST. The reaction was visualized by the addition of 50µL ABTS [2,2'-azino-bis (3-ethylbenzothiazoline-6-sulphonic acid)] chromogenic substrate for 15 minutes and stopped with 50µL 1% SDS. Absorbance at 405nm (OD405) was measured using an ELISA spectrophotometer plate reader. For each sample, HPSE activity was calculated as the difference between OD405 value with or without LMWH.

3.4 Statistical analysis

For data analysis and graph representation, Excel® and Origin® programs were used. Quantitative data were expressed as means ± standard error of the mean (s.e.m.) or means ± standard deviation (s.d.). For comparison between two distributions, the two-tailed t-test was used. For comparisons between more than two distributions, the one-way ANOVA with the Bonferroni correction was used. p-values < 0.05 were considered statistically significant.

3.5 Materials

3.5.1 Reagents

Product	Company	Catalog number
ABTS	Sigma-Aldrich	A3219
Acetic acid glacial	CARLO ERBA	401392
Agarose	HydraGen	R9112LE
Azocarmine G	Sigma-Aldrich	A1091
β-mercaptoethanol	Sigma-Aldrich	M7154
Blue loading buffer with DNA stain	Jena Bioscience	PCR-255-bl
Bovine serum albumin	Sigma-Aldrich	A2153
CCl_4	Sigma-Aldrich	87031
ColorBurst Electrophoresis Marker	Sigma-Aldrich	C1992
dNTPs Mix, 10mM Solution	Sigma-Aldrich	D7295
Chloroform	AppliChem	A3633
Eosin Y solution aqueous	Sigma-Aldrich	HT110232
Ethanol	Sigma-Aldrich	02860
Formalin solution, neutral buffered, 10%	Sigma-Aldrich	HT501128
Fluoromount aqueous mounting medium	Sigma-Aldrich	F4680
Hematoxylin solution according to Mayer	Sigma-Aldrich	51275
Hydrochloric acid	Sigma-Aldrich	08256
Glycine	Sigma-Aldrich	G8898
Glycerol	AppliChem	A2926
Isopropanol	Sigma-Aldrich	59304
Matrigel™ Basement Membrane Matrix	BD Bioscience	356234
Methanol	Sigma-Aldrich	32213
Methyl blue	Sigma-Aldrich	M5528
Non-fat dry milk	Santa Cruz	sc-2325
NaCl	AppliChem	A2942
Orange G	Sigma-Aldrich	O7252
Paraffin	Histo-Line	R0040SP
Protease Inhibitor Cocktail	Sigma-Aldrich	04693116001
Random Examer Primers	BIOLINE	BIO-38028
PBS	Sigma-Aldrich	D5652
SDS	Sigma-Aldrich	L4390

TRI Reagent	Sigma-Aldrich	T9424
Tri-Sodium citrate dihydrate	AppliChem	A4522
Tris	USB Affymetrix	75825
Triton X-100	Sigma-Aldrich	T8532
Water sterile-filtered	Sigma-Aldrich	W3500
Tween-20	Sigma-Aldrich	P2287
Xylene	Sigma-Aldrich	16446
100bp Opti-DNA Marker	abm	G016

3.5.2 Enzymes and commercial kits

Product	Company	Catalog number
DAB Peroxidase (HRP) Substrate Kit	VECTOR	SK-4100
MyTaq DNA Polymerase	BIOLINE	BIO-21105
Pierce^{TM} BCA Protein Assay Kit	Thermo scientific	23225
SensiFAST SYBER Hi-ROX Kit	BIOLINE	BIO-92005
SuperScript II	Invitrogen	18064-014
VECTASTAIN Elite ABC HRP Kit	VECTOR	PK-6101

3.5.3 Cell culture media and reagents

Product	Company	Catalog number
Collagenase NB4	SERVA	17454
DMEM-HG	Euroclone	ECB7501L
DMSO	Sigma-Aldrich	D8418
PBS	Aurogene	AU-L0625
PBS without $Ca2^{+}$ and $Mg2^{+}$	Aurogene	AU-L0615
Fetal Bovine Serum	Aurogene	AU-S1810
GBSS	Sigma-Aldrich	G9779
IL-1β	Peprotech	200-01B
IL-4	Peprotech	D0815
IFN-γ	[3]	

[3] IFN-γ was a gift from Dr.ssa Paola Aguiari (University of Padova, Padova)

Insulin from bovin pancreas	Sigma-Aldrich	I6634
L-Glutamine 200mM	Euroclone	ECB3000D
LPS	Santa Cruz	sc3535
Medium 199	Aurogene	AU-L0355
Optiprep Density Gradient Medium	Sigma-Aldrich	D1556
Penicillin/Streptomycin	Euroclone	ECB3001D
PMA	Sigma-Aldrich	P8139
RPMI 1640	Euroclone	ECB9006L
SST0001	[4]	
TNF-α	Sigma-Aldrich	T6674
Trypsin-EDTA 1X in PBS	Euroclone	ECB3052D
Trypan Blue	Euroclone	ECM0990D

[4] SST0001 was provided by Sigma-Tau Research Switzerland S.A. (Mendrisio, CH)

4. Results

4.1 Chronic administration of CCl_4 induces liver fibrosis in mice

To determine the involvement of HPSE in chronic liver disease, the hepatotoxin CCl_4 was used to induce liver fibrosis in mice. Repeated administration of CCl_4 to mice is a reliable model of chronic liver injury and liver fibrosis, recapitulating the pathological features observed in human patients. For our research purpose, Balb/cJ mice were treated twice a week with i.p. injections of CCl_4 for 1 and 2 weeks to induce an early chronic injury and for 8 and 12 weeks to induce a severe chronic injury and cirrhosis. Mice were weighed prior of each injection and the body weight of treated and control animals was monitored throughout the experimentation. CCl_4 administration was well tolerated, did not affect animal growth and all the animals were alive at their respective time of sacrifice. To evaluate the outcome of the treatment in term of histopathological changes and hepatic fibrogenesis, H-E and Azan Mallory stainings were respectively performed on control and CCl_4-treated livers. Liver sections from control mice stained with H-E showed normal liver lobular architecture at each time point. After 1 and 2 weeks of CCl_4 delivery, hepatic tissues showed high necro-inflammatory activity: livers exhibited confluent centrilobular necrotic areas, extensive inflammatory cells infiltration and hepatocyte ballooning. Deposition of calcium within the CCl_4-induced necrotic areas was also observed in multinucleated giant cells. Liver tissues from 8 and 12 week CCl_4-treated mice showed mild cell infiltration, disruption of tissue architecture. Micronodular cirrhosis was characterized by pseudolobules formation (Fig.11a). Azan-Mallory staining revealed a normal distribution of collagen fibers at the vascular walls of control livers at each time points. Perisinusoidal central fibrosis characterized by the deposition of fine collagen fibers in the sinusoids of the centrilobular region was found after 1 week of CCl_4 injection indicating the activation of a wound-healing process. Thin fibrotic septa occurred in 2 week CCl_4-treated livers which progressively led to porto-central and porto-portal bridging fibrosis after 8 and 12 weeks of CCl_4 administration (Fig.11b).

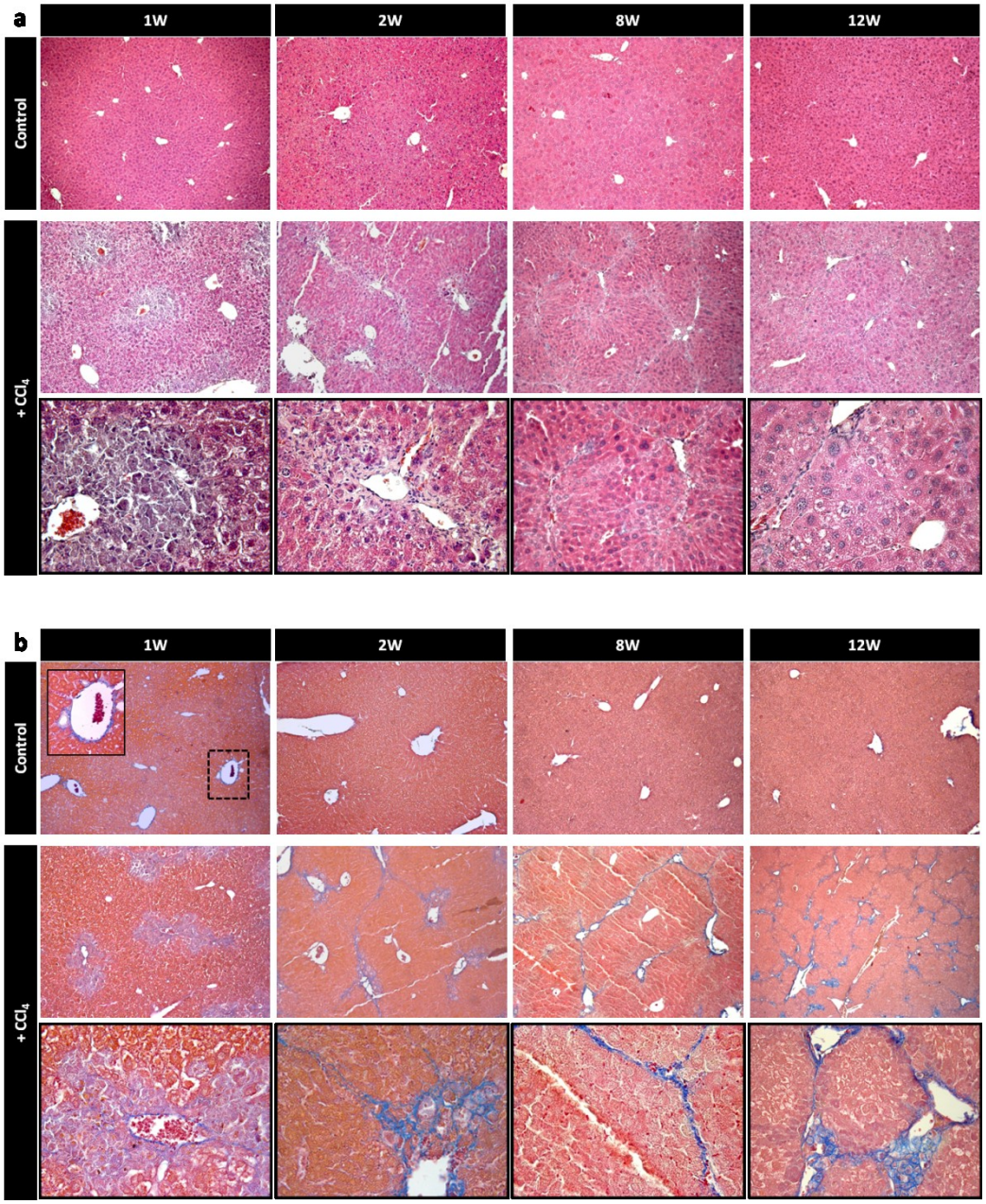

Figure 11. Histological assessment of CCl_4-induced liver fibrosis. (a) H-E staining and **(b)** Azan-Mallory staining of control and CCl_4-injured livers at the indicated time of treatment. Insert represents high magnification from black box, showing the stain of vascular collagen in control livers. (Original magnification, X100 and X400).

4.2 Heparanase expression is up-regulated in mice with early chronic liver injury

To analyze HPSE expression in the CCl_4-induced chronic injured livers, real time RT-PCR, Western blot and immunofluorescence analyses were performed. No significant changes in HPSE mRNA expression were measured between control livers at each time point. Compared to control groups, hepatic HPSE mRNA and protein levels were significantly up-regulated in the liver tissues of mice with early chronic liver disease (subjected to 1 and 2 weeks of CCl_4 administration) but not in mice with advance disease (subjected to 8 and 12 weeks of CCl_4 administration). HPSE mRNA levels were up-regulated in CCl_4-treated mice at week 1 (mean ± s.e.m.: 6.87 ± 0.77 *vs*. 1.27 ± 0.26 in CCl_4-treated and control mice respectively) and week 2 (mean ± s.e.m.: 3.11 ± 0.36 *vs*. 0.70 ± 0.05 in CCl_4-treated and control mice respectively). In contrast, HPSE levels were not significantly different as compared to controls after 8 weeks (mean ± s.e.m.: 2.09 ± 1.25 *vs*. 0.96 ± 0.35 in CCl_4-treated and control mice respectively) and 12 weeks of CCl_4 intoxication (mean ± s.e.m.: 2.17 ± 0.53 vs. 1.58 ± 0.41 in CCl_4-treated and control mice respectively). Moreover, HPSE mRNA levels were significantly reduced in liver of 2 week treated group compared to 1 week group (Fig.12a). These data indicated that HPSE transcription is up-regulated in the early stages of tissue damage and progressively decreased to basal levels in the late damage model. To test whether mRNA levels were reflected by protein translation, we performed Western blot analysis on protein extracts from liver tissues of control and CCl_4-treated mice. In line with real time RT-PCR data, CCl_4 injection caused a significant increase in HPSE protein levels in the early phases of tissue damage (1 and 2 weeks), as compared to control mice. On the contrary, prolonged and chronic treatment with CCl_4 (8 and 12 weeks) resulted in no significant changes in HPSE levels, supporting that HPSE protein content in liver tissues reflects mRNA expression (Fig.12b-c). Such a trend was confirmed by IF staining on formalin-fixed and paraffin embedded (FFPE) sections from mice treated with CCl_4 and their respective controls. Accordingly to Western blot results, immunofluorescence revealed a strong liver immunopositivity for HPSE after 1or 2 weeks of CCl_4 exposure as well as a low or absent HPSE staining after 8 and 12 weeks CCl_4 exposure (Fig.12d).

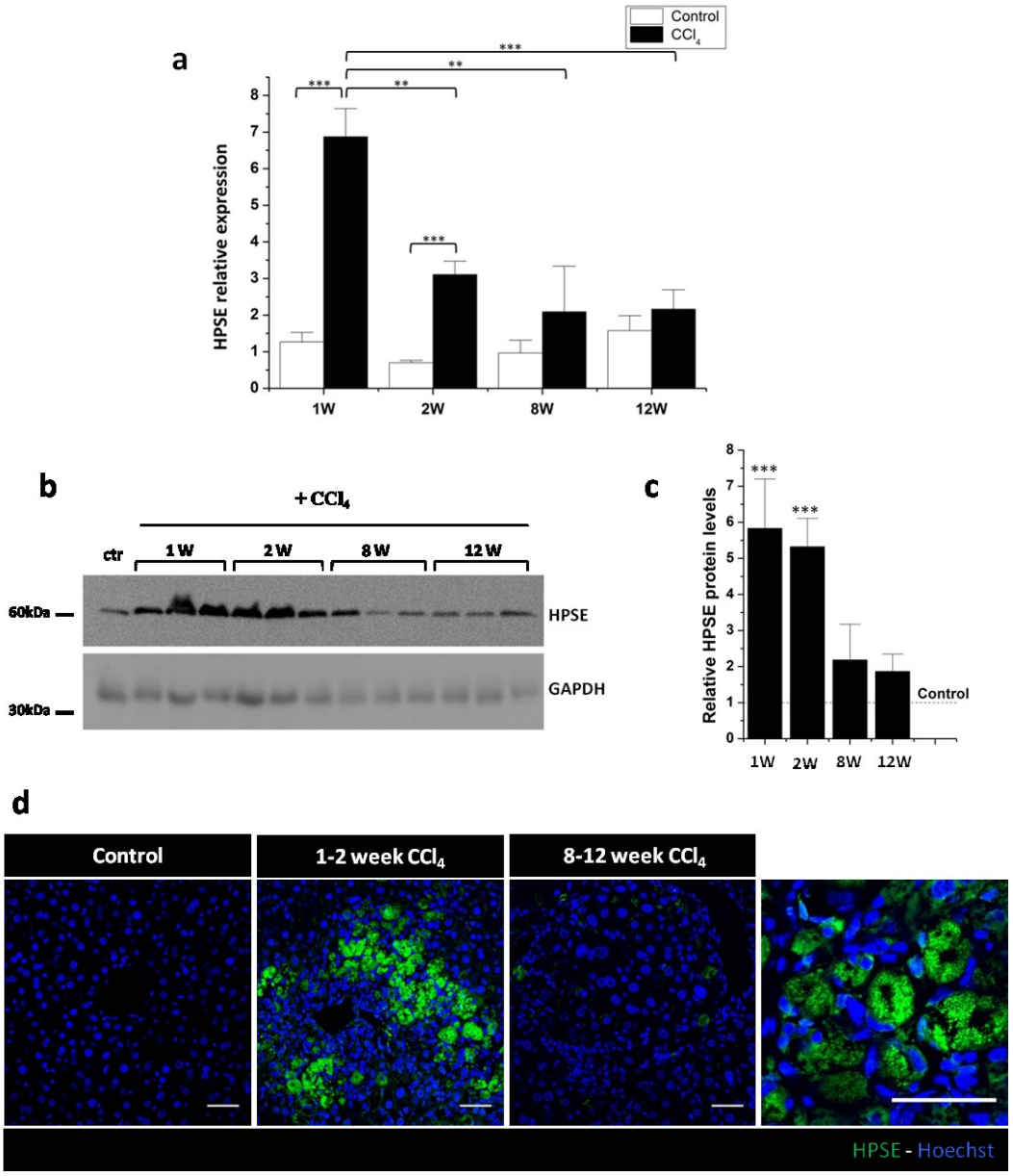

Figure 12. **HPSE is up-regulated in mice with early chronic liver injury. (a)** HPSE mRNA expression in livers from control and CCl_4-treated mice for the indicated time, measured by real-time RT-PCR analysis and normalized to GAPDH. Error bars represent s.e.m. *** $p < 0.001$, ** $p < 0.01$. **(b)** Western blot analysis for HPSE on whole liver protein extracts from CCl_4-induced fibrotic mice and control mice. **(c)** Densitometric quantification of HPSE from Western blot showed in panel (b). Error bars represent s.e.m. *** $p < 0.001$. **(d)** Confocal immunofluorescence staining for HPSE (green signal) and nuclei (blue signal) on liver sections from control mice and CCl_4-induced fibrotic mice at the indicated time. Right panel shows granular and diffuse pattern of HPSE distribution. Scale bar: 50µm.

4.3 Heparanase localization in early chronic CCl_4-injured livers

Immunofluorescence staining for HPSE in 1 week and 2 week injured livers, clearly showed that HPSE expression was not diffuse in the tissue but confined to distinct areas. Moreover, a combination of diffuse and granular pattern of distribution was observed (Fig.12d, right panel) indicating an extracellular and intracellular vesicular localization of HPSE respectively.

To better evaluate the intra-hepatic localization of increased HPSE in injured livers in response to the hepatotoxin CCl_4, immunohistochemical analysis for HPSE on FFPE sections was performed. As gene expression and protein analyses showed the hepatic up-regulation of HPSE at early time points in contrast to comparable levels between control and long time treated (8 and 12 weeks) mice, we investigated HPSE distribution only in liver tissues from mice with early chronic liver injury (1 and 2 weeks of CCl_4 delivery). Control healthy liver tissue was negatively stained for HPSE. In accordance to gene and protein expression results from real time RT-PCR, Western blot and immunofluorescence analyses, immunohistochemical stainings showed a marked expression of HPSE both in 1 and 2 week CCl_4-treated livers. Staining of HPSE suggested a centrilobular hepatic areas localization, in correspondence of necrotic tissues, perisinusidal fibrosis and inflammatory cell infiltrate. HPSE did not co-localized with healthy neighbouring hepatocytes. In addition, no HPSE staining was detected in portal triads. In term of hepatic acinus, HPSE stained areas corresponded to the centrilobular/zone 3 but not to the more peripheral zone 2 and zone 1 (Fig.13-14). This pattern of distribution reflected the CCl_4-affected regions of the liver.

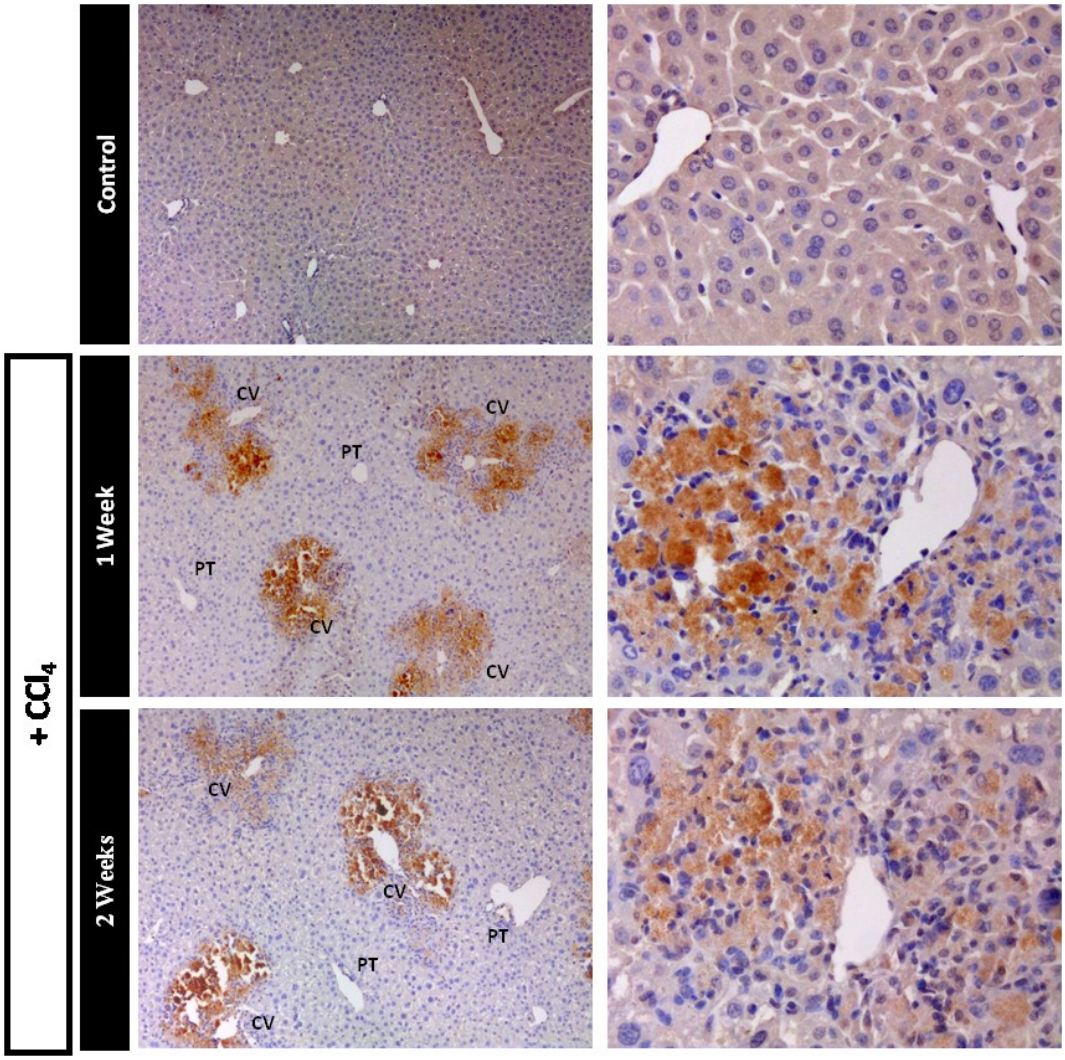

Figure 13. Expression of HPSE is restricted to centrilobular areas in early chronic injured mice. IHC on liver sections from control and CCl_4-treated mice at the indicated time points with anti-HPSE antibody. (Original magnification, X50 and X200). CV = central vein, PT = portal triads.

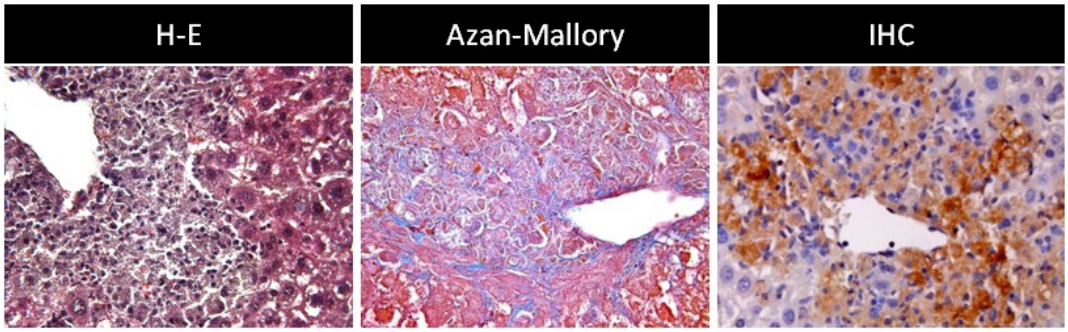

Figure 14. **Expression of HPSE is localized in centrilobular fibrotic areas in early chronic injured mice.** H-E (left), Azan-Mallory (middle) and IHC for HPSE (right) on liver sections from 1 week CCl_4-treated mice (original magnification, X200).

4.4 Heparanase expression by activated HSCs

Liver tissue injury by CCl_4 injections induced not only a local inflammatory response but also a rapid wound-healing process as demonstrated by the staining of collagen fibers in the affected centrilobular areas. ECM deposition is a consequence of myofibroblast cells activity with the aim of tissue restoration following injury. Prolonged insult to the centrilobular regions results in the activation and proliferation of perisinusoidal HSCs. Since HPSE localized in these fibrotic regions in 1 week and 2 week chronic CCl_4-injured livers (Fig.14), we questioned whether activated HSCs could contribute to its accretion. Accordingly, HPSE expression in both *in vitro* and *in vivo* activated HSCs was investigated. Isolation of quiescent HSCs and their culture on plastic dishes is a well established *in vitro* method to reproduce HSCs activation. Under this condition, HSCs undergo transdifferentiation into myofibroblast-like cells acquiring *de novo* expression of α-SMA and up-regulating ECM proteins. For our study, primary HSCs were isolated from rat livers and cultured on plastic plate to induce their spontaneous activation. Isolated cells were positively identified as HSCs by staining for intermediate filament desmin (Fig.15a). On uncoated culture plates, freshly isolated HSCs proliferated and changed their morphology acquiring the spindle shape phenotype of myofibroblast-like cells (Fig.15b). The expression of the myofibroblast marker α-SMA, the pro-fibrotic factor TGF-β and ECM proteins collagen I and fibronectin was measured in HSCs at different days post-isolation to verify the occurrence of *in vitro* activation. Collagen I and fibronectin mRNA levels increased after 15 days of culture compared to 7 days as showed by RT-PCR analysis (Fig.15c). Likewise, α-SMA and TGF-β mRNA were significantly up-regulated in 15 day cultured cells (149.32-fold and 2.36-fold increase, respectively), compared to 7 day cultured cells (Fig.15d). This data indicated the progressive activation of *in vitro* cultured cells. Concurrently, real time RT-PCR revealed that HPSE mRNA was significantly 1.94-fold up-regulated in 15 day *vs*. 7 day cultured HSCs (Fig.15d). Immunofluorescence staining for HPSE on HSCs at different days post-isolation was also performed. In line with real time RT-PCR data, HSCs increased α-SMA protein expression. While mild or absent staining was evident in freshly isolated cells (24 hours post-isolation), HPSE was detected in myofibroblast HSCs (15 days post-isolation). In activated

HSCs, HPSE showed a granular pattern of distribution localized in vesicles (most likely endosomes and lysosomes) (Fig.15e). Overall, these results indicated that HPSE is up-regulated by HSCs when activated to myfibrobalsts.

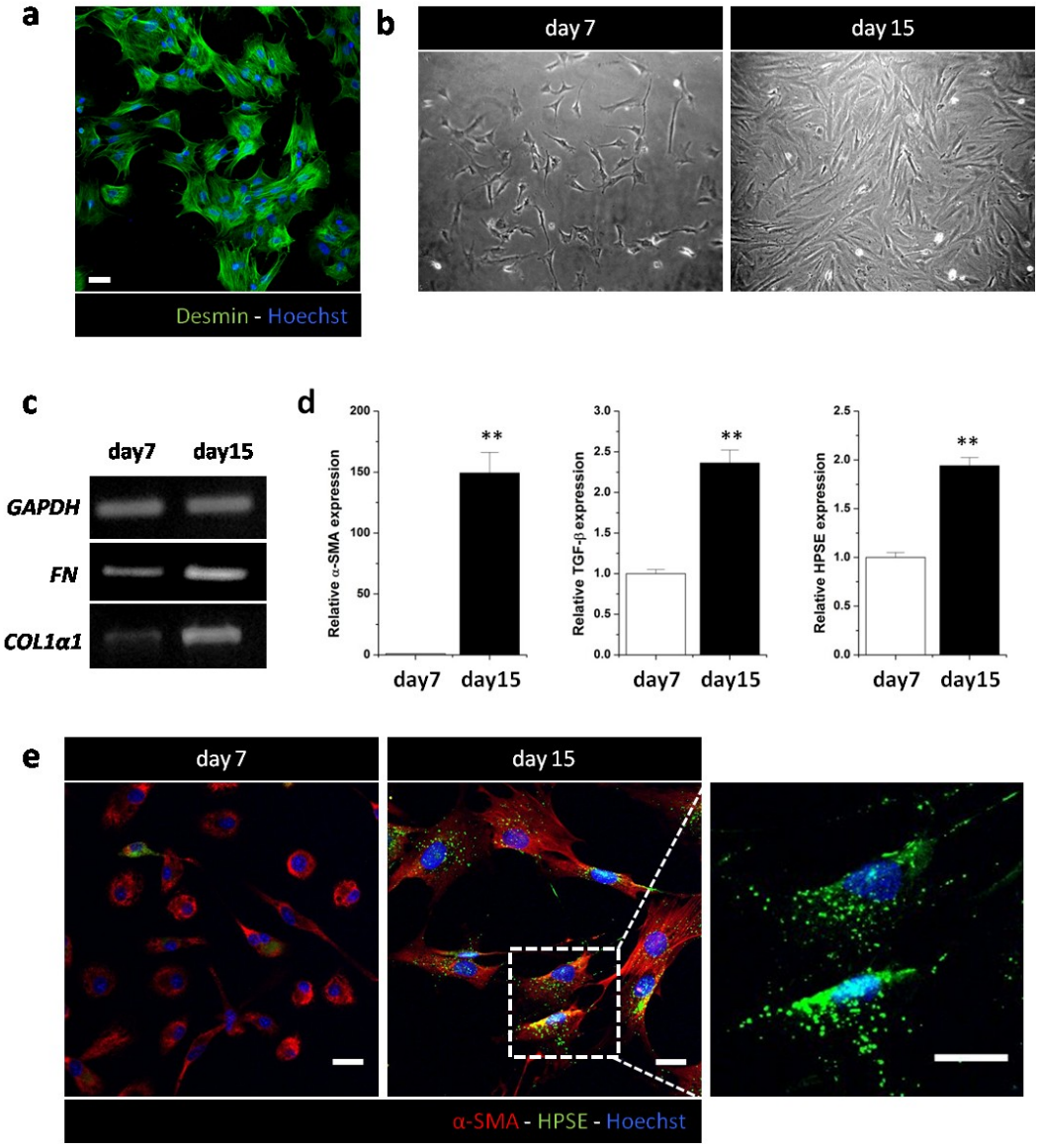

Figure 15 HSCs up-regulate HPSE during transdifferentiation to myofibroblasts. (a) Immune characterization of primary isolated rat HSCs for the presence of desmin marker. Scale bar: 20µm. **(b)** Bright field images of HSCs after 7 ad 15 days of culture on plastic dishes (original magnification, X100). **(c)** RT-PCR analysis for collagen I (Col1α1) and fibronectin (FN) in day4 and day15 cultured HSCs, normalized to GAPDH. **(d)** α-SMA, TGF-β and HPSE gene expression, measured in primary cultured HSCs at the indicated time. mRNA levels were determined by real time RT-PCR and normalized to GAPDH. Error bars represent s.d. ** $p < 0.01$. **(e)** Confocal immunofluorescence staining for α-SMA (red signal), HPSE (green signal) and nuclei (blue signal) on cultured HSCs at the indicated time. Right panel: high magnification from white box. Scale bar: 20µm.

In the light of these data from *in vitro* activated HSCs, we secondly addressed whether *in vivo* HSCs up-regulate HPSE in response to liver injury. HSCs activation in CCl_4-induced fibrosis could be monitored by expression of α-SMA. We therefore investigated the expression of α-SMA in control and fibrotic livers. As shown in Figure 16a, in control healthy mouse liver, α-SMA was observed only in vessel walls, as expressed by vascular smooth muscle cells. After CCl_4 exposure, α-SMA immunopositive cells increased at the site of injury. To address whether *in vivo* activated HSCs express HPSE, double immunofluorescence staining with anti-HPSE and anti-α-SMA antibodies was performed on early chronic injured livers (after 1 and 2 weeks of treatment). Although HPSE-positive HSCs could be detected after CCl_4 administration, HPSE was predominantly extracellularly distributed and localized in other neighbouring cells (Fig.16b). These data confirmed that activated HSCs increased HPSE expression but, most likely, they contributed minimally to its overload in liver tissue suggesting another major source.

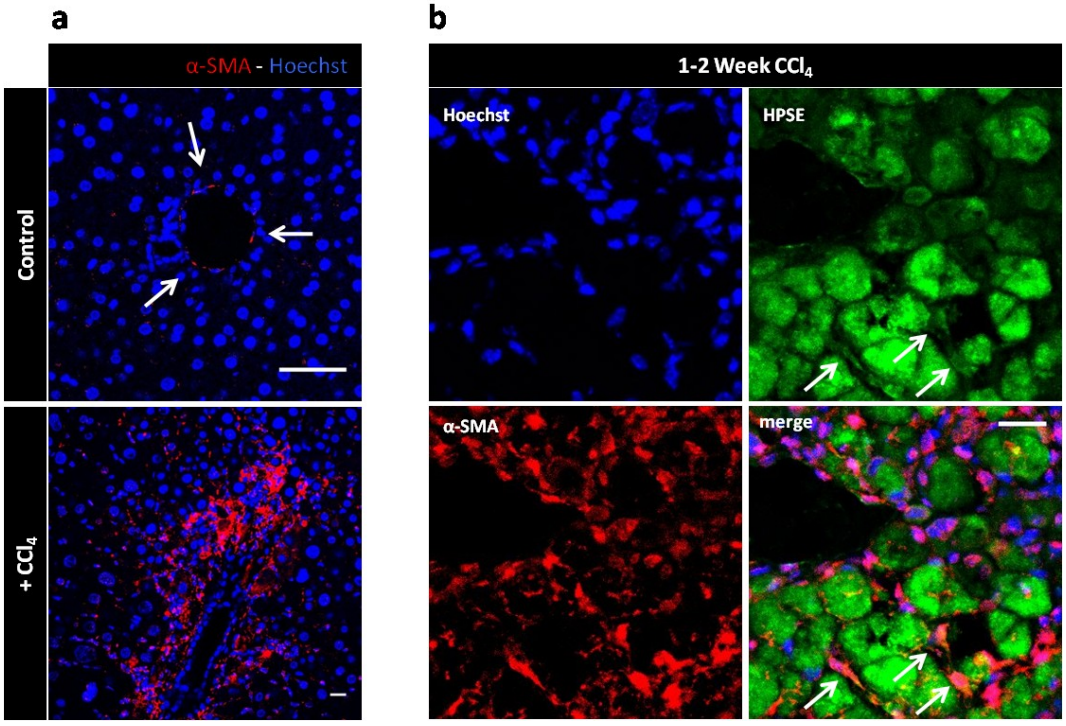

Figure 16. HPSE expression by *in vivo* activated HSCs (a) Left: Confocal immunofluorescence staining for α-SMA (red signal) and nuclei (blue signal) on liver sections from control and CCl_4-treated livers. In control liver, positive cells are indicated by white arrows. Scale bar: 50µm. **(b)** Representative confocal immunofluorescence staining for HPSE (green signal), α-SMA (red signal) and nuclei (blue signal) on liver tissue after 1 week and 2 weeks of CCl_4 administration. Some HPSE-positive HSCs are indicated by white arrows. Scale bar: 20µm.

4.5 Heparanase co-localizes with macrophages in early chronic CCl_4-injured livers

Necrosis/apoptosis of parenchymal cells is a stimulus not only for HSCs activation but also, and primarily, for inflammation through resident macrophages (Kupffer cells) activation and monocytes infiltration. Macrophages play a key role in chronic inflammation by the production of several pro-inflammatory and pro-fibrogenic mediators. Recent data have demonstrated a pro-inflammatory role for HPSE as well, by strongly enhancing macrophages activation. Starting from the evidence of the HPSE exclusive localization in necro-inflammatory areas, our second candidate source of HPSE in toxic injured liver were macrophages. To investigate the involvement of macrophages in HPSE up-regulation, we performed immunofluorescence staining for HPSE and F4/80 (a mouse macrophage-specific marker) in early chronic CCl_4-injured liver. In healthy mouse liver, F4/80 marked resident Kupffer cells lining sinusoids (Fig.17a, left panel). In the liver of mouse treated for 1 and 2 weeks with CCl_4, we detected increased F4/80 signal in support of both proliferation of resident Kupffer cells and activation of infiltrating monocytes. HPSE immunopositivity strongly overlapped with F4/80 after 1 and 2 weeks of CCl_4 administration, indicating the co-localization of HPSE with macrophages (Fig.17a, right panel). To further confirm this data, co-immunofluorescence with anti-CD68 (a pan-macrophage marker) antibody was also performed. In line with F4/80 results, co-localization of HPSE with CD68 was also evident (Fig.17b). Therefore, these results identified macrophages as a relevant source of HPSE in CCl_4-injured liver.

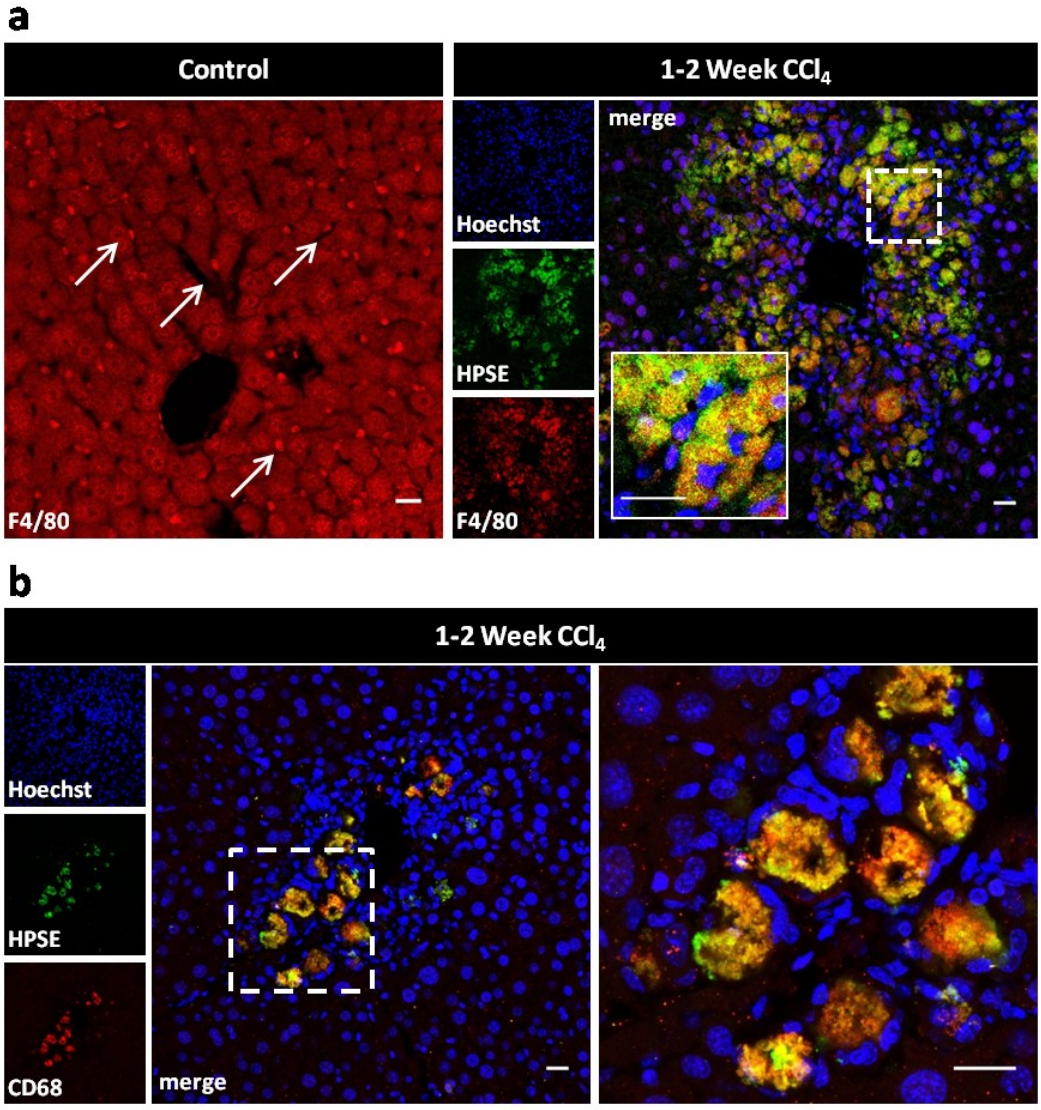

Figure 17. HPSE co-localizes with F4/80 and CD68 in early CCl_4-injured liver tissues. (a) Left: confocal immunofluorescence staining for F4/80 in control livers showing Kupffer cells lining sinusoid. White arrows indicate representative cells. Right: confocal immunofluorescence staining for HPSE (green signal), F4/80 (red signal) and nuclei (blue signal) on liver tissue after 1 week and 2 weeks of CCl_4 administration. Insert shows high magnification from white box. Scale bar: 20µm. **(b)** Confocal immunofluorescence staining for HPSE (green signal), CD68 (red signal) and nuclei (blue signal) on liver tissue after 1 week and 2 weeks of CCl_4 administration. Right panel: high magnification from white box. Scale bar: 20µm.

4.6 TNF-α regulates heparanase expression in macrophages

Different cytokines and pro-inflammatory mediators are known to induce HPSE in different cell lines. Lipopolisaccharide (LPS), a potent macrophage activator derived from Gram-negative bacteria cell wall, up-regulates HPSE in isolated PBMC [122] while TNF-α, IL-1β and IFN-γ induce HPSE expression in endothelial cells and different epithelial cell types [73, 74, 81, 123]. In the mouse models of diabetic nephropathy and chronic ulcerative colitis, HPSE is mild expressed by immune cells but up-regulated by glomerular cells in the first case and colonic epithelium in the second one. Up-regulation by epithelial cells is proposed to be sustained by secreted TNF-α from inflammatory macrophages [74, 81]. Differently from these systems of chronic injury, in our model of CCl_4-induced chronic liver disease, HPSE was primarily expressed by activated macrophages themselves.

To validate the role of inflammatory macrophages in HPSE accretion, rat liver Kupffer cells were isolated, treated with LPS and TNF-α for 6 hours and HPSE expression was analysed. Freshly isolated Kupffer cells were positively identified for ED1 (CD68) marker expression (Fig.18a). To verify Kupffer cells activation, the mRNA level of inflammatory cytokine IL-1β was measured in cells after treatments. Treating cells with LPS significantly up-regulated IL-1β mRNA levels compared to untreated cell (mean ± s.d.: 1721.97 ± 152.34 *vs*. 0.97 ± 0.04, respectively) (Fig.18c). IL-1β mRNA was ~4-fold increased in cells treated with TNF-α (mean ± s.d.: 3.99 ± 0.21 *vs*. 1.00 ± 0.06, respectively) (Fig.18d). Immunofluorescence staining for IL-1β in untreated and LPS-treated cells was also performed. After treatment with LPS, activated Kupffer cells acquire a spindle-shaped cell morphology and increased IL-1β protein. (Fig.18b). As shown by real time RT-PCR analysis, LPS treatment did not affect HPSE mRNA levels (mean ± s.d.: 0.81 ± 0.14 *vs*. 0.90 ± 0.14) (Fig.18c). Immunofluorescence revealed positive staining for HPSE in untreated Kupffer cells which, however, was not increased upon LPS treatment, confirming gene expression data (Fig.18b). As opposed to LPS, TNF-α induced HPSE gene transcription as demonstrated by the 2.17-fold mRNA significant increase in treated vs. untreated cells (mean ± s.d.: 2.24 ± 0.69 *vs*. 1.03 ± 0.36, respectively) (Fig.18d).

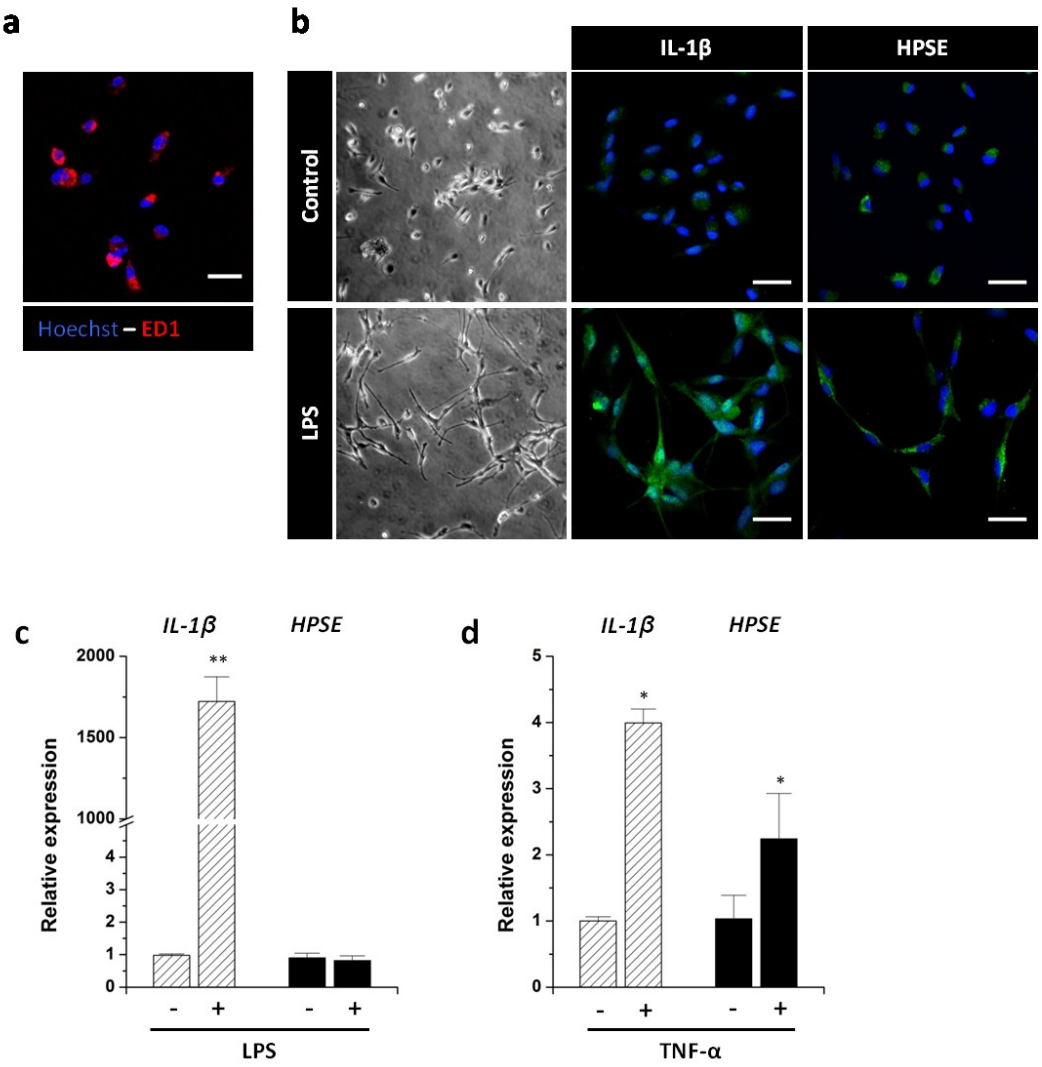

Figure 18. **TNF-α, but not LPS, stimulates HPSE expression in primary isolated Kupffer cells**. **(a)** Immune characterization of primary isolated rat Kupffer cells for presence of ED1 (CD68) macrophage marker. Scale bar: 20µm. **(b)** Bright field images (original magnification, X100) and confocal immunofluorescence staining for HPSE and IL-β in primary Kupffer cells treated with or without LPS (1µg/mL). Nuclei (blue signal) were counterstained with Hoechst. Scale bar: 20µm. **(c-d)** IL-1β and HPSE gene expression, measured in primary Kupffer cells incubated or not with LPS (1µg/mL) **(c)** and TNF-α (20ng/mL) **(d)**. mRNA levels were determined by real time RT-PCR and normalized to GAPDH. Error bars represent s.d. ** $p < 0.01$, * $p < 0.05$.

Similar results from TNF-α treatment were obtained utilizing the human monocyte/macrophage cell line U937. For these experiments, non-adherent U937 monocytes were treated with PMA for 48 hours to induce adherent macrophages differentiation. To determine the effect of TNF-α on HPSE expression, U937 macrophages were treated with increasing concentrations of TNF-α (0, 1, 10,

20ng/mL) for 24 hours. Dose response analysis of HPSE mRNA expression, together with pro-inflammatory cytokines IL-1β and TNF-α were examined by real time RT-PCR. TNF-α treatment resulted in a significant increase in IL-1β mRNA levels in a concentration-dependent manner. Expression was 1.38-fold increased in the presence of 1ng/mL TNF-α, 1.88-fold with 10ng/mL and 2.73-fold with 20ng/mL compared to untreated cells. TNF-α also induced a dose-dependent stimulation of itself mRNA expression (1.49-, 1.98- and 2.57-fold increase at 1, 10 and 20ng/mL TNF-α respectively). In addition to pro-inflammatory cytokines, HPSE gene transcription was induced in U937 macrophages by TNF-α, in a dose-dependent manner. Treating cells with 1ng/mL TNF-α induced a 1.95-fold increase in HPSE mRNA levels which reached 2.87- and 3.66-fold in the presence of 10 and 20ng/mL TNF-α (Fig.19a). To verify whether transcriptional changes was reflected in protein translation, U937 were treated with 1 and 10ng/mL and HPSE was detected by Western blot analysis. As shown in Figure 19b-c, HPSE protein levels were significantly increased after treatment, further demonstrating the regulatory function of TNF-α on HPSE expression in macrophages.

It is known that, in certain conditions, HPSE is a secretory protein which is released in the extracellular environment. Besides cellular localization, immunofluorescence staining of HPSE in 1 week and 2 week CCl_4-injured livers, showed also an extracellular distribution thus suggesting an active secretion of up-regulated HPSE (Fig.12d). Supported by the evidence of HPSE secretion by endothelial cells treated with TNF-α [123], we therefore investigated if TNF-α could also induce secretion of HPSE by TNF-α-activated inflammatory macrophages. To answer this question, U937 were treated with or without TNF-α (10ng/mL) for 24 hours and conditioned media were analyzed for HPSE protein level by Western blot. HPSE was undetectable in the conditioned medium of control cells but it strongly increased in the medium in response to TNF-α stimulation (Fig.19d). Overall these *in vitro* results supported the idea of an autocrine stimulation of HPSE by inflammatory macrophages through TNF-α. To further confirm our observations, TNF-α mRNA expression was measured in the fibrotic liver of mice treated with CCl_4. Compared to control mice, hepatic TNF-α mRNA levels significantly increased in the liver tissues of mice with early chronic

liver disease but not with advance fibrosis. Specifically, TNF-α mRNA levels were up-regulated in 1week (mean ± s.e.m.: 6.87 ± 0.77 *vs*. 1.27 ± 0.26 in CCl_4-treated and control mice respectively) and 2 week (mean ± s.e.m.: 3.11 ± 0.36 *vs*. 0.70 ± 0.05 in CCl_4-treated and control mice respectively) CCl_4-injured livers. On the contrary, no statistically significant difference was found after 8 weeks (mean ± s.e.m.: 2.09 ± 1.25 *vs*. 0.96 ± 0.35 in CCl_4-treated and control mice respectively) and 12 weeks (mean ± s.e.m.: 2.17 ± 0.53 *vs*. 1.58 ± 0.41 in CCl_4-treated and control mice respectively) of CCl_4 delivery (Fig.20a). Moreover, HPSE co-localized with TNF-α in fibrotic mouse livers after 1 and 2 weeks of CCl_4 administration (Fig.20b). The fact that the trend of TNF-α transcription observed during chronic CCl_4 treatment was comparable with that of HPSE expression and keeping in mind HPSE/TNF-α co-staining results, we strongly speculate a TNF-α-mediated HPSE up-regulation.

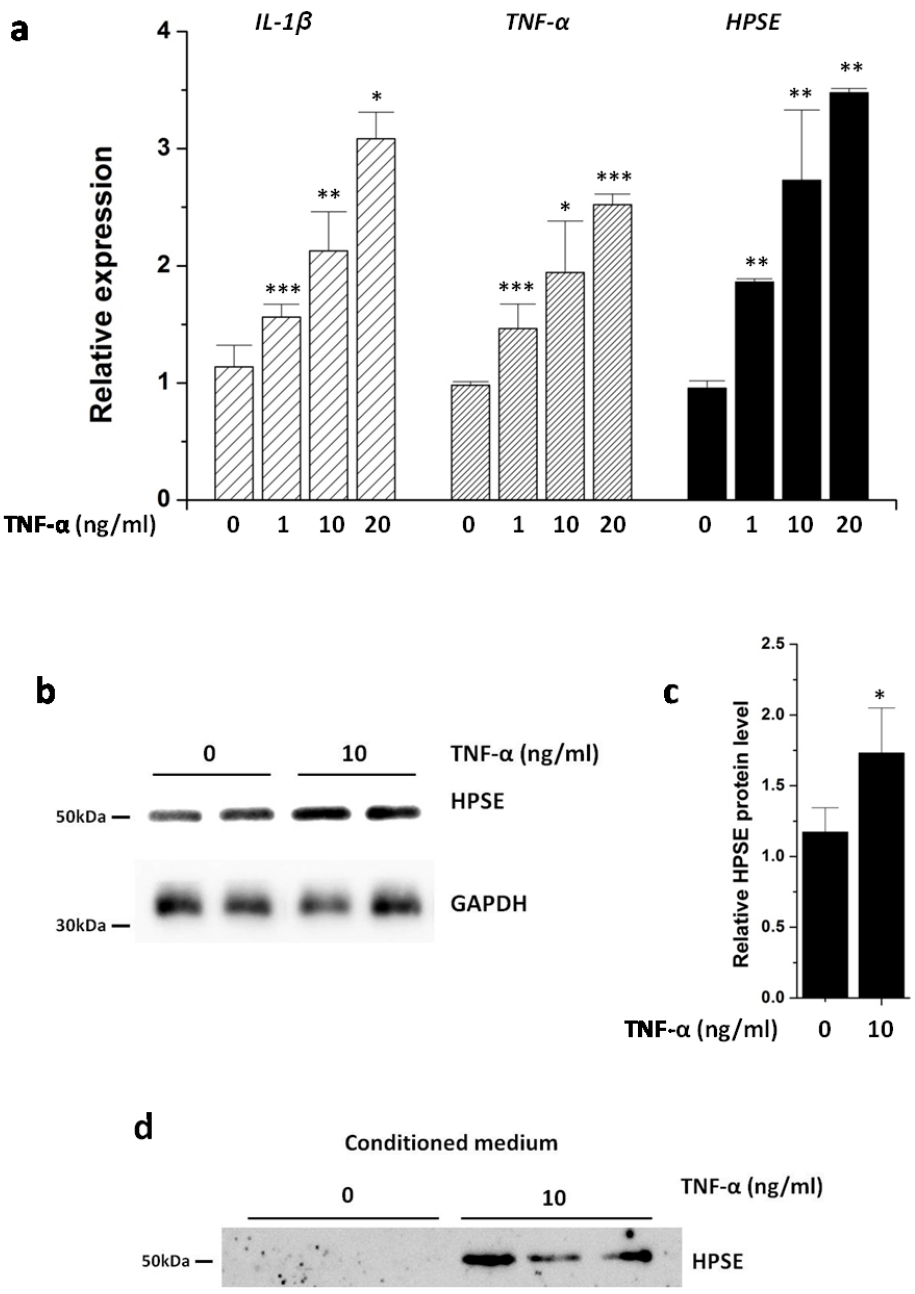

Figure 19. **TNF-α up-regulates HPSE expression and secretion in U937 macrophages**. **(a)** Real-time RT-PCR quantification of IL-1β, TNF-α and HPSE mRNA levels in lysates from U937 treated with different concentrations of TNF-α. mRNA levels were normalized to GAPDH. Error bars represent s.d. *** $p < 0.001$, ** $p < 0.01$, * $p < 0.05$. **(b)** Western blot analysis for HPSE on lysates from control and TNF-α-treated U937. **(c)** Densitometric quantification of HPSE from Western blot showed in panel b. Error bars represent s.d., * $p < 0.05$. **(d)** Western blot analysis for HPSE on conditioned medium from control and TNF-α-treated U937.

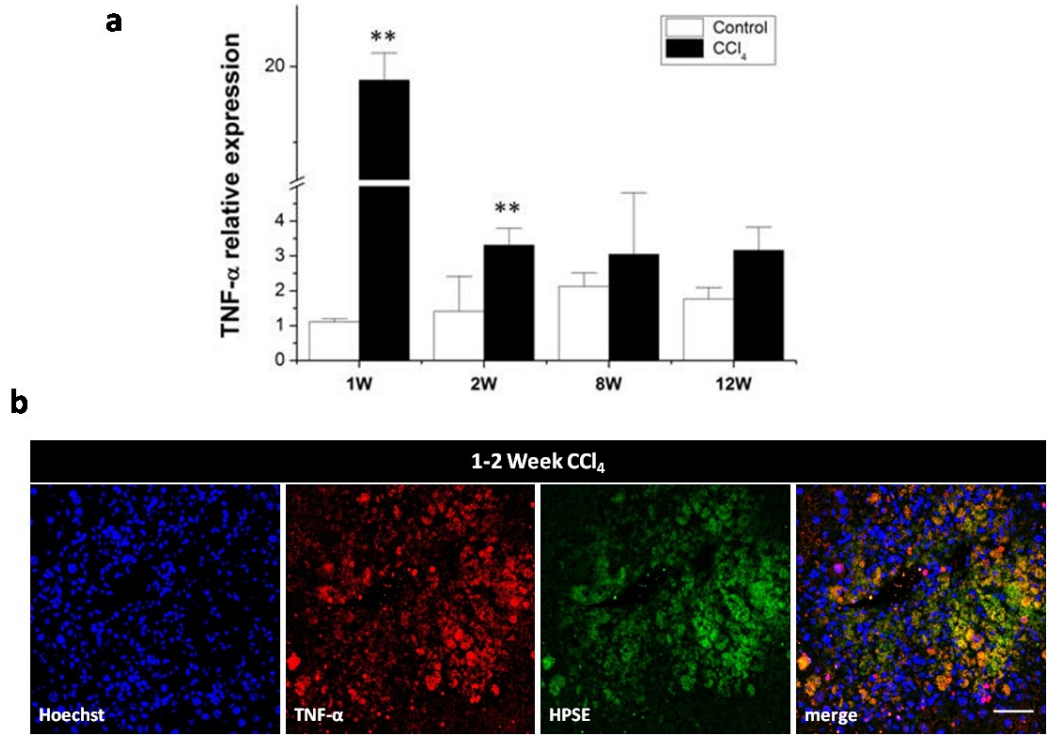

Figure 20. HPSE co-localizes with TNF-α in early CCl_4-injured liver tissues. (a) TNF-α mRNA expression in livers from control and CCl_4-treated mice for the indicated time, measured by real-time RT-PCR and normalized to GAPDH. Error bars represent s.e.m. ** $p < 0.01$. **(b)** Confocal immunofluorescence staining for TNF-α (red signal), HPSE (green signal) and nuclei (blue signal) on liver tissue after 1 week and 2 weeks of CCl_4 administration. Scale bar: 50µm.

4.7 Heparanase expression is up-regulated by IFN-γ and down-regulated by IL-4 in U937 macrophages

Our set of reported experiments highlighted that TNF-α had a regulatory function on HPSE expression in macrophages. We then moved our interest on inflammatory cytokines IL-1β and IFN-γ, supported by published data reporting that the expression of HPSE by endothelial cells is modulated by these molecules [73, 123].

In the initial phase of hepatic injury, Kupffer cells respond to damage by secretion of TNF-α and IL-1β. To test if IL-1β could modulate HPSE expression in macrophages, U937 were treated with IL-1β (10ng/mL) and mRNA levels were measured by real time RT-PCR. Differently from what has been reported for endothelial cells, IL-1β did not up-regulate HPSE expression in our experimental

setting (Fig.21). In the onset of chronic liver injury, DAMPs released by affected parenchymal cells are the first stimuli for Kupffer cells activation. As inflammation is established, other molecules participate in macrophage activation. Among these, IFN-γ is an important stimulus for Kupffer cells polarization into pro-inflammatory M1 macrophages [124]. In U937, HPSE expression was significantly 1.41-fold up-regulated in the presence of IFN-γ (20ng/mL) (Fig.21). Since IFN-γ is the major cytokines released by infiltrating T lymphocytes and NK cells, it is reasonable to suppose that these cells may contribute to HPSE up-regulation in M1 macrophages. As opposed to IFN-γ, IL-4 is one of the major stimulus for polarization in M2 "alternatively activated" or "anti-inflammatory" macrophages [124]. Interestingly, treating cells with IL-4 (20ng/mL) caused a significant down-regulation of HPSE (mean ± s.d.: 0,42 ± 0.02 vs. 1.02 ± 0.03 in treated and control cells respectively) (Fig.21). These results suggested that macrophages could differently express HPSE accordingly to M1or M2 direction of polarization.

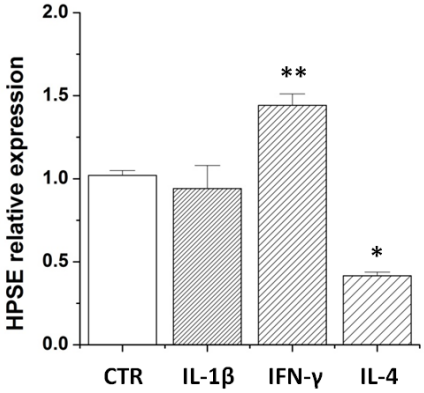

Figure 21. Effect of IL-1β, IFN-γ and IL-4 cytokines on HPSE expression in U937 macrophages. Determination of HPSE mRNA levels by real time RT-PCR in U937 treated with IL-1β, IFN-γ and IL-4 for 24 hours. Expression levels were normalized to GAPDH. Error bars represent s.d.
** $p < 0.01$, * $p < 0.01$.

4.8 Heparanase regulates HSCs activation

HSCs are the most important effector cells in liver fibrosis since they are responsible for ECM deposition. Activation of HSCs in the early stage of injury is

orchestrated by all neighboring liver cells through paracrine stimulation. Together with ROS from damaged hepatocytes and signals from liver sinusoidal endothelial cells, TGF-β and PDGF released by Kupffer cell drive HSCs early activation and proliferation [104]. The role of HPSE in regulating the bioavailability and activity of cytokines and growth factors by HS cleavage is well established and affects a variety of physiological and pathological processes. This notion together with the increased synthesis and secretion of HPSE in liver tissue in early chronic injury led us to hypothesize that HPSE may influence the behavior of HSCs.

To understand whether macrophage-derived HPSE could be a regulator of HSCs activation, we set up an experiment using HPSE-rich conditioned medium of U937. As schematically represented in Figure 22a, U937 were treated with or without TNF-α for 24 hours to induce HPSE expression. After treatment, medium was aspirated and replaced with fresh medium without serum. The conditioned media of treated cells (containing HPSE) and untreated cells (with low HPSE) were collected after 24 hours and used to treat LX-2 cells, a human HSCs cell line. To verify the role of HPSE, LX-2 cells were treated with U937 conditioned medium in the presence or absence of the heparin-derived HPSE inhibitor SST0001 (500µg/mL). LX-2 cells were treated 24 hours prior to RNA and protein extractions. The expression of the myofibroblast marker α-SMA and of fibronectin was measured in LX-2 cells by real time RT-PCR. Treatment with the conditioned medium of TNF-α activated macrophages, induced a significant 2.64-fold up-regulation of α-SMA and 1.59-fold up-regulation of fibronectin mRNA levels as compared to treatment with the conditioned medium of untreated U937. However, when LX-2 cells were treated with the conditioned medium of TNF-α activated macrophages in combination with SST0001, the increase of both α-SMA and fibronectin mRNA were significantly diminished (Fig.22b). Indeed, the expressions were 1.80-fold and 1.27-fold increased respectively compared to controls. These transcriptional data were also confirmed at protein level by Western blot analyses (Fig.22c). Among soluble mediators, VEGF is one of the major growth factor expressed and secreted by activated HSCs [125]. Since HPSE is known to regulate VEGF expression [59], we investigated if it could modulate its transcription also in HSCs. The expression of VEGF was 3.44 fold up-regulated in LX-2 stimulated with the conditioned medium of TNF-α activated U937 *vs*. cells stimulated with the conditioned medium of untreated U937. The

addition of SST0001, however, did not affect VEGF expression which was 3.61-fold increased (Fig.22b). Protein analysis by Western blot confirmed real time RT-PCR data (Fig.22c). These results implied that HPSE may modulate HSCs activation and highlighted a new mechanism by which inflammatory macrophages control HSCs activity.

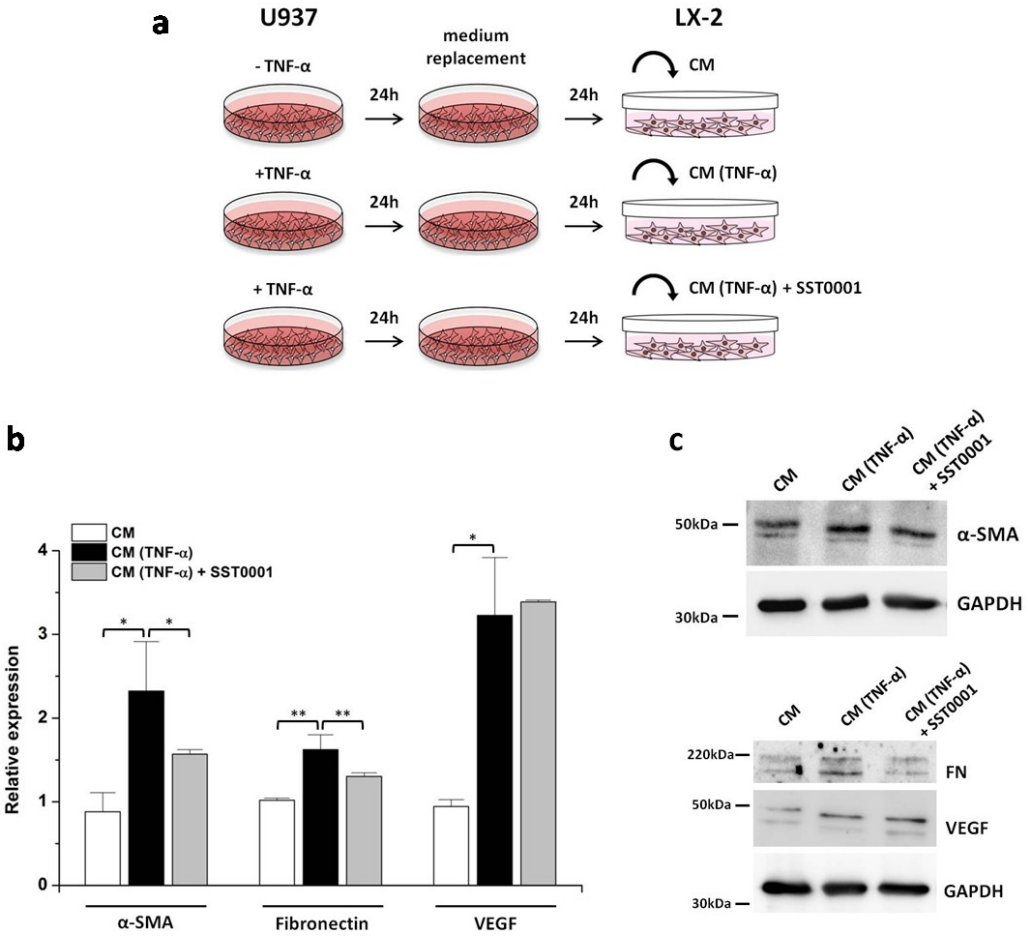

Figure 22. HPSE regulates HSCs activation. (a) Experimental protocol of conditioned medium experiment. U937 were incubated with or without TNF-α (10ng/mL) for 24 hours after which they were maintained 24 hours in medium -FCS. Conditioned media from untreated (CM) and pre-treated (CM (TNF-α)) U937 were collected and transferred to serum starved LX-2 with or without SST0001. **(b)** Gene expression of α-SMA, fibronectin and VEGF measured in LX-2 treated with CM, CM(TNF-α) and CM(TNF-α) + SST0001. mRNA levels were determined by real-time RT-PCR and normalized to GAPDH. Error bars represent s.d. ** $p < 0.01$, * $p < 0.05$. **(c)** Western blot of α-SMA, fibronectin and VEGF from LX-2 treated with CM, CM(TNF-α) and CM(TNF-α) + SST0001.

4.9 Heparanase regulates RAW 264.7 macrophages migration

Promotion of tumor cell migration through matrix disassembly is a well known pro-cancerous role of HPSE. HPSE facilitates immune cells extravasation as well, by altering the ECM integrity and by releasing HS-bound signaling molecules. HPSE favors cell migration also independently from its enzymatic activity. Indeed, HPSE can act on a cell surface receptor and switch on signaling pathways leading to migration [58, 126]. Macrophage migration to the site of injury is an hallmark of inflammation initiation. To evaluate the impact of exogenously added latent HPSE on macrophage migration, the wound healing assay was employed using the RAW 264.7 cell line. U937 were not considered for these set of experiments since the use of PMA to induce their differentiation results in loss of cell proliferative activity and in difficulty to obtain the confluence necessary for the assay.

RAW 264.7 confluent monolayers were scraped with a 200µL pipette tip and treated with or without latent HPSE (1µg/mL). The migration rate of RAW 264.7 treated with latent HPSE was also evaluated in addition to the HPSE inhibitor SST0001 (500µg/mL). Although this heparin-derived molecule is commonly used to inhibit HPSE enzymatic activity, it is known that an excess heparin competes with the binding of latent HPSE to membrane HSPGs and receptors thus preventing its uptake and other non-enzymatic functions [41]. Migration into the wounded areas was examined for 30 hours and images were captured at different time points after treatment (6, 24, 30 hours). The addition of latent HPSE stimulated an increase in RAW 264.7 migration as compared to untreated cells. During the entire course of the treatment HPSE-treated cells showed enhanced migration rate with respect to control cells reaching the statistic significance after 30 hours. As shown in Figure 23, after 6 hours from scratch, the percentage of wound area closed by HPSE-treated cells was 21.6% vs. 30.8% closed by untreated cells. After 24 hours wound closure increased to 42.4% in HPSE-treated cells and to 33.6% in untreated cells. At the end of the treatment (30 hours), 45.9% of wound area was closed by HPSE-treated cells while only 28.4% by control cells. Addition of HPSE together with SST0001, inhibited the migratory effect of latent HPSE. Migration rate of HPSE-treated cells was comparable to

that of untreated cells when the SST0001 inhibitor was added: 21.6% at 6 hours post scratch, 34.4% at 24 hours and 34% at 24 hours.

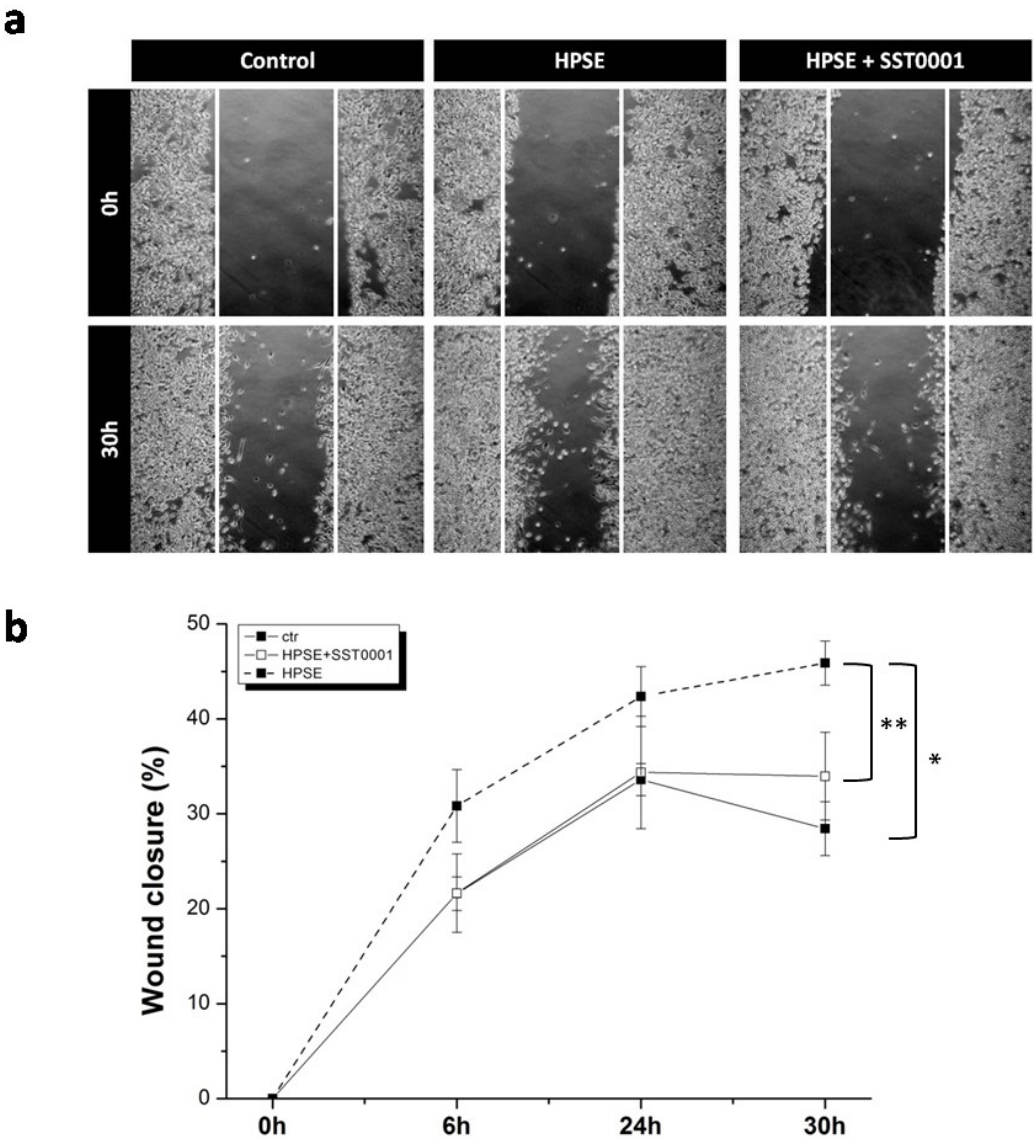

Figure 23. HPSE stimulates macrophage migration. (a) Wound healing assay of RAW 264.7 cells. Wounds was created after confluence and cells were treated with latent HPSE alone (1µg/mL) or plus SST0001 inhibitor (500µg/mL). Migration into the wound was monitored after 6, 24 and 30 hours post scratch. Representative images at 0 and 30 hours are shown (original magnification 10X). White lines indicate the boundary of scratch. **(b)** Quantification of wound closure. The area of the wound was measured at each time point and migration rate was expressed as percentage reduction of the initial scratch. Data are the mean ± s.e.m. of six measurement for each condition. ** $p < 0.01$, * $p < 0.05$.

4.10 Heparanase plasma activity negatively correlates with human liver stiffness

The study of HPSE expression in the CCl_4 mouse model of chronic liver disease revealed that HPSE increased in liver tissue in response to injury. However, its expression was not progressively enhanced with prolonged injury but decreased to basal control level suggesting its involvement only in the early stage of the disease. In patients affected by diseases in which HPSE is up-regulated (i.e. diabetes, renal disease, cancer), the level of HPSE increases also in biological fluids (plasma and/or urine) [90, 122, 127].

To further investigate HPSE role in the development of liver fibrosis, we aimed to correlate the stage of chronic liver disease with HPSE activity in the plasma of human patients. For this scope, HPSE activity was quantified in the collected plasma from 68 subjects utilizing a modified ELISA assay. The study population included 14 healthy volunteers and 68 patients with various chronic liver diseases and different fibrotic stages. According to the etiology, patients were categorized in two main subgroups: chronic autoimmune liver disease subgroup which included patients with AIH, PBC, PSC and overlap syndromes and chronic viral hepatitis subgroup which included patients with HBV and HCV. The stage of chronic liver disease, in terms of liver fibrosis, was determined by performing transient elastography (Fibroscan) which quantifies liver stiffness in kPa. The Fibroscan liver stiffness measurements were used to categorize patients according to their histological stage of fibrosis ranging from F0-1 (absent or mild fibrosis) to F2 (significant fibrosis), F3 (sever fibrosis) and F4 (cirrhosis). HPSE plasma activity was higher in patients with autoimmune liver disease at F0-F1 (n=17) and F2-F3 (n=13) stages of fibrosis (mean ± s.e.m.: 0.30 ± 0.03, 0.22 ± 0.03 respectively) with respect to healthy control group (mean ± s.e.m.: 0.06 ± 0.01) and these increases were statistically significant. However, HPSE plasma activity was not increased in patients with F4 fibrosis stage (n=7) (mean ± s.e.m.: 0.05 ± 0.02) compared to controls. In patients with chronic viral hepatitis, HPSE plasma activity was elevated in F0-F1 (n=8) and F2-F3 (n=6) fibrotic stages (mean ± s.e.m.: 0.35 ± 0.11, 0.29 ± 0.08 respectively) compared to healthy controls and these increases were statistically significant. As observed in cirrhotic patients with autoimmune liver diseases, also cirrhotic patients affected by HCV and HBV

(n=21) had basal plasma HPSE activity (mean ± s.e.m.: 0.08 ± 0.03) (Fig.24a). In summary, independently from the etiology of liver disease, HPSE plasma activity was markedly elevated in patients with mild, significant and severe liver fibrosis as compared to healthy controls but not in patients with cirrhosis. To better represent the trend of HPSE plasma activity in chronic liver disease progression, for each patient HPSE activity was plotted against liver stiffness, expressed in kPa. We found that HPSE activity negatively correlated with the organ stiffness both in autoimmune liver diseases (R=0.23, p=0.002) and viral hepatitis (R=0.24, p=0.004) (Fig.24b).

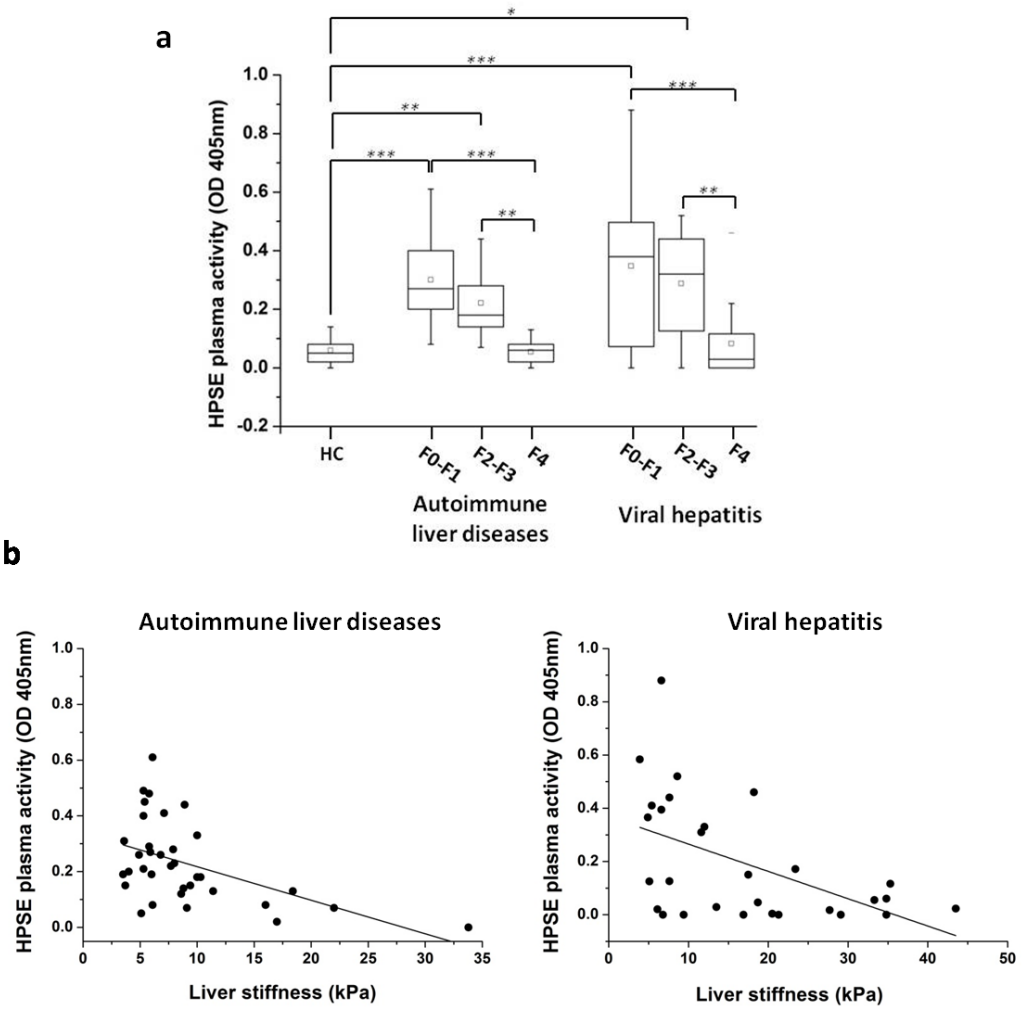

Figure 24. Heparanase plasma activity in patients with chronic liver diseases. (a) Box-plot of HPSE activity in the plasma of healthy controls (HC) (n=14) and patients with autoimmune liver diseases (n=37) and viral hepatitis (n=35). Patients were staged from F0 to F4 according to fibrosis. Squares represent mean values. *** $p < 0.001$, ** $p < 0.01$, * $P < 0.05$. **(b)** Scatter-plot of HPSE activity quantified in the plasma of patients with autoimmune liver diseases (left graph) and viral hepatitis (right graph) and correlated to liver stiffness. Trend lines are represented.

5. Discussion

Chronic liver injury is characterized by necrosis and inflammation which trigger fibrosis and may lead to cirrhosis and functional failure. Activation and proliferation of non-parenchymal cells (HSCs and resident macrophages) sustains the wound-healing response. In parallel, proliferation of parenchymal hepatocytes sustains the regenerative process. All these events aim at recovering and maintaining organ functions but, when deregulated by prolonged injury, result in uncontrolled fibrogenesis, ECM accumulation and disrupted organ architecture [103]. In this process, aberrant deposition of EMC proteins (collagens, fibronectin and laminin) is not counterbalanced by ECM degradation. Indeed, the major collagen-degrading enzymes, MMPs, are down-regulated by activated liver cells and substituted with their inhibitor TIMPs thus exacerbating fibrosis. However, ECM degradation also occurs during liver injury. In particular, at the initial steps of injury, migration of infiltrating cells at the site of injury and of myofibroblasts into the surrounding tissue, required the disruption of basal membranes which is mediated by MMPs [107]. In mammals, among the enzyme that degrade ECM and basal membranes, heparanase (HPSE) is the unique with the ability to degrade HS chains of HSPGs which are structural components of basal membranes. HPSE is able to cut these chains at specific sites, generating fragments of about 5-7kDa. Due to this function, intracellular endosomal HPSE promotes the turnover of cell surface-associated HSPGs while secreted HPSE promotes ECM remodeling and degradation [128]. Degradation of matrix by HPSE favours tumor cells invasion and migration in cancer and contributes to glomerular basement membrane disassembly and proteinuria in kidney diseases. Indirectly, extracellular HPSE activity plays fundamental roles both in physiological and pathological processes if considering the broad range of molecules (growth factors, cytokines, chemokines, enzymes) that negatively charged HS are able to bind and that are left to diffuse upon HPSE cleavage. In this sense, the release of VEGF and FGF-2, mediated by HPSE, is relevant for tumor angiogenesis. The release of HS-FGF-2 bioactive molecules is also relevant for tubular EMT induction in kidney interstitial fibrosis [42]. In the contest of inflammation, HPSE plays a role in inflammatory cells extravasation and macrophage activation. Interesting data have

emerged from chronic colitis and diabetic nephropathy mouse models both supporting a chronic inflammatory circuit connecting injured epithelial cells and inflammatory macrophages and mediated by HPSE [64]. Taken together, these studies highlight the importance of HPSE in sustaining inflammation and fibrosis which we hypothesized could be transposed to liver milieu as well. In particular, we questioned whether HPSE could be up-regulated by injured liver and which could be the implications for liver fibrogenesis.

The expression of HPSE by fibrotic liver has been already analysed in the mouse model of thioacetamide-induced fibrosis with contrasting results and with no deep investigation in its regulation and possible effects [48, 117]. To shed light into HPSE regulation during chronic liver disease, we investigated its tempo-spatial pattern of expression in the well-established animal model of CCl_4-induced fibrosis. BALB/cJ mice were used as most sensitive to fibrosis induction [129] and were injected with CCl_4 for 1, 2, 8 and 12 weeks. Periodic administration of CCl_4 in mice caused massive centrilobular hepatic inflammation and necrosis in the very early chronic liver injury. These histopathological modifications reflected the mechanism of CCl_4 toxicity and the different metabolizing properties of the parenchymal acinar zones. In fact, CCl_4 is predominantly metabolized by zone 3 hepatocytes which express cytochrome CYP21E, giving rise to toxic radicals [129]. HSCs, activated at the site of injury, started to produce and secrete collagen fibers leading to perisinusoidal fibrosis in the affected regions. CCl_4 delivery for prolonged time resulted in bridging fibrosis and micronodular cirrhosis. Herein, our data showed that HPSE underwent up-regulation in response to CCl_4 liver insult. Interestingly, HPSE expression did not increase concomitantly with fibrosis but progressively decreased during liver injury to return at basal level after 8 and 12 weeks of treatment. This time-limited expression suggests that HPSE may have a role in chronic disease only in the early period. In early fibrotic injured liver tissue, HPSE expression was also restricted in term of spatial distribution, being localized only at the necrotic and inflamed centrilobular zones with both a diffuse and a vesicular pattern indicating that HPSE up-regulation was accompanied by its secretion in the extracellular environment. Since HPSE was not localized within hepatocytes, we focused our investigation on non-parenchymal cells. During liver fibrosis, quiescent HSCs are

activated into fibrogenic α-SMA positive myofibroblasts by a plethora of paracrine and autocrine stimuli. These cells profoundly alter the microenvironment by the secretion of excessive ECM proteins [104]. Three main considerations let us to investigate on HPSE expression by HSCs: first, the need of HSCs to degrade basal membrane at early step of injury in order to migrate in the surrounding tissue [107]; second, the role of HPSE in regulating the transdifferentiation of cells [101]; third, the presence of abundant HPSE in centrilobular fibrotic area. To analyse HPSE expression by HSCs, primary cultures were established and characterized. Here we showed that HPSE expression increased during *in vitro* activation of HSCs together with α-SMA and ECM proteins and it was detected in perinuclear vesicles. Experiments of double immunostaining on early injured mouse liver samples confirmed HPSE expression by activated HSCs but revealed also that majority of signal was localized in neighbouring cells. Indeed, imunofluorescence analyses with the macrophage markers F4/80 and CD68 showed that HPSE strongly co-localized with inflammatory macrophages. It is well known that necrotic hepatocytes are a potent stimulus for the activation of resident macrophages (Kupffer cells) which, in turn, attract infiltrating monocytes through chemokines secretion [124]. In inflamed liver tissue, F4/80 and CD68 stainings alone are not sufficient to discriminate Kupffer cells from infiltrating monocyte-derived macrophages. It is reasonable to think that, under the same milieu, both resident and blood-derived macrophages can contribute to the increase of HPSE. Flow cytometry analysis of liver macrophage cells after CCl_4 injury would help us to better clarify this point. Thus, differently from chronic colitis and diabetic nephropathy in which HPSE increase is preferentially addicted to epithelial cells [74, 81], in our model HPSE was primarily expressed by inflammatory macrophages and, to a lesser extent, by activated HSCs in early chronic liver injury.

We next aimed to gain insight into the mechanism of HPSE up-regulation upon liver injury. Multiple inflammatory mediators (LPS, IL-1β, IFN-γ and TNF-α) affect HPSE expression in different cell types. These molecules were tested on primary isolated Kupffer cells and U937 cell line to measure HPSE expression. Although the classical inflammatory stimulus LPS up-regulates HPSE in isolated peripheral blood mononuclear cells (PBMC) [122], we observed that treating primary Kupffer cells with LPS did not affect HPSE expression. This result was

confirmed also at protein level by immunofluorescence analysis in which, however, HPSE was detected both in untreated and treated cells. A possible explanation for the unexpected HPSE immunopositivity in primary isolated Kupffer cells could be the protocol used for their isolation (see paragraph 3.2.1.1). Accordingly to this protocol, Kupffer cells are selectively isolated after about 15 days of culture during which they proliferate by semi-adhering on a monolayer of a parenchymal cell-rich population. It is plausible that this co-culture system with different cell crass-talk may affect gene expression including that of HPSE.

Conversely, TNF-α induced augmented HPSE mRNA level in Kupffer cells and U937. Increased HPSE protein in response to TNF-α was also detected in U937. These data further support the ability of TNF-α to regulate HPSE expression that was already observed in epithelial and endothelial cells. In their work on HPSE regulation by inflammatory cytokines, Chen *et al*., showed that TNF-α and IL-β induce HPSE expression and secretion in endothelial cells [123]. Herein, we showed that TNF-α, but not IL-1β, induced HPSE transcription in U937. In chronic diseases, TNF-α is a major inflammatory cytokine secreted by macrophages in response to damaged cells. The role of TNF-α in regulating HPSE expression has emerged also in chronic colitis and diabetic nephropathy in which macrophage-derived TNF-α induces HPSE expression in epithelial cells (colonic and tubular cells respectively) [74, 81]. Interestingly, in our model of chronic liver disease, TNF-α functioned also as an autocrine stimulus for macrophages themselves which were induced to produce and secrete HPSE. Our *in vitro* results were also supported by two *in vivo* observations: i) HPSE strongly co-localized with TNF-α in 1 and 2 week CCl_4-treated livers and ii) TNF-α mRNA expression was significantly higher only at early time point of CCl_4 injury (in agreement with the necro-inflammatory activity that we observed histologically) and this trend corresponded to that of HPSE expression.

Among other inflammatory stimuli, IFN-γ and IL-4 were also tested on U937 macrophages. These cytokines are well known antagonist in macrophage polarization, promoting M1 phenotype the first and M2 phenotype the second [124]. Interestingly, these molecules acted antagonistically also in regulating HPSE gene expression. Indeed we found that IFN-γ stimulated HPSE gene transcription. In contrast, IL-4 down-regulated its expression. Considering the

inflammatory milieu of chronic liver injured tissue with an heterogeneous pool of cytokines and growth factors, it is plausible that different molecules derived from different cells may cooperate to HPSE up-regulation. In this sense, TNF-α and IFN-γ from T-lymphocytes and NK cells could both increase HPSE in macrophages. These results also opened interesting questions about HPSE expression from differently polarized macrophages which could be investigated in the future. Thus, with this PhD thesis, we provided evidences that hepatic HPSE increased in early stage of injury and that this increase was strictly dependent on inflammatory macrophages in response to TNF-α stimulation and presumably to IFN-γ. To a lesser extent, HSCs contributed to the HPSE rise as well.

The interest on the effect of HPSE on macrophages activation in chronic inflammation is increasing and led to the discovery that HPSE modulates inflammatory phenotype of macrophages through TLRs thus exacerbating chronic inflammation [79]. Since this role has been deeply investigated and is plausible that could be transposed in liver context, we decided to move our investigation from inflammation to fibrosis and we wondered what might be the effects of HPSE up-regulation on fibrogenesis. We therefore evaluated whether HPSE could influence HSCs and macrophage behaviour. In the complex cellular cross-talk that characterize chronic liver injury, activated Kupffer cells are the major stimulus for HSCs activation at early steps, by releasing pro-fibrogenic growth factors [103]. A tight proximity of HSCs and extracellular HPSE was clearly evident in our immunofluorescence stainings and it opened the question whether macrophage-derived HPSE could have a role in HSCs activation. To analyse such interaction, the conditioned medium of activated U937 cells, enriched in HPSE by pre-treatment with TNF-α, was used to stimulate LX-2 cells. The involvement of HPSE was verified by the addition of an HPSE inhibitor. We provided evidence that HPSE participated in the regulation of fibrogenic α-SMA and fibronectin expression by activated HSCs. The induction of VEGF, whose expression is known to be induced by HPSE in endothelial cells [59], was not regulated by HPSE in HSCs. A pro-fibrogenic role of HPSE has been already demonstrated in kidney fibrosis by our group, through the regulation of FGF-2 and TGF-β bioavailability [42] and HPSE regulation of the activity of these pro-fibrotic factors on HSCs will be studied. We then investigated whether HPSE could affect macrophage migration. The role of HPSE in extracellular matrix remodeling and

the fact that this activity affects cell migration is obvious both in physiological and pathological processes, in particular in tumors. In liver context of important tissue destruction in which high levels of HPSE were detected, it is discounted that HPSE may favour cellular migration through ECM degradation. This is the reason why we focused our attention on non enzymatic activity of HPSE. A suggestion derived from recent data that HPSE stimulates cell migration independently from enzymatic activity and through activation of specific signaling pathways [58, 126]. Herein we showed that treatment of macrophages with latent HPSE caused a significant increase in cell migration, indicating that also HPSE precursor may affect macrophage behaviour.

Considering the transient HPSE expression observed in the CCl_4 mouse model of liver fibrosis, HPSE activity was measured in the plasma of patients with chronic liver disease and correlated with the stage of the pathology. Elevated levels of HPSE activity were found in the plasma of patients with mild, significant and severe fibrosis but dramatically decreased to basal levels in cirrhotic patients. This observation strongly supported *in vivo* data from the animal model and it provided further evidence of an early involvement of HPSE in liver disease. Moreover, the fact that these results were observed both in patients with autoimmune liver disease and with viral hepatitis indicated that the pathological events that lead to HPSE up-regulation could be reproducible in chronic liver disease of different etiology.

6. Conclusions

The interest on HPSE in acute and chronic inflammatory disease and cancer-related inflammation is increased in the last decade and has led to the discovery of novel pro-inflammatory and pro-fibrogenic roles for this enzyme. This work represent the first study aimed at investigating the involvement of HPSE in chronic liver disease. With a set of *in vitro*, *in vivo* and *ex vivo* experiments we provided evidences that HPSE is involved in chronic liver injury but it is not correlated with the progression of the disease. Collectively, our proposed model of cascade of events can be summarized as follow. In response to damaged parenchymal cells, Kupffer cells trigger inflammation by secretion of inflammatory cytokines and chemokines. Among these, TNF-α, acting on macrophages themselves, induces the expression and secretion of HPSE. We suppose that macrophage-derived HPSE sustains early steps of fibrogenesis through basal membrane degradation for cell migration and the release of ECM-bound growth factors that trigger HSCs activation. HSCs themselves up-regulate HPSE upon their activation. HPSE has also a pro-migratory effect on macrophages independently from its enzymatic activity.

The fact that HPSE is involved in the initial steps of the disease acquires even more relevance if considering that the probability of fibrosis resolution decreases with advance disease and that the discovery of early pharmacological targets is crucial. With these premises, to better elucidate the biological significance and the functional role of HPSE in chronic liver disease is necessary to understand if HPSE may be a target for therapeutic intervention in patients with liver fibrosis/cirrhosis. In this efforts, we are now planning to evaluate the effects of CCl_4 chronic administration in heparanase-null (HPSE-KO) mice. HPSE-KO mice are fertile and viable. In the STZ-induced diabetes model, these mice do not develop diabetic nephropathy compared to wild type mice. In addition, kidney tissue from KO-mice showed less F4/80 and TGF-β expression and less interstitial fibrosis [85]. These observations further encourage us to investigate the response of HPSE-KO mice to hepatotoxin delivery.

In conclusion, this work of PhD thesis unveils a novel role for HPSE in the early onset of liver fibrogenesis, connecting inflammation to tissue remodelling.

7. Bibliography

1. Couchman, J.R. and C.A. Pataki, *An introduction to proteoglycans and their localization.* J Histochem Cytochem, 2012. **60**(12): p. 885-97.
2. Iozzo, R.V. and L. Schaefer, *Proteoglycan form and function: A comprehensive nomenclature of proteoglycans.* Matrix Biol, 2015. **42**: p. 11-55.
3. Farrugia, B.L., et al., *Can we produce heparin/heparan sulfate biomimetics using "mother-nature" as the gold standard?* Molecules, 2015. **20**(3): p. 4254-76.
4. Bishop, J.R., M. Schuksz, and J.D. Esko, *Heparan sulphate proteoglycans fine-tune mammalian physiology.* Nature, 2007. **446**(7139): p. 1030-7.
5. Sarrazin, S., W.C. Lamanna, and J.D. Esko, *Heparan sulfate proteoglycans.* Cold Spring Harb Perspect Biol, 2011. **3**(7).
6. Mohammadi, M., S.K. Olsen, and O.A. Ibrahimi, *Structural basis for fibroblast growth factor receptor activation.* Cytokine Growth Factor Rev, 2005. **16**(2): p. 107-37.
7. Manon-Jensen, T., Y. Itoh, and J.R. Couchman, *Proteoglycans in health and disease: the multiple roles of syndecan shedding.* FEBS J, 2010. **277**(19): p. 3876-89.
8. Iozzo, R.V., *Basement membrane proteoglycans: from cellar to ceiling.* Nat Rev Mol Cell Biol, 2005. **6**(8): p. 646-56.
9. Bezakova, G. and M.A. Ruegg, *New insights into the roles of agrin.* Nat Rev Mol Cell Biol, 2003. **4**(4): p. 295-308.
10. Marneros, A.G. and B.R. Olsen, *Physiological role of collagen XVIII and endostatin.* FASEB J, 2005. **19**(7): p. 716-28.
11. Kolset, S.O. and H. Tveit, *Serglycin--structure and biology.* Cell Mol Life Sci, 2008. **65**(7-8): p. 1073-85.
12. Jin, L., et al., *The anticoagulant activation of antithrombin by heparin.* Proc Natl Acad Sci U S A, 1997. **94**(26): p. 14683-8.
13. Stewart, M.D. and R.D. Sanderson, *Heparan sulfate in the nucleus and its control of cellular functions.* Matrix Biol, 2014. **35**: p. 56-9.

14. Rivara, S., F.M. Milazzo, and G. Giannini, *Heparanase: a rainbow pharmacological target associated to multiple pathologies including rare diseases.* Future Med Chem, 2016. **8**(6): p. 647-80.
15. Dong, J., et al., *Genomic organization and chromosome localization of the newly identified human heparanase gene.* Gene, 2000. **253**(2): p. 171-8.
16. Vlodavsky, I., et al., *Mammalian heparanase: gene cloning, expression and function in tumor progression and metastasis.* Nat Med, 1999. **5**(7): p. 793-802.
17. Toyoshima, M. and M. Nakajima, *Human heparanase. Purification, characterization, cloning, and expression.* J Biol Chem, 1999. **274**(34): p. 24153-60.
18. Hulett, M.D., et al., *Cloning of mammalian heparanase, an important enzyme in tumor invasion and metastasis.* Nat Med, 1999. **5**(7): p. 803-9.
19. Kussie, P.H., et al., *Cloning and functional expression of a human heparanase gene.* Biochem Biophys Res Commun, 1999. **261**(1): p. 183-7.
20. Miao, H.Q., et al., *Cloning, expression, and purification of mouse heparanase.* Protein Expr Purif, 2002. **26**(3): p. 425-31.
21. Goldshmidt, O., et al., *Expression pattern and secretion of human and chicken heparanase are determined by their signal peptide sequence.* J Biol Chem, 2001. **276**(31): p. 29178-87.
22. Nasser, N.J., et al., *Adaptive evolution of heparanase in hypoxia-tolerant Spalax: gene cloning and identification of a unique splice variant.* Proc Natl Acad Sci U S A, 2005. **102**(42): p. 15161-6.
23. Kizaki, K., et al., *Cloning and localization of heparanase in bovine placenta.* Placenta, 2003. **24**(4): p. 424-30.
24. McKenzie, E., et al., *Cloning and expression profiling of Hpa2, a novel mammalian heparanase family member.* Biochem Biophys Res Commun, 2000. **276**(3): p. 1170-7.
25. Levy-Adam, F., et al., *Heparanase 2 interacts with heparan sulfate with high affinity and inhibits heparanase activity.* J Biol Chem, 2010. **285**(36): p. 28010-9.
26. Peterson, S.B. and J. Liu, *Multi-faceted substrate specificity of heparanase.* Matrix Biol, 2013. **32**(5): p. 223-7.

27. Gong, F., et al., *Processing of macromolecular heparin by heparanase.* J Biol Chem, 2003. **278**(37): p. 35152-8.
28. Simizu, S., et al., *Secretion of heparanase protein is regulated by glycosylation in human tumor cell lines.* J Biol Chem, 2004. **279**(4): p. 2697-703.
29. Ben-Zaken, O., et al., *Low and high affinity receptors mediate cellular uptake of heparanase.* Int J Biochem Cell Biol, 2008. **40**(3): p. 530-42.
30. Ben-Zaken, O., et al., *Heparanase induces Akt phosphorylation via a lipid raft receptor.* Biochem Biophys Res Commun, 2007. **361**(4): p. 829-34.
31. Shteingauz, A., N. Ilan, and I. Vlodavsky, *Processing of heparanase is mediated by syndecan-1 cytoplasmic domain and involves syntenin and alpha-actinin.* Cell Mol Life Sci, 2014. **71**(22): p. 4457-70.
32. Wu, L., et al., *Structural characterization of human heparanase reveals insights into substrate recognition.* Nat Struct Mol Biol, 2015. **22**(12): p. 1016-22.
33. Levy-Adam, F., et al., *Identification and characterization of heparin/heparan sulfate binding domains of the endoglycosidase heparanase.* J Biol Chem, 2005. **280**(21): p. 20457-66.
34. Fux, L., et al., *Structure-function approach identifies a COOH-terminal domain that mediates heparanase signaling.* Cancer Res, 2009. **69**(5): p. 1758-67.
35. van den Hoven, M.J., et al., *Heparanase in glomerular diseases.* Kidney Int, 2007. **72**(5): p. 543-8.
36. Shafat, I., I. Vlodavsky, and N. Ilan, *Characterization of mechanisms involved in secretion of active heparanase.* J Biol Chem, 2006. **281**(33): p. 23804-11.
37. Riaz, A., et al., *Characterization of heparanase-induced phosphatidylinositol 3-kinase-AKT activation and its integrin dependence.* J Biol Chem, 2013. **288**(17): p. 12366-75.
38. Wang, F., et al., *Fatty acid-induced nuclear translocation of heparanase uncouples glucose metabolism in endothelial cells.* Arterioscler Thromb Vasc Biol, 2012. **32**(2): p. 406-14.

39. Nobuhisa, T., et al., *Translocation of heparanase into nucleus results in cell differentiation.* Cancer Sci, 2007. **98**(4): p. 535-40.
40. Yang, Y., et al., *Nuclear heparanase-1 activity suppresses melanoma progression via its DNA-binding affinity.* Oncogene, 2015. **34**(47): p. 5832-42.
41. Schubert, S.Y., et al., *Human heparanase nuclear localization and enzymatic activity.* Lab Invest, 2004. **84**(5): p. 535-44.
42. Secchi, M.F., et al., *Recent data concerning heparanase: focus on fibrosis, inflammation and cancer.* Biomol Concepts, 2015. **6**(5-6): p. 415-21.
43. Shteper, P.J., et al., *Role of promoter methylation in regulation of the mammalian heparanase gene.* Oncogene, 2003. **22**(49): p. 7737-49.
44. Baraz, L., et al., *Tumor suppressor p53 regulates heparanase gene expression.* Oncogene, 2006. **25**(28): p. 3939-47.
45. Vlodavsky, I., et al., *Expression of heparanase by platelets and circulating cells of the immune system: possible involvement in diapedesis and extravasation.* Invasion Metastasis, 1992. **12**(2): p. 112-27.
46. Nasser, N.J., *Heparanase involvement in physiology and disease.* Cell Mol Life Sci, 2008. **65**(11): p. 1706-15.
47. D'Souza, S.S., et al., *Heparanase expression and function during early pregnancy in mice.* Biol Reprod, 2007. **77**(3): p. 433-41.
48. Goldshmidt, O., et al., *Heparanase expression during normal liver development and following partial hepatectomy.* J Pathol, 2004. **203**(1): p. 594-602.
49. Zcharia, E., et al., *Heparanase regulates murine hair growth.* Am J Pathol, 2005. **166**(4): p. 999-1008.
50. Malgouries, S., et al., *Heparanase 1: a key participant of inner root sheath differentiation program and hair follicle homeostasis.* Exp Dermatol, 2008. **17**(12): p. 1017-23.
51. Zcharia, E., et al., *Heparanase accelerates wound angiogenesis and wound healing in mouse and rat models.* FASEB J, 2005. **19**(2): p. 211-21.
52. Nadir, Y., *Heparanase and coagulation-new insights.* Rambam Maimonides Med J, 2014. **5**(4): p. e0031.
53. Nadir, Y., et al., *Heparanase induces tissue factor expression in vascular endothelial and cancer cells.* J Thromb Haemost, 2006. **4**(11): p. 2443-51.

54. Nadir, Y., et al., *Heparanase induces tissue factor pathway inhibitor expression and extracellular accumulation in endothelial and tumor cells.* Thromb Haemost, 2008. **99**(1): p. 133-41.
55. Nadir, Y., et al., *Heparanase enhances the generation of activated factor X in the presence of tissue factor and activated factor VII.* Haematologica, 2010. **95**(11): p. 1927-34.
56. Nadir, Y. and B. Brenner, *Heparanase multiple effects in cancer.* Thromb Res, 2014. **133 Suppl 2**: p. S90-4.
57. Masola, V., et al., *Heparanase as a target in cancer therapy.* Curr Cancer Drug Targets, 2014. **14**(3): p. 286-93.
58. Gingis-Velitski, S., et al., *Heparanase induces endothelial cell migration via protein kinase B/Akt activation.* J Biol Chem, 2004. **279**(22): p. 23536-41.
59. Zetser, A., et al., *Heparanase induces vascular endothelial growth factor expression: correlation with p38 phosphorylation levels and Src activation.* Cancer Res, 2006. **66**(3): p. 1455-63.
60. Nadir, Y. and B. Brenner, *Heparanase procoagulant activity in cancer progression.* Thromb Res, 2016. **140 Suppl 1**: p. S44-8.
61. Levy-Adam, F., et al., *Heparanase facilitates cell adhesion and spreading by clustering of cell surface heparan sulfate proteoglycans.* PLoS One, 2008. **3**(6): p. e2319.
62. Yang, Y., et al., *Heparanase enhances syndecan-1 shedding: a novel mechanism for stimulation of tumor growth and metastasis.* J Biol Chem, 2007. **282**(18): p. 13326-33.
63. Purushothaman, A., et al., *Heparanase stimulation of protease expression implicates it as a master regulator of the aggressive tumor phenotype in myeloma.* J Biol Chem, 2008. **283**(47): p. 32628-36.
64. Vlodavsky, I., et al., *Significance of heparanase in cancer and inflammation.* Cancer Microenviron, 2012. **5**(2): p. 115-32.
65. Jiang, P., et al., *Cloning and characterization of the human heparanase-1 (HPR1) gene promoter: role of GA-binding protein and Sp1 in regulating HPR1 basal promoter activity.* J Biol Chem, 2002. **277**(11): p. 8989-98.

66. Andela, V.B., et al., *Tumor metastasis and the reciprocal regulation of prometastatic and antimetastatic factors by nuclear factor kappaB.* Cancer Res, 2000. **60**(23): p. 6557-62.
67. Cao, H.J., et al., *Tumor metastasis and the reciprocal regulation of heparanase gene expression by nuclear factor kappa B in human gastric carcinoma tissue.* World J Gastroenterol, 2005. **11**(6): p. 903-7.
68. Ogishima, T., et al., *Promoter CpG hypomethylation and transcription factor EGR1 hyperactivate heparanase expression in bladder cancer.* Oncogene, 2005. **24**(45): p. 6765-72.
69. Ogishima, T., et al., *Increased heparanase expression is caused by promoter hypomethylation and up-regulation of transcriptional factor early growth response-1 in human prostate cancer.* Clin Cancer Res, 2005. **11**(3): p. 1028-36.
70. Lu, W.C., et al., *Trans-activation of heparanase promoter by ETS transcription factors.* Oncogene, 2003. **22**(6): p. 919-23.
71. Elkin, M., et al., *Regulation of heparanase gene expression by estrogen in breast cancer.* Cancer Res, 2003. **63**(24): p. 8821-6.
72. Li, J.P. and I. Vlodavsky, *Heparin, heparan sulfate and heparanase in inflammatory reactions.* Thromb Haemost, 2009. **102**(5): p. 823-8.
73. Edovitsky, E., et al., *Role of endothelial heparanase in delayed-type hypersensitivity.* Blood, 2006. **107**(9): p. 3609-16.
74. Lerner, I., et al., *Heparanase powers a chronic inflammatory circuit that promotes colitis-associated tumorigenesis in mice.* J Clin Invest, 2011. **121**(5): p. 1709-21.
75. Schmidt, E.P., et al., *The pulmonary endothelial glycocalyx regulates neutrophil adhesion and lung injury during experimental sepsis.* Nat Med, 2012. **18**(8): p. 1217-23.
76. Waterman, M., et al., *Heparanase upregulation by colonic epithelium in inflammatory bowel disease.* Mod Pathol, 2007. **20**(1): p. 8-14.
77. Li, R.W., et al., *Dramatic regulation of heparanase activity and angiogenesis gene expression in synovium from patients with rheumatoid arthritis.* Arthritis Rheum, 2008. **58**(6): p. 1590-600.

78. Blich, M., et al., *Macrophage activation by heparanase is mediated by TLR-2 and TLR-4 and associates with plaque progression.* Arterioscler Thromb Vasc Biol, 2013. **33**(2): p. e56-65.
79. Goldberg, R., et al., *Versatile role of heparanase in inflammation.* Matrix Biol, 2013. **32**(5): p. 234-40.
80. Meirovitz, A., et al., *Heparanase in inflammation and inflammation-associated cancer.* FEBS J, 2013. **280**(10): p. 2307-19.
81. Goldberg, R., et al., *Role of heparanase-driven inflammatory cascade in pathogenesis of diabetic nephropathy.* Diabetes, 2014. **63**(12): p. 4302-13.
82. Goodall, K.J., et al., *Soluble heparan sulfate fragments generated by heparanase trigger the release of pro-inflammatory cytokines through TLR-4.* PLoS One, 2014. **9**(10): p. e109596.
83. van den Hoven, M.J., et al., *Regulation of glomerular heparanase expression by aldosterone, angiotensin II and reactive oxygen species.* Nephrol Dial Transplant, 2009. **24**(9): p. 2637-45.
84. Maxhimer, J.B., et al., *Heparanase-1 gene expression and regulation by high glucose in renal epithelial cells: a potential role in the pathogenesis of proteinuria in diabetic patients.* Diabetes, 2005. **54**(7): p. 2172-8.
85. Gil, N., et al., *Heparanase is essential for the development of diabetic nephropathy in mice.* Diabetes, 2012. **61**(1): p. 208-16.
86. Levidiotis, V., et al., *Heparanase is involved in the pathogenesis of proteinuria as a result of glomerulonephritis.* J Am Soc Nephrol, 2004. **15**(1): p. 68-78.
87. Levidiotis, V., et al., *A synthetic heparanase inhibitor reduces proteinuria in passive Heymann nephritis.* J Am Soc Nephrol, 2004. **15**(11): p. 2882-92.
88. van den Hoven, M.J., et al., *Increased expression of heparanase in overt diabetic nephropathy.* Kidney Int, 2006. **70**(12): p. 2100-8.
89. Katz, A., et al., *Involvement of human heparanase in the pathogenesis of diabetic nephropathy.* Isr Med Assoc J, 2002. **4**(11): p. 996-1002.
90. Shafat, I., et al., *Heparanase levels are elevated in the urine and plasma of type 2 diabetes patients and associate with blood glucose levels.* PLoS One, 2011. **6**(2): p. e17312.

91. Chen, S., et al., *Protective effect of sulodexide on podocyte injury in adriamycin nephropathy rats.* J Huazhong Univ Sci Technolog Med Sci, 2009. **29**(6): p. 715-9.
92. Masola, V., et al., *A new mechanism of action of sulodexide in diabetic nephropathy: inhibits heparanase-1 and prevents FGF-2-induced renal epithelial-mesenchymal transition.* J Transl Med, 2012. **10**: p. 213.
93. Zeisberg, M. and R. Kalluri, *Cellular mechanisms of tissue fibrosis. 1. Common and organ-specific mechanisms associated with tissue fibrosis.* Am J Physiol Cell Physiol, 2013. **304**(3): p. C216-25.
94. Rockey, D.C., P.D. Bell, and J.A. Hill, *Fibrosis--A Common Pathway to Organ Injury and Failure.* N Engl J Med, 2015. **373**(1): p. 96.
95. Zeisberg, M. and E.G. Neilson, *Mechanisms of tubulointerstitial fibrosis.* J Am Soc Nephrol, 2010. **21**(11): p. 1819-34.
96. Masola, V., et al., *Regulation of heparanase by albumin and advanced glycation end products in proximal tubular cells.* Biochim Biophys Acta, 2011. **1813**(8): p. 1475-82.
97. Masola, V., et al., *Impact of heparanase on renal fibrosis.* J Transl Med, 2015. **13**: p. 181.
98. Lan, H.Y., *Tubular epithelial-myofibroblast transdifferentiation mechanisms in proximal tubule cells.* Curr Opin Nephrol Hypertens, 2003. **12**(1): p. 25-9.
99. Iwano, M., *EMT and TGF-beta in renal fibrosis.* Front Biosci (Schol Ed), 2010. **2**: p. 229-38.
100. Strutz, F., et al., *Role of basic fibroblast growth factor-2 in epithelial-mesenchymal transformation.* Kidney Int, 2002. **61**(5): p. 1714-28.
101. Masola, V., et al., *Heparanase and syndecan-1 interplay orchestrates fibroblast growth factor-2-induced epithelial-mesenchymal transition in renal tubular cells.* J Biol Chem, 2012. **287**(2): p. 1478-88.
102. Masola, V., et al., *Heparanase is a key player in renal fibrosis by regulating TGF-beta expression and activity.* Biochim Biophys Acta, 2014. **1843**(9): p. 2122-8.
103. Pellicoro, A., et al., *Liver fibrosis and repair: immune regulation of wound healing in a solid organ.* Nat Rev Immunol, 2014. **14**(3): p. 181-94.

104. Elpek, G.O., *Cellular and molecular mechanisms in the pathogenesis of liver fibrosis: An update.* World J Gastroenterol, 2014. **20**(23): p. 7260-76.
105. Friedman, S.L., *Hepatic stellate cells: protean, multifunctional, and enigmatic cells of the liver.* Physiol Rev, 2008. **88**(1): p. 125-72.
106. Puche, J.E., Y. Saiman, and S.L. Friedman, *Hepatic stellate cells and liver fibrosis.* Compr Physiol, 2013. **3**(4): p. 1473-92.
107. Iredale, J.P., A. Thompson, and N.C. Henderson, *Extracellular matrix degradation in liver fibrosis: Biochemistry and regulation.* Biochim Biophys Acta, 2013. **1832**(7): p. 876-83.
108. Hemmann, S., et al., *Expression of MMPs and TIMPs in liver fibrosis - a systematic review with special emphasis on anti-fibrotic strategies.* J Hepatol, 2007. **46**(5): p. 955-75.
109. Xie, G. and A.M. Diehl, *Evidence for and against epithelial-to-mesenchymal transition in the liver.* Am J Physiol Gastrointest Liver Physiol, 2013. **305**(12): p. G881-90.
110. Xu, J., et al., *The types of hepatic myofibroblasts contributing to liver fibrosis of different etiologies.* Front Pharmacol, 2014. **5**: p. 167.
111. Carmel, J., et al., *Heparanase accelerates the proliferation of both hepatocytes and endothelial cells early after partial hepatectomy.* Exp Mol Pathol, 2012. **92**(2): p. 202-9.
112. Xiao, Y., et al., *Heparanase expression in hepatocellular carcinoma and the cirrhotic liver.* Hepatol Res, 2003. **26**(3): p. 192-198.
113. El-Assal, O.N., et al., *The clinicopathological significance of heparanase and basic fibroblast growth factor expressions in hepatocellular carcinoma.* Clin Cancer Res, 2001. **7**(5): p. 1299-305.
114. Ikeguchi, M., Y. Hirooka, and N. Kaibara, *Heparanase gene expression and its correlation with spontaneous apoptosis in hepatocytes of cirrhotic liver and carcinoma.* Eur J Cancer, 2003. **39**(1): p. 86-90.
115. Liu, C.J., et al., *Adjuvant heparanase inhibitor PI-88 therapy for hepatocellular carcinoma recurrence.* World J Gastroenterol, 2014. **20**(32): p. 11384-93.

116. Liu, C.J., et al., *Heparanase inhibitor PI-88 as adjuvant therapy for hepatocellular carcinoma after curative resection: a randomized phase II trial for safety and optimal dosage.* J Hepatol, 2009. **50**(5): p. 958-68.

117. Ohayon, O., et al., *Halofuginone upregulates the expression of heparanase in thioacetamide-induced liver fibrosis in rats.* Lab Invest, 2008. **88**(6): p. 627-33.

118. Liu, Y., et al., *Animal models of chronic liver diseases.* Am J Physiol Gastrointest Liver Physiol, 2013. **304**(5): p. G449-68.

119. Kitani, H., et al., *A simple and efficient method to isolate macrophages from mixed primary cultures of adult liver cells.* J Vis Exp, 2011(51).

120. Liang, C.C., A.Y. Park, and J.L. Guan, *In vitro scratch assay: a convenient and inexpensive method for analysis of cell migration in vitro.* Nat Protoc, 2007. **2**(2): p. 329-33.

121. Castera, L., X. Forns, and A. Alberti, *Non-invasive evaluation of liver fibrosis using transient elastography.* J Hepatol, 2008. **48**(5): p. 835-47.

122. Zaza, G., et al., *Dialysis-related transcriptomic profiling: the pivotal role of heparanase.* Exp Biol Med (Maywood), 2014. **239**(1): p. 52-64.

123. Chen, G., et al., *Inflammatory cytokines and fatty acids regulate endothelial cell heparanase expression.* Biochemistry, 2004. **43**(17): p. 4971-7.

124. Tacke, F. and H.W. Zimmermann, *Macrophage heterogeneity in liver injury and fibrosis.* J Hepatol, 2014. **60**(5): p. 1090-6.

125. Zhao, Y., et al., *Hepatic stellate cells produce vascular endothelial growth factor via phospho-p44/42 mitogen-activated protein kinase/cyclooxygenase-2 pathway.* Mol Cell Biochem, 2012. **359**(1-2): p. 217-23.

126. Ma, X.M., et al., *Heparanase promotes human gastric cancer cells migration and invasion by increasing Src and p38 phosphorylation expression.* Int J Clin Exp Pathol, 2014. **7**(9): p. 5609-21.

127. Kelly, T., et al., *High heparanase activity in multiple myeloma is associated with elevated microvessel density.* Cancer Res, 2003. **63**(24): p. 8749-56.

128. Vreys, V. and G. David, *Mammalian heparanase: what is the message?* J Cell Mol Med, 2007. **11**(3): p. 427-52.

129. Liedtke, C., et al., *Experimental liver fibrosis research: update on animal models, legal issues and translational aspects.* Fibrogenesis Tissue Repair, 2013. **6**(1): p. 19.